

Fig. 12– Block diagram of a system using a "losser"-type tone-control circuit.

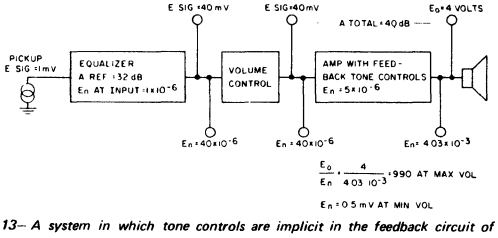


Fig. 13– A system in which tone controls are implicit in the feedback circuit of the power amplifier.

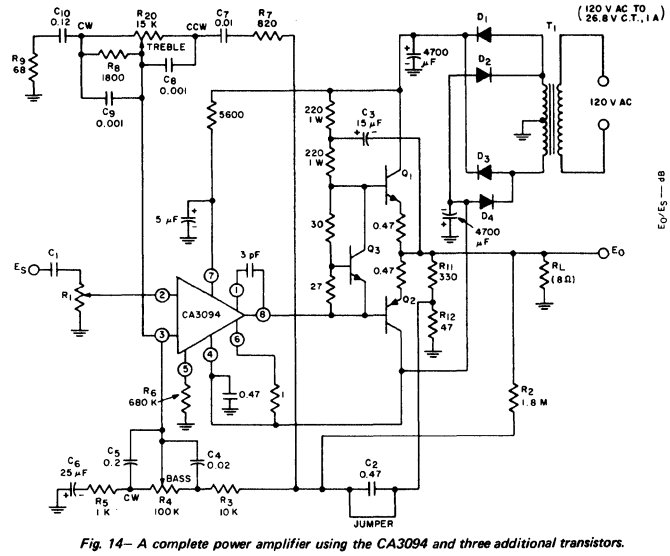


Fig. 14– A complete power amplifier using the CA3094 and three additional transistors.

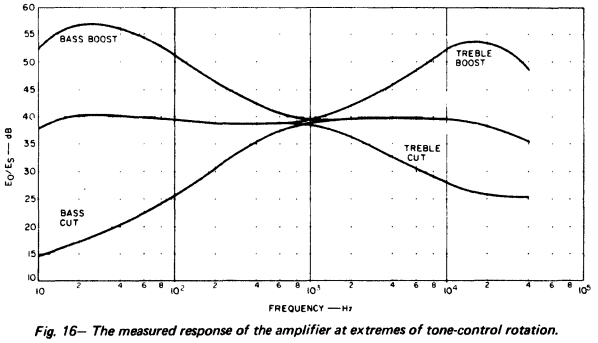


Fig. 16– The measured response of the amplifier at extremes of tone-control rotation.

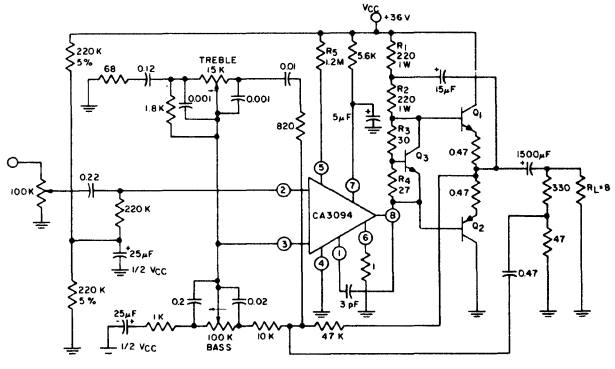


Fig. 15– A power amplifier operated from a single supply.

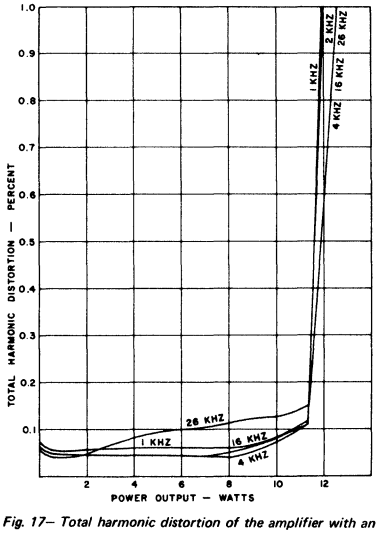


Fig. 17– Total harmonic distortion of the amplifier with an unregulated power supply.

network includes R3, R4, R5, C4, and C5. C6 blocks the dc from the feedback network so that the dc gain from input to the feedback takeoff point is unity. The residual dc-output-voltage at the speaker terminals is then $I_{ABC} R_1 \frac{R_{11} + R_{12}}{R_{12}}$ where R_1 is the source resistance. The input bias current is then $\frac{I_{ABC}}{2\beta} = -\frac{(V_{CC} - V_{be})}{2\beta R6}$. The treble network consists of R7, R8, R9, R10, C7, C8, C9, and C10. Resistors R7 and R9 limit the maximum available cut and boost, respectively. The boost limit is useful in curtailing heating due to finite turn-off time in the output units. The limit is also desirable when there are tape recorders nearby. The cut limit aids the stability of the amplifier by cutting the loop gain at higher frequencies where phase shifts become significant.

In cases in which absolute stability under all load conditions is required, it may be necessary to insert a small inductor in the output lead to isolate the circuit from capacitive loads. A 3-microhenry inductor (1 ampere) in parallel with a 22-ohm resistor is adequate. The derivation of circuit constants is shown in Appendix B. Curves of control action versus electrical rotation are also given.

Performance

Fig. 16 is a plot of the measured response of the complete amplifier at the extremes of tone-control rotation. A comparison of Fig. 16 with the computed curves of Fig. B4 (Appendix B) shows good agreement. The total harmonic distortion of the amplifier with an unregulated power supply is shown in Fig. 17; IM distortion is plotted in Fig. 18. Hum and noise are typically 700 microvolts at the output, or 83-dB down.

COMPANION RIAA PREAMPLIFIER

Many available preamplifiers are capable of providing the drive for the power amplifier of Fig. 14. Yet the unique characteristics of the amplifier – its power supply, input impedance, and gain – make possible the design of an RIAA

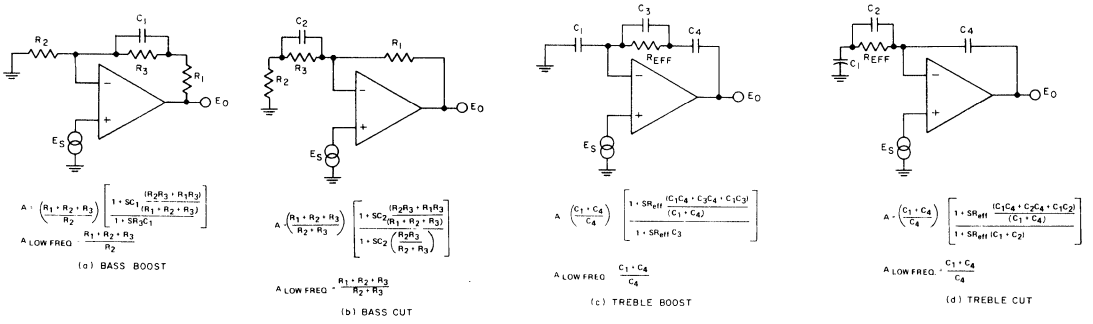


Fig. B1– Four operational-amplifier circuit configurations and the gain expressions for each.

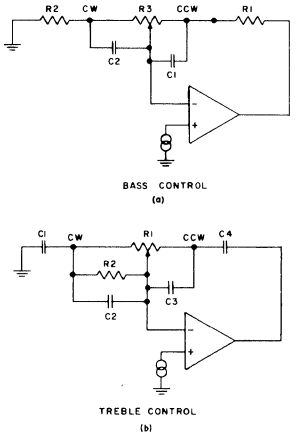


Fig. B2– Cut and boost bass and treble controls that have the characteristics of the circuits of Fig. B1.

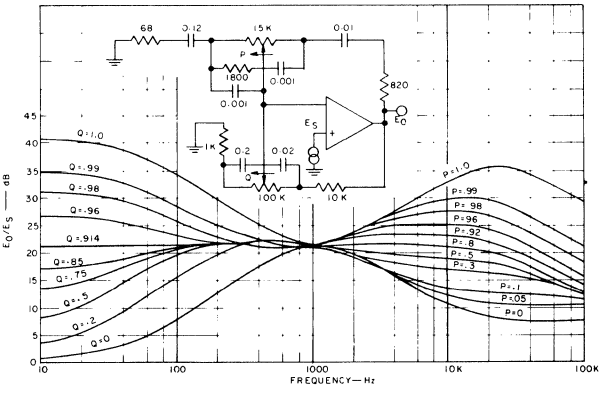


Fig. B3– A plot of the response of the circuit of Fig. 14 with bass and treble tone controls combined at various settings of both controls.

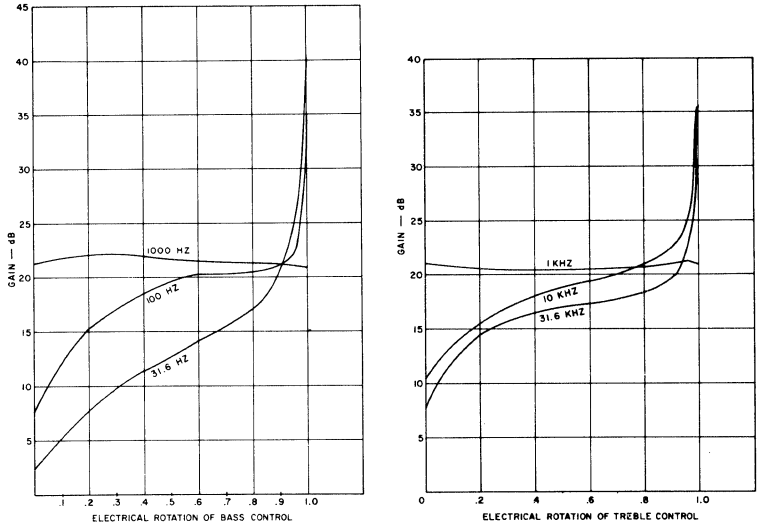


Fig. B4– The information of Fig. B3 plotted as a function of electrical rotation.

91-percent of its total resistance. The amplitude response of the treble control is, however, never completely "flat"; a computer was used to generate response curves as controls were varied.

Fig. B3 is a plot of the response with bass and treble tone controls combined at various settings of both controls. The values shown are the practical ones used in the actual design. Fig. B4 shows the information of Fig. B3 replotted as a function of electrical rotation. The ideal taper for each control would be the complement of the 100-Hz plot for the bass control and the 10-kHz response for the treble control. The mechanical center should occur at the crossover point in each case.

References*

1. "Applications of the CA3080 and CA3080A High-Performance Operational Transconductance Amplifiers," H. A. Wittlinger, RCA Application Note ICAN-6668
2. "A New Wide-band Amplifier Technique," B. Gilbert, IEEE Journal of Solid State Circuits, Vol. SC-3, No. 4, December, 1968.
3. "Trackability," James A. Kogar, *Audio*, December 1966
4. *RCA Linear Integrated Circuits Manual*, RCA Technical Series IC-42

*RCA publications available through RCA Solid State Division, Box 3200, Somerville, N.J., 08876.

teristics for various values of R_{SC} are shown in Fig. 4.

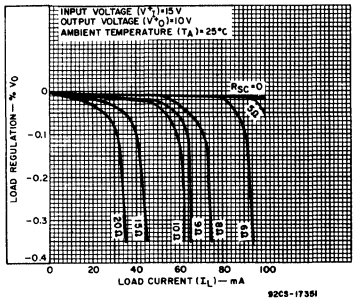


Fig. 4– Load regulation characteristics for circuit of Fig. 3.

When this circuit is used to provide high output currents at low output voltages, care must be exercised to avoid excessive IC dissipation. In the circuit of Fig. 3, this dissipation control can be accomplished by increasing the primary-to-secondary transformer ratio (a reduction in V_I) or by using a dropping resistor between the rectifier and the CA3085 regulator. Fig. 5 gives data on dissipation limitation (V_I-V_O vs. I_O) for CA3085-series circuits.

The short-circuit current is determined as follows:

$$I_{SC} = \frac{V_{BE}}{R_{SC}} \approx \frac{0.7}{R_{SC}} \text{ amperes} \qquad (2)$$

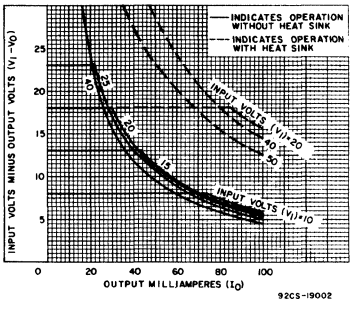


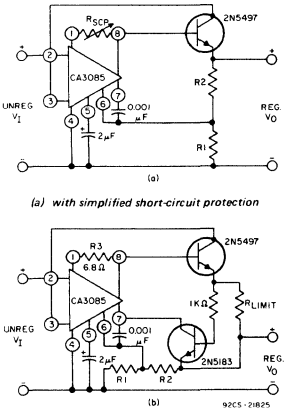
Fig. 5– Dissipation limitation ($V_I - V_O$ vs. I_O) for CA3085 series circuits.

The line- and load-regulation characteristics for the circuit shown in Fig. 3 are approximately 0.05 per cent of the output voltage.

High-Current Voltage Regulator

When regulated voltages at currents greater than 100 milliamperes are required, the CA3085 can be used in conjunction with an external n-p-n pass-transistor as shown in the circuits of Fig. 6. In these circuits the output current available from the regulator is increased in accordance with the h_{FE} of the external n-p-n pass-transistor. Output currents up to 8 amperes can be regulated with these circuits. A Darlington power transistor can be substituted for the 2N5497 transistor when currents greater than 8 amperes are to be regulated.

A simplified method of short-circuit protection is used in connection with the circuit of Fig. 6(a). The variable resistor R_{SCP} serves two purposes: (1) it can be adjusted to optimize the base drive requirements (h_{FE}) of the particular 2N5497 transistor being used, and (2) in the event of a short-circuit in the regulated output voltage the base drive current in the 2N5497 will increase, thereby increasing the voltage drop across R_{SCP}. As this voltage-drop increases the short-circuit protection system within the CA3085 correspondingly reduces the output current available at terminal 8, as described previously. It should be noted that the degree of short-circuit protection depends on the value of R_{SCP}, i.e., design compromise is required in choosing the value of R_{SCP} to provide the desired base drive for the 2N5497 while maintaining the desired short-circuit protection. Fig. 6(b) shows an alternate circuit in which an additional transistor (2N5183) and two resistors have been added as an auxiliary short-circuit protection feature. Resistor R3 is used to establish the desired base drive for the 2N5497, as described above. Resistor R_{limit} now controls the short-circuit output current because, in the event of a short-circuit, the voltage drop developed across its terminals increases sufficiently to increase the base drive to the 2N5183 transistor. This increase in base drive results in reduced output from the CA3085 because collector current flow in the 2N5183 diverts base drive from the Darlington output stage of the CA3085 (see Fig. 2) through terminal 7. The load regulation of this circuit is typically 0.025 per cent with 0 to 3-ampere load-current variation; line regulation is typically 0.025 per cent/volt change in input voltage.



(a) with simplified short-circuit protection

(b) with auxiliary short-circuit protection

Fig. 6– High-current voltage regulator using n-p-n pass transistor.

Voltage Regulator with Low V_I-V_O Difference

In the voltage regulators described in the previous section, it is necessary to maintain a minimum difference of about 4 volts between the input and output voltages. In some applications this requirement is prohibitive. The circuit shown in Fig. 7 can deliver an output current in the order of 2 amperes with a V_I-V_O difference of only one volt.

It employs a single external p-n-p transistor having its base and emitter connected to terminals 2 and 3, respectively, of the CA3085. In this circuit, the emitter of the output transistor (Q14 in Fig. 2) in the CA3085 is returned to the negative supply rail through an external resistor (R_{SCP}) and two series-connected diodes (D1, D2). These forward-biased diodes maintain Q6 in the CA3085 within linear-mode operation. The

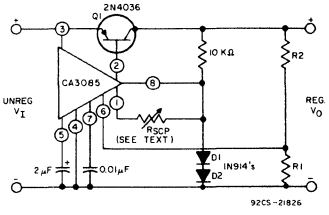


Fig. 7– Voltage regulator for low $V_I - V_O$ difference.

choice of resistors R1 and R2 is made in accordance with Eq. (1). Adequate frequency compensation for this circuit is provided by the 0.01-microfarad capacitor connected between terminal 7 of the CA3085 and the negative supply rail.

Fig. 8, which shows the output impedance of the circuit of Fig. 7 as a function of frequency, illustrates the excellent ripple-rejection characteristics of this circuit at frequencies below 1 kHz. Lower output impedances at the higher frequencies can be provided by connecting an appropriate capacitor across the output voltage terminals. The addition of a capacitor will, however, degrade the ability of the system to react to transient-load conditions.

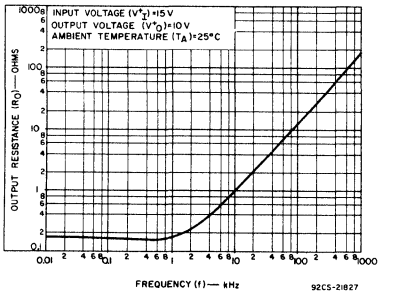


Fig. 8– Output resistance vs. frequency for circuit of Fig. 7.

High-Voltage Regulator

Fig. 9 shows a circuit that uses the CA3085 as a voltage-reference and regulator control device for high-voltage power supplies in which the voltages to be regulated are well above the input-voltage ratings of the CA3085-series circuits. The external transistors Q1 and Q2 require voltage ratings in excess of the maximum input voltage to be regulated. Series-pass transistor Q2 is controlled by the collector current of Q1, which in turn is controlled by the normally regulated current output supplied by the CA3085. The input voltage for the CA3085 regulator at terminal 3 is supplied through dropping resistor R3 and the clamping zener diode D1. The values for resistor R1 and R2 are determined in accordance with Eq. (1).

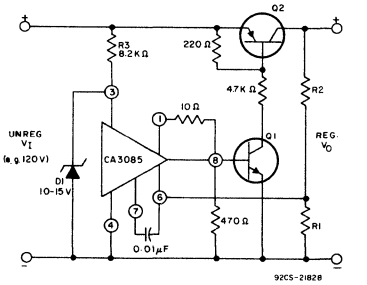


Fig. 9– High-voltage regulator.

Negative-Voltage Regulator

The CA3085 is used as a negative-supply voltage regulator in the circuit shown in Fig. 10. Transistor Q3 is the series-pass transistor. It should be noted that the CA3085 is effectively connected across the load-side of the regulated system. Diode D1 is used initially in a "circuit-starter" function; transistor Q2 "latches" D1 out of its starter-circuit function so that the CA3085 can assume its role in controlling the pass-transistor Q3 by means of Q1.

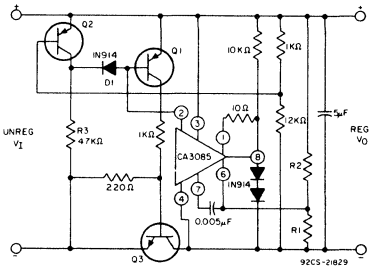


Fig. 10– Negative-voltage regulator.

Operation of the circuit is as follows: current through R3 and D1 provides base drive for Q1, which in turn provides

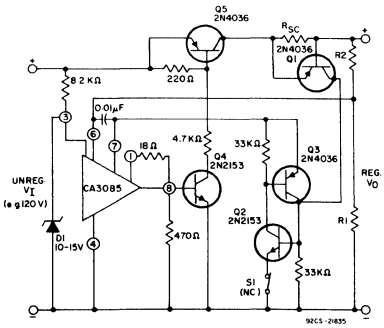


Fig. 16– High-voltage regulator incorporating current "snap-back" protection.

Switching Regulator

When large input-to-output voltage differences are necessary, the regulators described above are inefficient because they dissipate significant power in the series-pass transistor. Under these conditions, high-efficiency operation can be achieved by using a switching-type regulator of the generic type shown in Fig. 17(a). Transistor Q1 acts as a keyed switch and operates in

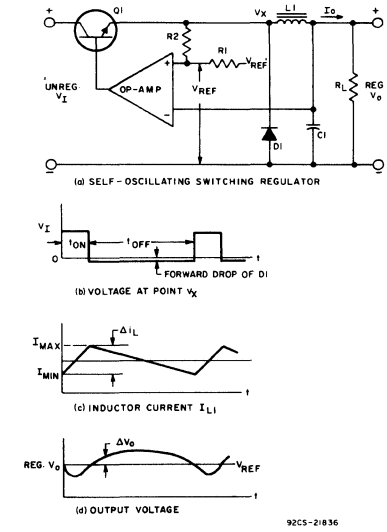


Fig. 17– Switching regulator and associated waveforms.

either a saturated or cut-off condition to minimize dissipation. When transistor Q1 is conductive, diode D1 is reverse-biased and current in the inductance L1 increases in accordance with the following relationship:

$$i_L = \frac{1}{L}\int_{t_o}^{t_1} V dt \qquad (10)$$

where V is the voltage across the inductance L1. The current through the inductance charges the capacitor C1 and supplies current to the load. The output voltage rises until it slightly exceeds the reference voltage V_{ref}. At this point the op-amp removes base drive to Q1 and the unregulated input voltage V_I is "switched off". The energy stored in the inductor L1 now causes the voltage at V_X to swing in the negative direction and current flows through diode D1, while continuing to supply current into the load R_L. As the current in the inductor falls below the load current, the capacitor C1 begins to discharge and V_O decreases. When V_O falls slightly below the value of V_{ref}, the op-amp turns on Q1 and the cycle is repeated. It should be apparent that the output voltage oscillates about V_{ref} with an amplitude determined by R1 and R2. Actually, the value of V_{ref} varies from being slightly more positive than V_{ref} when Q1 is conducting, to being slightly more negative than V_{ref} when D1 is conducting. The voltage and current waveforms are shown in Fig. 17(b), (c), and (d).

Design Example: The following specifications are used in decomputations for a switching regulator:

$V_I = 30$ V, $V_O = 5$ V, $I_O = 500$ mA,
switching frequency = 20 kHz,
output ripple = 100 mV.

If it is assumed that transistor Q1 is in steady-state saturated operation with a low voltage-drop, the current in the inductor is given by Eq. 10, as follows:

$$i_L = \frac{1}{L}\int_{t_o}^{t_1} V dt = \left(\frac{V_I - V_O}{L1}\right) t_{on} \qquad (11)$$

When transistor Q1 is off, the current in the inductor is given by:

$$i_L \cong \frac{(V_O + V_{D1})\ t_{off}}{L1} \qquad (12)$$

From Eq. 11,

$$L_1 = \frac{(V_I - V_O)}{i_L} \cdot \frac{1}{f} \cdot \frac{V_O}{V_I} \qquad (13)$$

If i_{max} is 1.3 I_L, then during t_{on} the current in the inductor (i_L) will be 0.5 A x 1.3 = 0.65 A; therefore, Δi_L = 0.15 A

Substitution in Eq. 13 yields

$$L_1 = \frac{(30-5)}{0.15} \cdot \frac{1}{(20 \times 10^3)} \cdot \frac{5}{30} = 1.4 \text{ mH} \qquad (14)$$

Current discharge from the capacitor C1 is given by:

$$i_c = C\frac{dv}{dt} \qquad (15)$$

Thus, $\Delta i_c = C\frac{\Delta v}{\Delta t}$, or $C = \frac{\Delta i_c\ \Delta t}{\Delta v}$

Since $i_c = i_L$ and $\Delta t = t_{off}$, then

$$C = \frac{\Delta i_L\ t_{off}}{\Delta v}$$

Substitution for the value of i_L from Eq. 13 yields

$$C = \frac{\left(\frac{V_I - V_O}{L1}\right) \cdot \frac{1}{f} \cdot \left(\frac{V_O}{V_I}\right) \cdot t_{off}}{\Delta v} \qquad (16)$$

The total period $T = t_{off} + t_{on}$, and $T = \frac{1}{f}$. Therefore,

$$t_{off} = \frac{1}{f} - t_{on} \qquad (17)$$

For optimum efficiency t_{on} should be

$$\cong \left(\frac{V_O}{V_I}\right) T \cong \left(\frac{V_O}{V_I}\right) \frac{1}{f} \qquad (18)$$

Substitution for t_{on} in Eq. 18 yields

$$t_{off} = \frac{1}{f} - \left(\frac{V_O}{V_I}\right)\frac{1}{f} = \frac{1}{f}\left(1 - \frac{V_O}{V_I}\right) \qquad (19)$$

Substitution for t_{off} in Eq. 16 yields

$$C = \frac{\frac{(V_I - V_O)}{L_1} \cdot \frac{1}{f} \cdot \frac{V_O}{V_I} \cdot \frac{1}{f} \cdot \left(1 - \frac{V_O}{V_I}\right)}{\Delta v}$$

Substitution of numerical values in Eq. 20 produces the following value for C:

$$C = \frac{\frac{30-5}{1.4 \times 10^{-3}} \cdot \frac{1}{20 \times 10^3} \cdot \frac{5}{30} \cdot \frac{1}{20 \times 10^3} \cdot \left(1 - \frac{5}{30}\right)}{10^{-1}} = 63\ \mu F$$

A switching-regulator circuit using the CA3085 is shown in Fig. 18. The values of L and C (1.5 millihenries and 50 microfarads, respectively) are commercially available components having values approximately equal to the computed values in the previous design example.

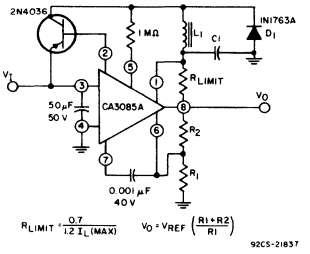
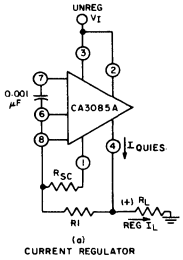


Fig. 18– Typical switching regulator circuit.

Current Regulators

The CA3085 series of voltage regulators can be used to provide a constant source or sink current. A regulated-current supply capable of delivering up to 100 milliamperes is shown in Fig. 19(a). The regulated load current is controlled by R1 because the current flowing through this resistor must establish a voltage difference between terminals 6 and 4 that is equal to the internal reference voltage developed between terminals 5 and 4. The actual regulated current, reg I_L, is the sum of the quiescent regulator current and the current through R1, i.e.,

$$\text{reg } I_L = I_{quiescent} + I_{R1}$$



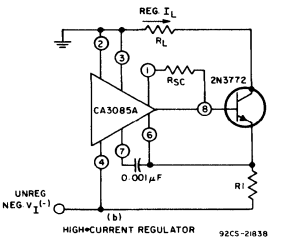


Fig. 19– Constant current regulators.

Fig. 19(b) shows a high-current regulator using the CA3085 in conjunction with an external n-p-n transistor to regulate currents up to 3 amperes. In this circuit the quiescent regulator current does not flow through the load and the output current can be directly programmed by R1, i.e.,

$$\text{Reg } I_L = \frac{V_{ref}}{R1}$$

With this regulator currents between 1 milliampere and 3 amperes can be programmed directly. At currents below 1 milliampere inaccuracies may occur as a result of leakage in the external transistor.

A Dual-Tracking Voltage Regulator

A dual-tracking voltage regulator using a CA3085 and a CA3094A* is shown in Fig. 20. The CA3094A is basically an op-amp capable of supplying 100 milliamperes of output current.

Features and Applications of RCA Integrated-Circuit Zero-Voltage Switches (CA3058, CA3059, and CA3079)

by A.C.N. Sheng, G.J. Granieri, J. Yellin, and T. McNulty

RCA-CA3058, CA3059 and CA3079 zero-voltage switches are monolithic integrated circuits designed primarily for use as trigger circuits for thyristors in many highly diverse ac power-control and power-switching applications. These integrated-circuit switches operate from an ac input voltage of 24, 120, 208 to 230, or 277 volts at 50, 60, or 400 Hz.

The CA3059 and CA3079 are supplied in a 14-terminal dual-in-line plastic package. The CA3058 is supplied in a 14-terminal dual-in-line ceramic package. The electrical and physical characteristics of each type are detailed in RCA Data Bulletin File No. 490.

RCA zero-voltage switches (ZVS) are particularly well suited for use as thyristor trigger circuits. These switches trigger the thyristors at zero-voltage points in the supply-voltage cycle. Consequently, transient load-current surges and radio-frequency interference (RFI) are substantially reduced. In addition, use of the zero-voltage switches also reduces the rate of change of on-state current (di/dt) in the thyristor being triggered, an important consideration in the operation of thyristors. These switches can be adapted for use in a variety of control functions by use of an internal differential comparator to detect the difference between two externally developed voltages. In addition, the availability of numerous terminal connections to internal circuit points greatly increases circuit flexibility and further expands the types of ac power-control applications to which these integrated circuits may be adapted. The excellent versatility of the zero-voltage switches is demonstrated by the fact that these circuits have been used to provide transient-free temperature control in self-cleaning ovens, to control gun-muzzle temperature in low-temperature environments, to provide sequential switching of heating elements in warm-air furnaces, to switch traffic signal lights at street intersections, and to effect other widely different ac power-control functions.

FUNCTIONAL DESCRIPTION

RCA zero-voltage switches are multistage circuits that employ a diode limiter, a zero-crossing (threshold) detector, an on-off sensing amplifier (differential comparator), and a Darlington output driver (thyristor gating circuit) to provide the basic switching action. The dc operating voltages for these stages is provided by an internal power supply that has sufficient current capability to drive external circuit elements, such as transistors and other integrated circuits. An important feature of the zero-voltage switches is that the output trigger pulses can be applied directly to the gate of a triac or a silicon controlled rectifier (SCR). The CA3058 and CA3059 also feature an interlock (protection) circuit that inhibits the application of these pulses to the thyristor in the event that the external sensor should be inadvertently opened or shorted. An external inhibit connection (terminal No. 1) is also available so that an external signal can be used to inhibit the output drive. This feature is not included in the CA3079; otherwise, the three integrated-circuit zero-voltage switches are electrically identical.

Over-all Circuit Operation

Fig. 1 shows the functional interrelation of the zero-voltage switch, the external sensor, the thyristor being triggered, and the load elements in an on-off type of ac power-control system. As shown, each of the zero-voltage switches incorporates four functional blocks as follows:

(1) Limiter-Power Supply – Permits operation directly from an ac line.

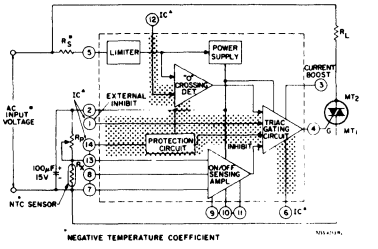
(2) Differential On/Off Sensing Amplifier – Tests the condition of external sensors or command signals. Hysteresis or proportional-control capability may easily be implemented in this section.

(3) Zero-Crossing Detector – Synchronizes the output pulses of the circuit at the time when the ac cycle is at a zero-voltage point and thereby eliminates radio-frequency inteference (RFI) when used with resistive loads.

(4) Triac Gating Circuit – Provides high-current pulses to the gate of the power-controlling thyristor.

In addition, the CA3058 and CA3059 provide the following important auxiliary functions (shown in Fig. 1):

(1) A built-in protection circuit that may be actuated to remove drive from the triac if the sensor opens or shorts.



AC Input Voltage (50/60 or 400 Hz) V AC	Input Series Resistor (R_S) k Ω	Dissipation Rating for R_S W
24	2	0.5
120	10	2
208/230	20	4
277	25	5

Fig. 1 – Functional block diagrams of the zero-voltage switches CA3058, CA3059, and CA3079.

(2) Thyristor firing may be inhibited through the action of an internal diode gate connected to terminal 1.

(3) High-power dc-comparator operation is provided by overriding the action of the zero-crossing detector. This override is accomplished by connecting terminal 12 to terminal 7. Gate current to the thyristor is continuous when terminal 13 is positive with respect to terminal 9.

Fig. 2 shows the detailed circuit diagram for the integrated-circuit zero-voltage switches. (The diagrams shown in Figs. 1 and 2 are representative of all three RCA zero-voltage switches, i.e., the CA3058, CA3059, and CA3079; the shaded areas indicate the circuitry that is not included in the CA3079.)

The limiter stage of the zero-voltage switch clips the incoming ac line voltage to approximately ±8 volts. This signal is then applied to the zero-voltage-crossing detector, which generates an output pulse each time the line voltage passes through zero. The limiter output is also applied to a rectifying diode and an external capacitor, C_F, that comprise the dc power supply. The power supply provides approximately 6 volts as the V_{CC} supply to the other stages of the zero-voltage switch. The on-off sensing amplifier is basically a differential comparator. The thyristor gating circuit contains a driver for direct triac triggering. The gating circuit is enabled when all the inputs are at a "high" voltage, i.e., the line voltage must be approximately zero volts, the sensing-amplifier output must be "high," the external voltage to terminal 1 must be a logical "0", and, for the CA3058 and CA3059, the output of the fail-safe circuit must be "high." Under these conditions, the thyristor (triac or SCR) is triggered when the line voltage is essentially zero volts.

Thyristor Triggering Circuits

The diodes D_1 and D_2 in Fig. 2 form a symmetrical clamp that limits the voltages on the chip to ±8 volts; the diodes D_7 and D_{13} form a half-wave rectifier that develops a positive voltage on the external storage capacitor, C_F.

The output pulses used to trigger the power-switching thyristor are actually developed by the zero-crossing detector and the thyristor gating circuit. The zero-crossing detector consists of diodes D_3 through D_6, transistor Q_1, and the associated resistors shown in Fig. 2. Transistors Q_1 and Q_6 through Q_9 and the associated resistors comprise the thyristor gating circuit and output driver. These circuits generate the output pulses when the ac input is at a zero-voltage point so that RFI is virtually eliminated when the zero-voltage switch and thyristor are used with resistive loads.

The operation of the zero-crossing detector and thyristor gating circuit can be explained more easily if the on state (i.e., the operating state in which current is being delivered to the thyristor gate through terminal 4) is considered as the operating condition of the gating circuit. Other circuit elements in the zero-voltage switch inhibit the gating circuit unless certain conditions are met, as explained later.

In the on state of the thyristor gating circuit, transistors Q_8 and Q_9 are conducting, transistor Q_7 is off, and transistor Q_6 is on. Any action that turns on transistor Q_7 removes the drive from transistor Q_8 and thereby turns off the thyristor. Transistor Q_7 may be turned on directly by application of a minimum of ±1.2 volts at 10 microamperes to the external-inhibit input, terminal 1. (If a voltage of more than

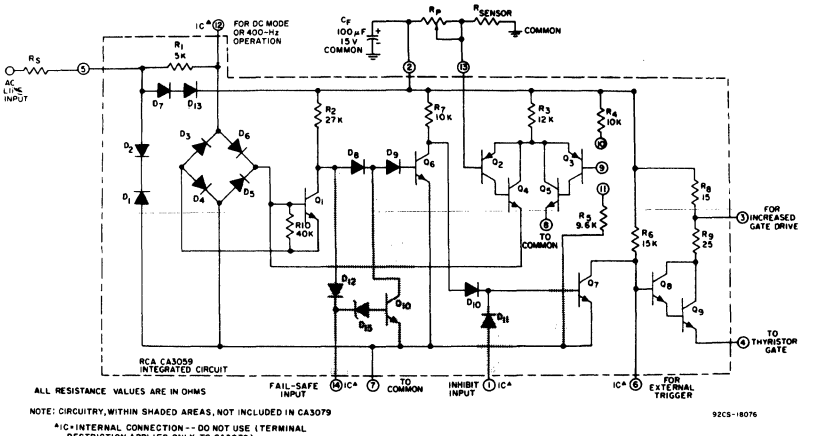


Fig. 2 – Schematic diagram of zero-voltage switches CA3058, CA3059, and CA3079.

more positive than the breakdown voltage of diode D_{15}, activation of the protection circuit is not possible. For this reason, loading the internal supply may cause this circuit to malfunction, as may selection of the wrong external supply voltage. Fig. 7 shows a guide for the proper operation of the protection circuit when an external supply is used with a typical integrated-circuit zero-voltage switch.

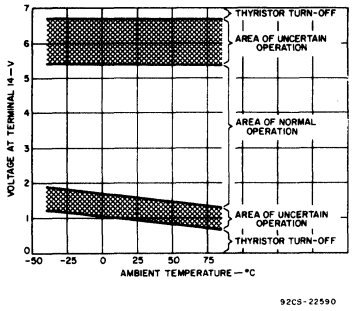


Fig. 7 – Operating regions for built-in protection circuits of a typical zero-voltage switch.

SPECIAL APPLICATION CONSIDERATIONS

As pointed out previously, the RCA integrated-circuit zero-voltage switches (CA3058, CA3059, and CA3079) are exceptionally versatile units that can be adapted for use in a wide-variety of power-control applications. Full advantage of this versatility can be realized, however, only if the user has a basic understanding of several fundamental considerations that apply to certain types of applications of the zero-voltage switches.

Operating-Power Options

Power to the zero-voltage switch may be derived directly from the ac line, as shown in Fig. 1, or from an external dc power supply connected between terminals 2 and 7, as shown in Fig. 8. When the zero-voltage switch is operated directly from the ac line, a dropping resistor R_S of 5,000 to 10,000 ohms must be connected in series with terminal 5 to limit the current in the switch circuit. The optimum value for this resistor is a function of the average current drawn from the internal dc power supply, either by external circuit elements or by the thyristor trigger circuits, as shown in Fig. 9. The chart shown in Fig. 1 indicates the value and dissipation rating of the resistor R_S for ac line voltages of 24, 120, 208 to 230, and 277 volts.

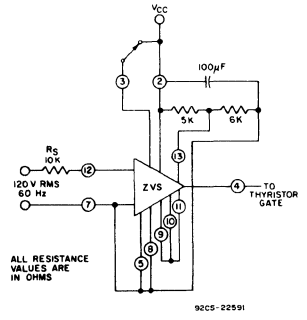


Fig. 8 – Operation of the zero-voltage switch from an external dc power supply connected between terminals 2 and 7.

Half-Cycling Effect

The method by which the zero-voltage switch senses the zero crossing of the ac power results in a half-cycling phenomenon at the control point. Fig. 10 illustrates this phenomenon. The zero-voltage switch senses the zero-voltage

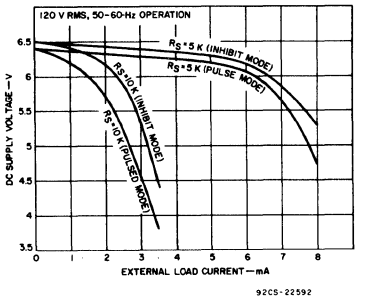


Fig. 9 – DC supply voltage as a function of external load current for several values of dropping resistance R_S.

crossing every half-cycle, and an output, for example pulse No. 4, is produced to indicate the zero crossing. During the remaining 8.3 milliseconds, however, the differential amplifier in the zero-voltage switch may change state and inhibit any further output pulses. The uncertainity region of the differential amplifier, therefore, prevents pulse No. 5 from triggering the triac during the negative excursion of the ac line voltage.

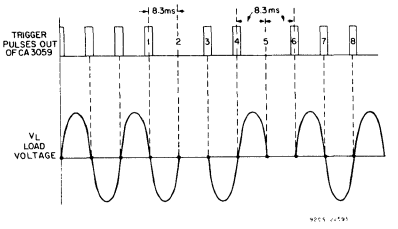


Fig. 10 – Half-cycling phenomenon in the zero-voltage switch.

When a sensor with low sensitivity is used in the circuit, the zero-voltage switch is very likely to operate in the linear mode. In this mode, the output trigger current may be sufficient to trigger the triac on the positive-going cycle, but insufficient to trigger the device on the negative-going cycle of the triac supply voltage. This effect introduces a half-cycling phenomenon, i.e., the triac is turned on during the positive half-cycle and turned off during the negative half-cycle.

Several techniques may be used to cope with the half-cycling phenomenon. If the user can tolerate some hystersis in the control, then positive feedback can be added around the differential amplifier. Fig. 11 illustrates this technique. The tabular data in the figure lists the recommended values of resistors R_1 and R_2 for different sensor impedances at the control point.

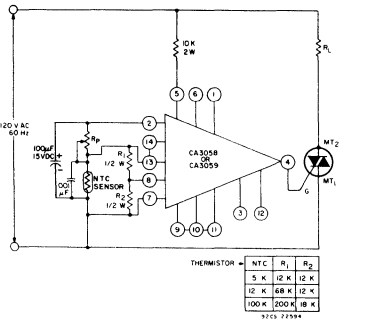


Fig. 11 – CA3058 or CA3059 on-off controller with hysteresis.

If a significant amount (greater than ±10%) of controlled hysteresis is required, then the circuit shown in Fig. 12 may be employed. In this configuration, external transistor Q_1 can be used to provide an auxiliary timed-delay function.

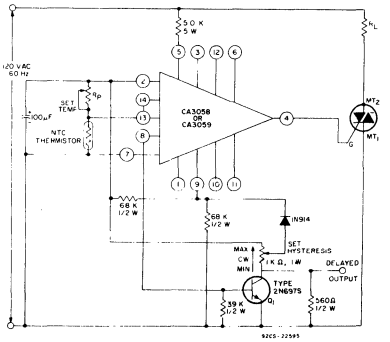


Fig. 12 – CA3058 or CA3059 on-off controller with controlled hysteresis.

For applications that require complete elimination of half-cycling without the addition of hysteresis, the circuit shown in Fig. 13 may be employed. This circuit uses a CA3098E integrated-circuit programmable comparator with a zero-voltage switch. A block diagram of CA3098E is shown in Fig. 14. Because the CA3098E contains an integral flip-flop, its output will be in either a "0" or "1" state. Consequently the zero-voltage switch cannot operate in the linear mode, and spurious half-cycling operation is prevented. When the signal-input voltage at terminal 8 of the CA3098E is equal to or less than the "low" reference voltage (LR), current flows from the power supply through resistor R_1 and R_2, and a logic "0" is

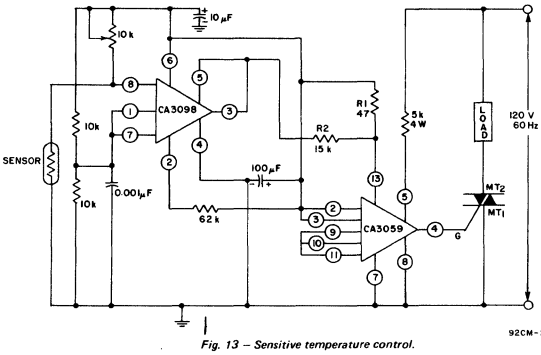


Fig. 13 – Sensitive temperature control.

Circuits that use a sensitive-gate triac to shift the firing point of the power triac by approximately 90 degrees have been designed. If the primary load is inductive, this phase shift corresponds to firing at zero current in the load. However, changes in the power factor of the load or tolerances of components will cause errors in this firing time.

The circuit shown in Fig. 19 uses a CA3086 integrated-circuit transistor array to detect the absence of load current by sensing the voltage across the triac. The internal zero-crossing detector is disabled by connection of terminal 12 to terminal 7, and control of the output is made through the external inhibit input, terminal 1. The circuit permits an output only when the voltage at point A exceeds two V_{BE} drops, or 1.3 volts. When A is positive, transistors Q_3 and Q_4 conduct and reduce the voltage at terminal 1 below the inhibit state. When A is negative, transistors Q_1 and Q_2 conduct. When the voltage at point A is less than ±1.3 volts, neither of the transistor pairs conducts; terminal 1 is then pulled positive by the current in resistor R_3, and the output in inhibited.

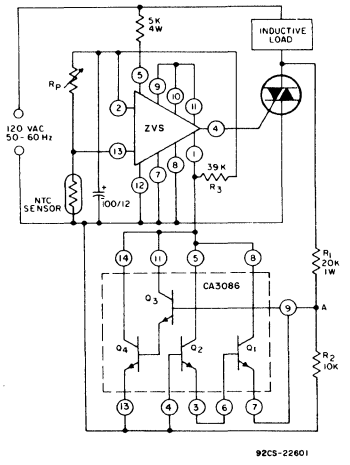


Fig. 19 – Use of the CA3058 or CA3059 together with CA3086 for switching inductive loads.

The circuit shown in Fig. 19 forms a pulse of gate current and can supply high peak drive to power traics with low average current drain on the internal supply. The gate pulse will always last just long enough to latch the thyristor so that there is no problem with delaying the pulse to an optimum time. As in other circuits of this type, RFI results if the load is not suitably inductive because the zero-crossing detector is disabled and initial turn-on occurs at random.

The gate pulse forms because the voltage at point A when the thyristor is on is less than 1.3 volts: therefore, the output of the zero-voltage switch is inhibited, as described above. The resistor divider R_1 and R_2 should be selected to assure this condition. When the triac is on, the voltage at point A is approximately one-third of the instantaneous on-state voltage (v_T) of the thyristor. For most RCA thyristors, v_T (max) is less than 2 volts, and the divider shown is a conservative one. When the load current passes through zero, the triac commutates and turns off. Because the circuit is still being driven by the line voltage, the current in the load attempts to reverse, and voltage increases rapidly across the "turned-off" triac. When this voltage exceeds 4 volts, one portion of the CA3086 conducts and removes the inhibit signal to permit application of gate drive. Turning the triac on causes the voltage across it to drop and thus ends the gate pulse. If the latching current has not been attained, another gate pulse forms, but no discontinuity in the load current occurs.

Provision of Negative Gate Current

Triacs trigger with optimum sensitivity when the polarity of the gate voltage and the voltage at the main terminal 2 are similar (I^+ and II^- modes). Sensitivity is degraded when the polarities are opposite (I^- and III^+ modes). Although RCA triacs are designed and specified to have the same sensitivity in both I^- and III^+ modes, some other types have very poor sensitivity in the III^+ condition. Because the zero-voltage switch supplies positive gate pulses, it may not directly drive some higher-current triacs of these other types.

The circuit shown in Fig. 20(a) uses the negative-going voltage at terminal 3 of the zero-voltage switch to supply a negative gate pulse through a capacitor. The curve in Fig. 20(b) shows the approximate peak gate current as a function of gate voltage V_G. Pulse width is approximately 80 microseconds.

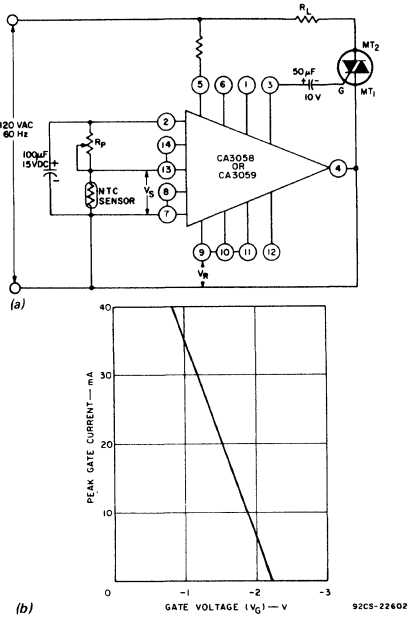


Fig. 20 – Use of the CA3058 or CA3059 to provide negative gate pulses: (a) schematic diagram; (b) peak gate current (at terminal 3) as a function of gate voltage.

Operation with Low-Impedance Sensors

Although the zero-voltage switch can operate satisfactorily with a wide range of sensors, sensitivity is reduced when sensors with impedances greater than 20,000 ohms are used. Typical sensitivity is one per cent for a 5000-ohm sensor and increases to three per cent for a 0.1-megohm sensor.

Low-impedance sensors present a different problem. The sensor bridge is connected across the internal power supply and causes a current drain. A 5000-ohm sensor with its associated 5000-ohm series resistor draws less than 1 milliampere. On the other hand, a 300-ohm sensor draws a current of 8 to 10 milliampers from the power supply.

Fig. 21 shows the 600-ohm load line of a 300-ohm sensor on a redrawn power-supply regulation curve for the zero-voltage switch. When a 10,000-ohm series resistor is used, the voltage across the circuit is less than 3 volts and both sensitivity and output current are significantly reduced. When a 5000-ohm series resistor is used, the supply voltage is nearly 5 volts, and operation is approximately normal. For more consistent operation, however, a 4000-ohm series resistor is recommended.

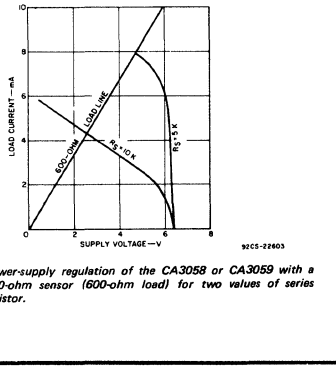


Fig. 21 – Power-supply regulation of the CA3058 or CA3059 with a 300-ohm sensor (600-ohm load) for two values of series resistor.

Although positive-temperature-coefficient (PTC) sensors rated at 5 kilohms are available, the existing sensors in ovens are usually of a much lower value. The circuit shown in Fig. 22 is offered to accommodate these inexpensive metal-wound

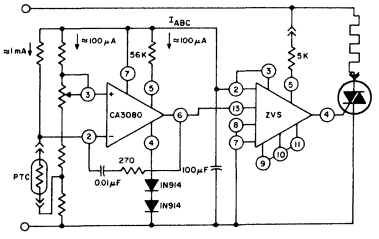


Fig. 22 – Schematic diagram of circuit for use with low-resistance sensor.

sensors. A schematic diagram of the RCA CA3080 integrated-circuit operational transconductance amplifier used in Fig. 22, is shown in Fig. 23. With an amplifier bias current, I_{ABC}, of 100 microamperes, a forward transconductance of 2 milliohms is achieved in this configuration. The CA3080 switches when the voltage at terminal 2 exceeds the voltage at terminal 3. This action allows the sink current, I_s, to flow from terminal 13 of the zero-voltage switch (the input impedance to terminal 13 of the zero-voltage switch is approximately 50 kilohms); gate pulses are no longer applied to the triac because Q_2 of the zero-voltage switch is on. Hence, if the PTC sensor is cold, i.e., in the low resistance state, the load is energized. When the temperature of the PTC sensor increases to the desired temperature, the sensor enters the high resistance state, the voltage on terminal 2 becomes greater than that on terminal 3, and the triac switches the load off.

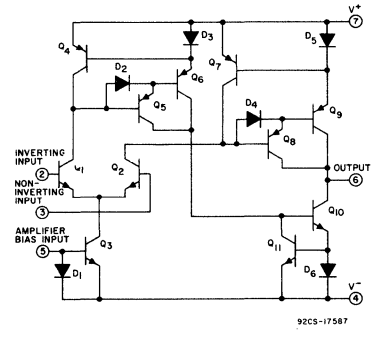


Fig. 23 – Schematic diagram of the CA3080.

Further cycling depends on the voltage across the sensor. Hence, very low values of sensor and potentiometer resistance can be used in conjunction with the zero-voltage switch power supply without causing adverse loading effects and impairing system performance.

Interfacing Techniques

Fig. 24 shows a system diagram that illustrates the role of the zero-voltage switch and thyristor as an interface between the logic circuitry and the load. There are several basic interfacing techniques. Fig. 25(a) shows the **direct input** technique. When the logic output transistor is switched from the on state (saturated) to the off state, the load will be turned on at the next zero-voltage crossing by means of the interfacing zero-voltage switch and the triac. When the logic output transistor is switched back to the on state, zero-crossing pulses from the zero-voltage switch to the triac

TEMPERATURE CONTROLLERS

Fig. 29 shows a triac used in an on-off temperature-controller configuration. The triac is turned on at zero voltage whenever the voltage V_s exceeds the reference

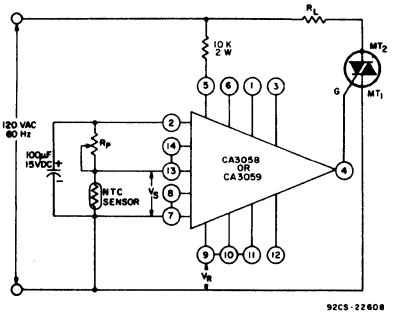


Fig. 29 – CA3058 or CA3059 on-off temperature controller.

voltage V_r. The transfer characteristic of this system, shown in Fig. 30(a), indicates significant thermal overshoots and undershoots, a well-known characteristic of such a system. The differential or hysteresis of this system, however, can be further increased, if desired, by the addition of positive feedback.

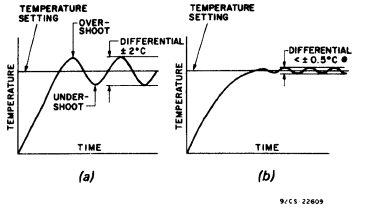


Fig. 30 – Transfer characteristics of (a) on-off and (b) proportional control systems.

For precise temperature-control applications, the proportional-control technique with synchronous switching is employed. The transfer curve for this type of controller is shown in Fig. 30(b). In this case, the duty cycle of the power supplied to the load is varied with the demand for heat required and the thermal time constant (inertia) of the system. For example, when the temperature setting is increased in an on-off type of controller, full power (100 per cent duty cycle) is supplied to the system. This effect results in significant temperature excursions because there is no anticipatory circuit to reduce the power gradually before the actual set temperature is achieved. However, in a proportional control technique, less power is supplied to the load (reduced duty cycle) as the error signal is reduced (sensed temperature approaches the set temperature).

Before such a system is implemented, a time base is chosen so that the on-time of the triac is varied within this time base. The ratio of the on-to-off time of the triac within this time interval depends on the thermal time constant of the system and the selected temperature setting. Fig. 31 illustrates the principle of proportional control. For this operation, power is supplied to the load until the ramp voltage reaches a value greater than the dc control signal supplied to the opposite side of the differential amplifier. The triac then remains off for the remainder of the time-base period. As a result, power is "proportioned" to the load in a direct relation to the heat demanded by the system.

For this application, a simple ramp generator can be realized with a minimum number of active and passive components. A ramp having good linearity is not required for proportional operation because of the nonlinearity of the

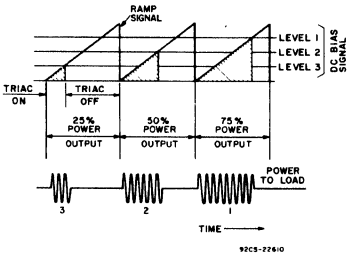


Fig. 31 – Principles of proportional control.

thermal system and the closed-loop type of control. In the circuit shown in Fig. 32, the ramp voltage is generated when the capacitor C_1 charges through resistors R_0 and R_1. The time base of the ramp is determined by resistors R_2 and R_3, capacitor C_2, and the breakover voltage of the D3202U* diac.

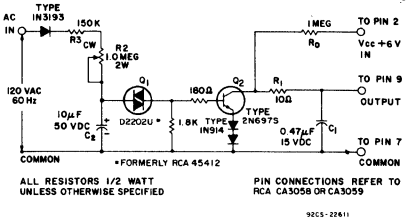


Fig. 32 – Ramp generator.

When the voltage across C_2 reaches approximately 32 volts, the diac switches and turns on the 2N697S transistor and 1N914 diodes. The capacitor C_1 then discharges through the collector-to-emitter junction of the transistor. This discharge time is the retrace or flyback time of the ramp. The circuit shown can generate ramp times ranging from 0.3 to 2.0 seconds through adjustment of R_2. For precise temperature regulation, the time base of the ramp should be shorter than the thermal time constant of the system, but long with respect to the period of the 60-Hz line voltage. Fig. 33 shows a triac connected for the proportional mode.

lag the incoming line voltage. The motors, however, are switched by the triacs at zero current, as shown in Fig. 34(b).

The problem of driving inductive loads such as these motors by the narrow pulses generated by the zero-voltage switch is solved by use of the sensitive-gate RCA-40526 triac. The high sensitivity of this device (3 milliamperes maximum) and low latching current (approximately 9 milliamperes) permit synchronous operation of the temperature-controller circuit. In Fig. 34(a), it is apparent that, though the gate pulse V_g of triac Y_1 has elapsed, triac Y_2 is switched on by the current through R_{L1}. The low latching current of the RCA-40526 triac results in dissipation of only 2 watts in R_{L1}, as opposed to 10 to 20 watts when devices that have high latching currents are used.

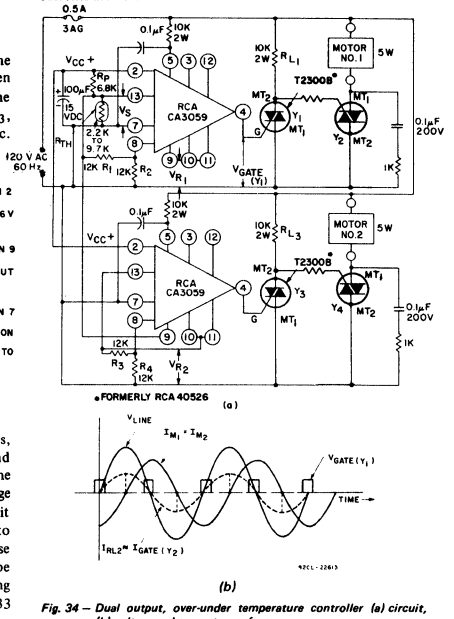


Fig. 34 – Dual output, over-under temperature controller (a) circuit, (b) voltage and current waveforms.

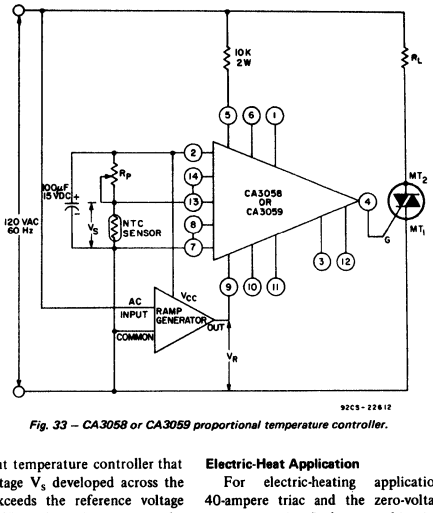


Fig. 33 – CA3058 or CA3059 proportional temperature controller.

Fig. 34(a) shows a dual-output temperature controller that drives two triacs. When the voltage V_s developed across the temperature-sensing network exceeds the reference voltage V_{R1}, motor No. 1 turns on. When the voltage across the network drops below the reference voltage V_{R2}, motor No. 2 turns on. Because the motors are inductive, the currents I_{M1}

Electric-Heat Application

For electric-heating applications, the RCA-2N5444 40-ampere triac and the zero-voltage switch constitute an optimum pair. Such a combination provides synchronous switching and effectively replaces the heavy-duty contactors which easily degrade as a result of pitting and wearout from

* Formerly RCA 45412

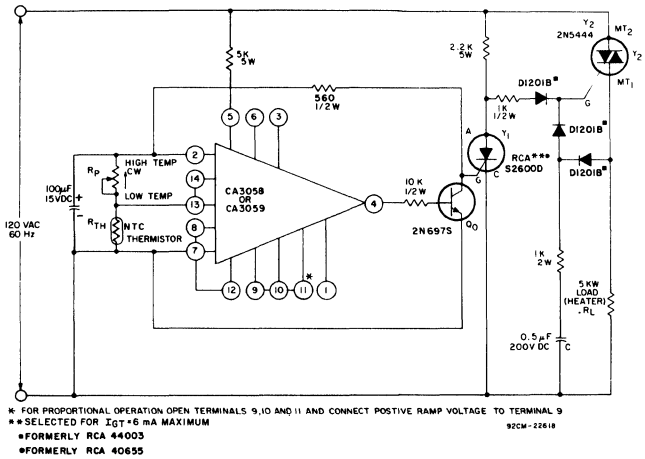


Fig. 39 – CA3058 or CA3059 integral-cycle temperature controller that features a protection circuit and no half-cycling effect.

When the ac line swings negative, capacitor C discharges through the triac gate to trigger the triac on the negative half-cycle. The diode-resistor-capacitor "slaving network" triggers the triac on negative half-cycle to provide only **integral cycles** of ac power to the load.

When the temperature being controlled reaches the desired value, as determined by the thermistor, then a positive voltage level appears at terminal 4 of the zero-voltage switch. The SCR then starts to conduct at the beginning of the positive input cycle to shunt the trigger current away from the gate of the triac. The triac is then turned off. The cycle repeats when the SCR is again turned OFF by the zero-voltage switch.

The circuit shown in Fig. 39 is similar to the configuration in Fig. 38 except that the protection circuit incorporated in the zero-voltage switch can be used. In this new circuit, the NTC sensor is connected between terminals 7 and 13, and transistor Q_0 inverts the signal output at terminal 4 to nullify the phase reversal introduced by the SCR (Y_1). The internal power supply of the zero-voltage switch supplies bias current to transistor Q_0.

Of course, the circuit shown in Fig. 39 can readily be converted to a **true proportional integral-cycle temperature controller** simply by connection of a positive-going ramp voltage to terminal 9 (with terminals 10 and 11 open), as previously discussed in this Note.

Thermocouple Temperature Control

Fig. 40 shows the CA3080A operating as a pre-amplifier for the zero-voltage switch to form a zero-voltage switching circuit for use with thermocouple sensors.

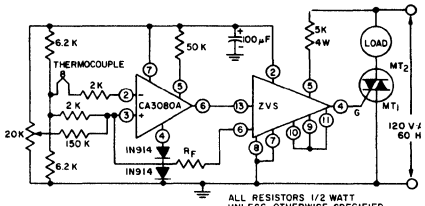


Fig. 40 – Thermocouple temperature control with zero-voltage switching.

Thermocouple Temperature Control with Zero-Voltage Load Switching

Fig. 41 shows the circuit diagram of a thermocouple temperature control system using zero-voltage load switching. It should be noted that one terminal of the thermocouple is connected to one leg of the supply line. Consequently, the thermocouple can be "ground-referenced", provided the appropriate leg of the ac line is maintained at ground. The comparator, A_1 (a CA3130), is powered from a 6.4-volt source of potential provided by the zero-voltage-switch (ZVS) circuit (a CA3079). The ZVS, in turn, is powered off-line through a series-dropping resistor R6. Terminal 4 of the ZVS provides trigger-pulses to the gate of the load-switching triac in response to an appropriate control signal at terminal 9.

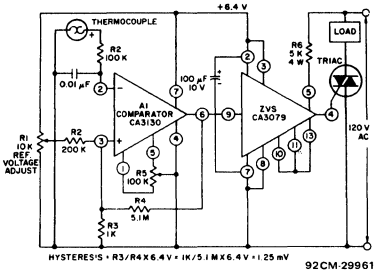


Fig. 41 – Thermocouple temperature control with zero-voltage switching.

The CA3130 is an ideal choice for the type of comparator circuit shown in Fig. 41 because it can "compare" low voltages (such as those generated by a thermocouple) in the proximity of the negative supply rail. Adjustment of potentiometer R1 drives the voltage-divider network R3, R4 so that reference voltages over the range of 0 to 20 millivolts can be applied to noninverting terminal 3 of the comparator. Whenever the voltage developed by the thermocouple at terminal 2 is more positive than the reference voltage applied at terminal 3, the comparator output is toggled so as to sink current from terminal 9 of the ZVS; gate pulses are then no longer applied to the triac. As shown in Fig. 41, the circuit is provided with a control-point "hysteresis" of 1.25 millivolts.

Nulling of the comparator is performed by means of the following procedure: Set R1 at the low end of its range and short the thermocouple output signal appropriately. If the triac is in the conductive mode under these conditions, adjust nulling potentiometer R5 to the point at which triac conduction is interrupted. On the other hand, if the triac is in the non-conductive mode under the conditions above, adjust R5 to the point at which triac conduction commences. The thermocouple output signal should then be unshorted, and R1 can be set to the voltage threshold desired for control-circuit operation.

MACHINE CONTROL AND AUTOMATION

The earlier section on interfacing techniques indicated several techniques of controlling ac loads through a logic system. Many types of automatic equipment are not complex enough or large enough to justify the cost of a flexible logic system. A special circuit, designed only to meet the control requirements of a particular machine, may prove more economical. For example, consider the simple machine shown in Fig. 42; for each revolution of the motor, the belt is advanced a prescribed distance, and the strip is then punched. The machine also has variable speed capability.

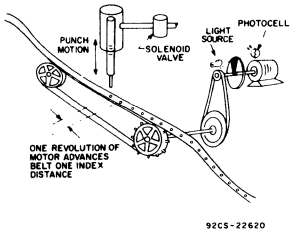


Fig. 42 – Step-and-punch machine.

The typical electromechanical control circuit for such a machine might consist of a mechanical cambank driven by a separate variable speed motor, a time delay relay, and a few logic and power relays. Assuming use of industrial-grade controls, the control system could get quite costly and large. Of greater importance is the necessity to eliminate transients generated each time a relay or switch energizes and deenergizes the solenoid and motor. Fig. 43 shows such transients, which might not affect the operation of this machine, but could affect the more sensitive solid-state equipment operating in the area.

A more desirable system would use triacs and zero-voltage switching to incorporate the following advantages:

a. Increased reliability and long life inherent in solid-state devices as opposed to moving parts and contacts associated with relays.

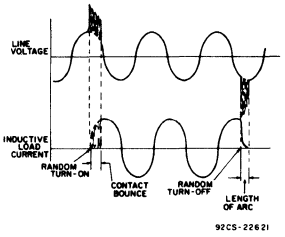


Fig. 43 – Transients generated by relay-contact bounce and non-zero turn-off of inductive load.

b. Minimized generation of EMI/RFI using zero-voltage switching techniques in conjunction with thyristors.
c. Elimination of high-voltage transients generated by relay-contact bounce and contacts breaking inductive loads, as shown in Fig. 42.
d. Compactness of the control system.

The entire control system could be on one printed-circuit board, and an over-all cost advantage would be achieved. Fig. 44 is a timing diagram for the proposed solid-state

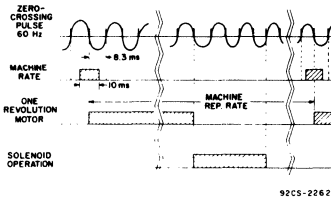


Fig. 44 – Timing diagram for proposed solid-state machine control.

SYNCHRONOUS LIGHT FLASHER

Fig. 50 shows a simplified version of the synchronous-switching traffic light flasher shown in Fig. 49.

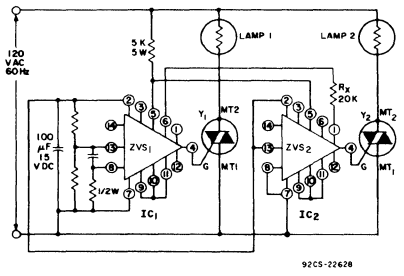


Fig. 50 – Synchronous light flasher.

Flash rate is set by use of the curve shown in Fig. 16. If a more precise flash rate is required, the ramp generator described previously may be used. In this circuit, ZVS_1 is the master control unit and ZVS_2 is slaved to the output of ZVS_1 through its inhibit terminal (terminal 1). When power is applied to lamp No. 1, the voltage of terminal 6 on ZVS_1 is high and ZVS_2 is inhibited by the current in R_x. When lamp No. 1 is off, ZVS_2 is not inhibited, and triac Y_2 can fire. The power supplies operate in parallel. The on-off sensing amplifier in ZVS_2 is not used.

TRANSIENT-FREE SWITCH CONTROLLERS

The zero-voltage switch can be used as a simple solid-state switching device that permits ac currents to be turned on or off with a minimum of electrical transients and circuit noise.

The circuit shown in Fig. 51 is connected so that, after the control terminal 14 is opened, the electronic logic waits until the power-line voltage reaches a zero crossing before power is applied to the load Z_L. Conversely, when the control terminals are shorted, the load current continues until it reaches a zero crossing. This circuit can switch a load at zero current whether it is resistive or inductive.

The circuit shown in Fig. 52 is connected to provide the opposite control logic to that of the circuit shown in Fig. 51. That is, when the switch is closed, power is supplied to the load, and when the switch is opened, power is removed from the load.

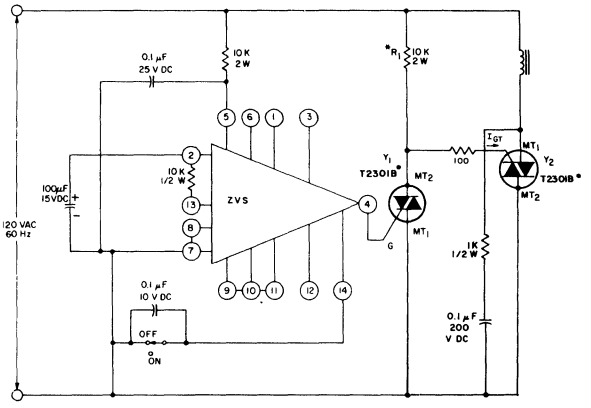
In both configurations, the maximum rms load current that can be switched depends on the rating of triac Y_2. If Y_2 is an RCA-2N5444 triac, an rms current of 40 amperes can be switched.

DIFFERENTIAL COMPARATOR FOR INDUSTRIAL USE

Differential comparators have found widespread use as limit detectors which compare two analog input signals and provide a go/no-go, logic 'one" or logic "zero" output, depending upon the relative magnitudes of these signals. Because the signals are often at very low voltage levels and very accurate discrimination is normally required between them, differential comparators in many cases employ differential amplifiers as a basic building block. However, in many industrial control applications, a high-performance differential comparator is not required. That is, high resolution, fast switching speed, and similar features are not essential. The zero-voltage switch is ideally suited for use in such applications. Connection of terminal 12 to terminal 7 inhibits the zero-voltage threshold detector of the zero-voltage switch, and the circuit becomes a differential comparator.

Fig. 53 shows the circuit arrangement for use of the zero-voltage switch as a differential comparator. In this application, no external dc supply is required, as is the case with most commercially available integrated-circuit comparators; of course, the output-current capability of the zero-voltage switch is reduced because the circuit is operating in the dc mode. The 1000-ohm resistor R_G, connected between terminal 4 and the gate of the triac, limits the output current to approximately 3 milliamperes.

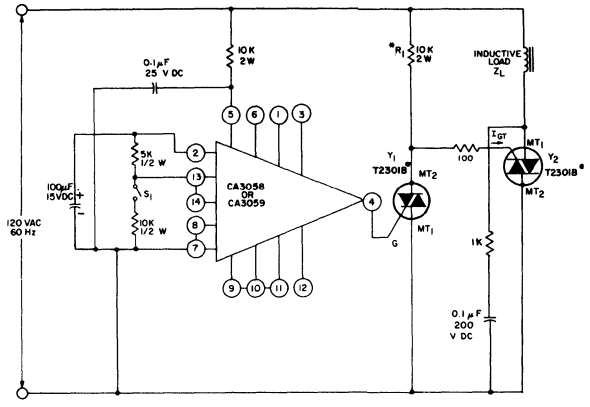
When the zero-voltage switch is connected in the dc mode, the drive current for terminal 4 can be determined from a curve of the external load current as a function of dc voltage



*IF Y_2, FOR EXAMPLE, IS A 40-AMPERE TRIAC, THEN R_1 MUST BE DECREASED TO SUPPLY SUFFICIENT I_{GT} FOR Y_2.

• FORMERLY RCA 40691

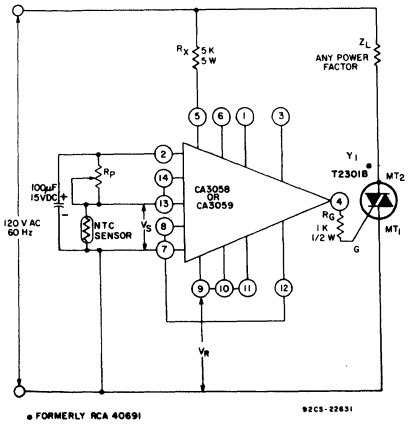
Fig. 51 – Zero-voltage switch transient-free switch controller in which power is supplied to the load when the switch is open.



*IF Y_2, FOR EXAMPLE, IS A 40-AMPERE TRIAC, R_1 MUST BE DECREASED TO SUPPLY SUFFICIENT I_{GT} FOR Y_2

• FORMERLY RCA 40691

Fig. 52 – Zero-voltage switch transient-free switch controller in which power is applied to the load when the switch is closed.



• FORMERLY RCA 40691

Fig. 53 – Differential comparator using the CA3058 or CA3059 integrated-circuit zero-voltage switch.

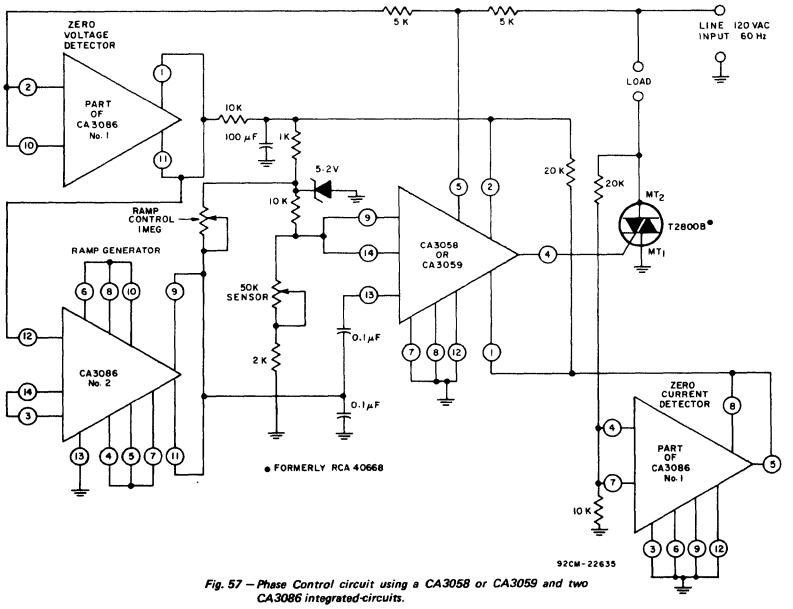


Fig. 57 – Phase Control circuit using a CA3058 or CA3059 and two CA3086 integrated-circuits.

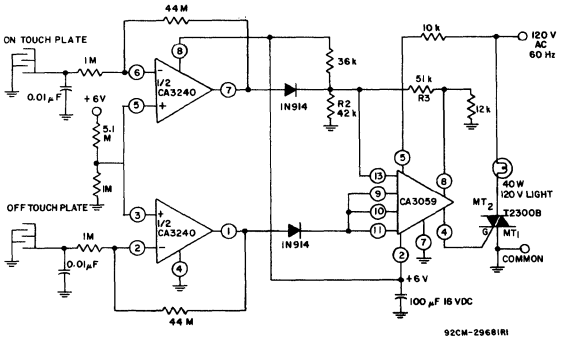


Fig. 58 – On-off touch switch.

control circuits. This signal must be electrically isolated from the three-phase power system.

3. Three separate triac gating signals are required.
4. For operation with resistive loads, the zero-voltage switching technique should be used to minimize any radio-frequency interference (RFI) that may be generated.

Isolation of DC Logic Circuitry

As explained earlier under **Special Application Considerations**, isolation of the dc logic circuitry* from the ac line, the triac, and the load circuit is often desirable even in many single-phase power-control applications. In control circuits for polyphase power systems, however, this type of isolation is essential, because the common point of the dc logic circuitry cannot be referenced to a common line in all phases.

In the three-phase circuits described in this section, photo-optic techniques (i.e., photo-coupled isolators) are used to provide the electrical isolation of the dc logic command signal from the ac circuits and the load. The photo-coupled isolators consist of an infrared light-emitting diode aimed at a silicon photo transistor, coupled in a common package. The light-emitting diode is the input section, and the photo transistor is the output section. The two components provide a voltage isolation typically of 1500 volts. Other isolation techniques, such as pulse transformers, magnetoresistors, or reed relays, can also be used with some circuit modifications.

Resistive Loads

Fig. 59 illustrates the basic phase relationships of a balanced three-phase resistive load, such as may be used in heater applications, in which the application of load power is controlled by zero-voltage switching. The following conditions are inherent in this type of application:

1. The phases are 120 degrees apart; consequently, all three phases cannot be switched on simultaneously at zero voltage.
2. A single phase of a wye configuration type of three-wire system cannot be turned on.
3. Two phases must be turned on for initial starting of the system. These two phases form a single-phase circuit which is out of phase with both of its component phases. The single-phase circuit leads one phase by 30 degrees and lags the other phase by 30 degrees.

These conditions indicate that in order to maintain a system in which no appreciable RFI is generated by the switching action from initial starting through the steady-state operating condition, the system must first be turned on, by zero-voltage switching, as a single-phase circuit and then must revert to synchronous three-phase operation.

Fig. 60 shows a simplified circuit configuration of a three-phase heater control that employs zero-voltage synchronous switching in the steady-state operating condition, with random starting. In this system, the logic command to turn on the system is given when heat is required, and the command to turn off the system is given when heat is not required. Time proportioning heat control is also possible through the use of logic commands.

The three photo-coupled inputs to the three zero-voltage switches change state simultaneously in response to a "logic command". The zero-voltage switches then provide a positive pulse, approximately 100 microseconds in duration, only at a zero-voltage crossing relative to their particular phase. A balanced three-phase sensing circuit is set up with the three zero-voltage switches each connected to a particular phase on their common side (terminal 7) and referenced at their high side (terminal 5), through the current-limiting resistors R4, R5, and R6, to an established artificial neutral point. This artificial neutral point is electrically equivalent to the inaccessible neutral point of the wye type of three-wire load and, therefore, is used to establish the desired phase relationships. The same artificial neutral point is also used to establish the proper phase relationships for a delta type of three-wire load. Because only one triac is pulsed on at a time, the diodes (D1, D2, and D3) are necessary to trigger the opposite-polarity triac, and, in this way, to assure initial latching-on of the system. The three resistors (R1, R2, and R3) are used for current limiting of the gate drive when the opposite-polarity triac is triggered on by the line voltage.

In critical applications that require suppression of all generated RFI, the circuit shown in Fig. 61 may be used. In addition to synchronous steady-state operating conditions, this circuit also incorporates a zero-voltage starting circuit. The start-up condition is zero-voltage synchronized to a single-phase, 2-wire, line-to-line circuit, comprised of phases A and B. The logic command engages the single-phase start-up zero-voltage switch and three-phase photo-coupled isolators OC13, OC14, OC15 through the photo-coupled

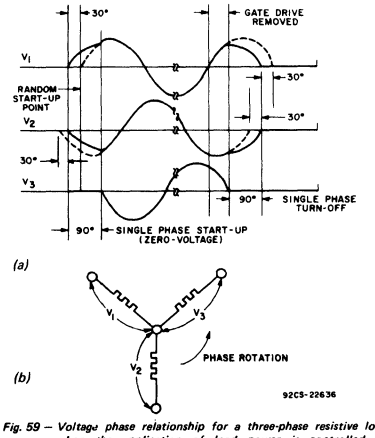


Fig. 59 – Voltage phase relationship for a three-phase resistive load when the application of load power is controlled by zero-voltage switching: (a) voltage waveforms, (b) load-circuit orientation of voltages. (The dashed lines indicate the normal relationship of the phases under steady-state conditions. The deviation at start-up and turn-off should be noted.)

* The dc logic circuitry provides the low-level electrical signal that dictates the state of the load. For temperature controls, the dc logic circuitry includes a temperature sensor for feedback. The RCA integrated-circuit zero-voltage switch, when operated in the dc mode with some additional circuitry, can replace the dc logic circuitry for temperature controls.

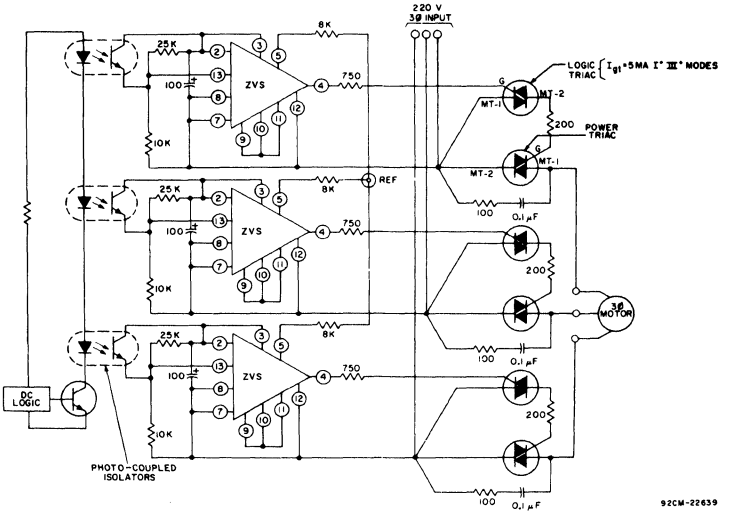


Fig. 62 – Triac three-phase control circuit for an inductive load, i.e., three-phase motor.

Considerations in Low-Noise Performance

Fig.5 shows the schematic diagram of a noise model useful in a review of the considerations pertinent to optimizing low-noise performance in amplifier operation.

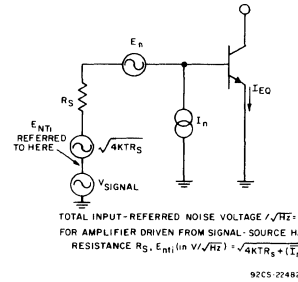


Fig. 5 – Sources of noise in the transistor-amplifier stage.

This model illustrates that consideration must be given to three major sources of noise:

1. Noise contributed by the "thermal-noise" voltage developed across the signal-source resistance, R_s. The magnitude of this voltage in $V/\sqrt{Hz}$ is approximately equal to $\sqrt{4KTR_s}$ for a 1-cycle bandwidth, where k is Boltzmann's constant (1.38 x 10^{-23} joule/°K), T is the temperature in degrees Kelvin, and R_s is the source resistance in ohms.
2. The noise voltage, E_n, resulting from the combined effects of shot noise due to emitter current flow and thermal noise due to transistor base resistance. These effects add in rms fashion to give a total E_n equal to $(E_{shot}^2 + 4KTr_b')^{1/2}$. The shot-noise component, E_{shot}, is inversely proportional to the square root of I_{EQ}, and has a value

$$E_{shot} = \frac{14.2 \times 10^{-12}}{\sqrt{I_{EQ}}} (V/Hz.)$$

   In super-beta transistors, the base resistance component of E_n tends to dominate, particularly at currents greater than 10 microamperes. In addition, this component of E_n has been experimentally found to be inversely related to operating current. Therefore, the total value of E_n is inversely related to operating current I_{EQ}. For example, the CA3095E has a total 1-kHz E_n of approximately 15 nV/$\sqrt{Hz}$ at a collector current of 5 microamperes and approximately 8 nV/$\sqrt{Hz}$ at 50 microamperes.
3. The noise current, I_n, resulting from the combined "shot noise" generated by the flow of base current and the 1/f noise generated in the transistor. The magnitude of I_n is approximately proportional to $\sqrt{I_{IB}}$, where I_{IB} is the base current. The value of I_n is typically 0.12 pA/$\sqrt{Hz}$ at f = 10 Hz when the super-beta differential-cascode amplifier in the CA3095E is operating at I_{EQ} = 5 μA. I_n decreases to approximately 0.03 pA$\sqrt{Hz}$ at f = 1 kHz.

When each input terminal in a differential amplifier is driven from a source resistance (R_s), the total noise voltage (referred to the input, see Fig. 5) per unit bandwidth is given by:

$$E_{nti}\ (in\ V/\sqrt{Hz}) = \sqrt{2KTR_s + 2(\overline{I_nR_s})^2 + (E_n)^2}$$

When amplifiers are driven from low source impedances, E_n is the predominant factor in noise contributions, whereas the effect of I_n predominates when input signals are supplied from high source impedances. Consequently, since the CA3095E operates with very high beta at very low operating currents, it has exceptionally low values of I_n, and is an excellent choice to amplify signals from high source resistances when low amplifier noise contribution is desired. Additionally, the incidence of "popcorn" (burst) noise[2] is low in the CA3095E, a characteristic which further enhances its suitability for use in amplifying signals supplied from high-impedance sources. Figs. 6 and 7 show typical data on I_n and E_n characteristics, respectively, as a function of frequency, for the super-beta transistors in the CA3095E.

Because the operating current of the super-beta transistors in the CA3095E is adjustable over a wide range, the circuit designer can optimize the operating current for maximum

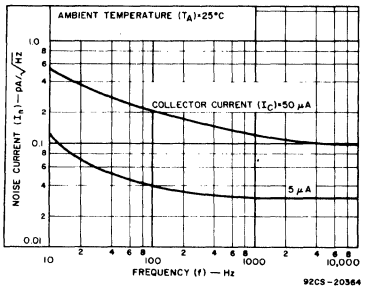


Fig. 6 – Noise current I_n as a function of frequency f for each super-beta cascode-amplifier transistor pair (Q_1 - Q_3 and Q_2 - Q_4).

signal-to-noise ratio at a particular frequency and source resistance. This adjustment is accomplished by selecting an operating point for which E_n is approximately equal to $\sqrt{2}\,I_n\,R_s$. For example, the optimum operating collector currents in the differential-cascode amplifier are about 5 microamperes when the amplifier is to be driven from two 300-kilohm source resistors. For operation from higher source resistances, the currents should be proportionately lower, and vice versa. Operating currents in the range from 0.1 to 1.0 milliampere are recommended when the amplifier is to be operated as a low-noise video amplifier. At these current levels, the gain-bandwidth product (f_T) is increased significantly with respect to low collector current operation.

ILLUSTRATIVE CIRCUIT APPLICATIONS

Like other RCA transistor-array IC's, the CA3095E offers the circuit designer a class of solid-state devices featuring matched electrical and thermal characteristics, compactness, ease of physical handling, economy, and versatility of use. The

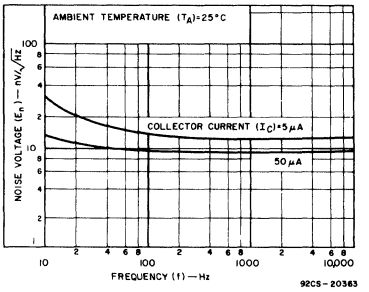


Fig.7 – Noise voltage E_n as a function of frequency f for each super-beta cascode-amplifier transistor pair (Q_1–Q_3 and Q_2–Q_4).

CA3095E is an electronic "building block" which permits the designer to optimize performance of a particular circuit for gain, noise, power consumption, bandwidth, and/or other specific considerations. Some typical circuit applications of the CA3095E are described below.

High-Input-Resistance Low-Noise Amplifier

The CA3095E contains all the transistors necessary for the construction of a low-noise, feedback amplifier having a high input resistance ($R_{IN} \cong 20$ MΩ) and a 3-dB bandwidth of about 50 kHz. In the circuit shown in Fig. 8, voltage gain is provided by a cascade of two stages, the differential-cascode stage (Q_1, Q_3 - Q_2, Q_4) and the differential stage (Q_7, Q_8). Transistor Q_6 is an interstage emitter-follower. The voltage gain of the amplifier (approximately 30 dB with the circuit values shown) is essentially established by the ratio of R_8 to the parallel combination of R_5 and R_6. The R_8, C_2 network couples feedback around the entire amplifier. Capacitor C_4 provides stabilizing compensation. The output-voltage swing (E_O) is typically 3 volts, peak-to-peak. Typical noise-figure data are shown in Fig. 8. Power consumption of the amplifier

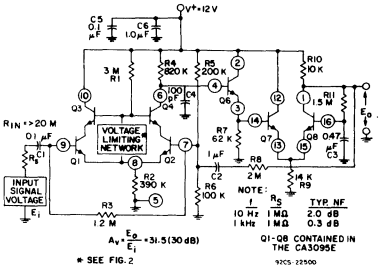


Fig. 8 – High-input-resistance, low-noise amplifier circuit.

is typically about 750 microamperes at a supply voltage of 12 volts, although the current in transistors Q_1 and Q_2 is less than 5 microamperes.

Low-Noise Video Amplifier

The circuit shown in Fig. 9 illustrates the use of super-beta transistors in the input stage of a video amplifier. The circuit is capable of delivering 4 volts, peak-to-peak, of output signal with a typical gain of 33 dB across a bandwidth from dc to 10 MHz (3-dB point). In this application, each super-beta transistor is biased for operation at about 400 microamperes to achieve wideband operation. The super-beta transistor characteristics minimize the contributions to noise generated by noise current (I_n) in the input stage. The equivalent input-noise-voltage-vs-frequency characteristics for the entire amplifier circuit are shown in Fig.10. Transistors Q_1 through Q_4 are connected as an emitter-coupled pair of cascode amplifiers with a single-ended load resistor, R_3, to drive a discrete transistor Q-PNP. This combination provides sufficient current gain to drive Q_6, the voltage-gain-stage transistor, with load resistor R_8. Resistor R_7 provides a path for dc and ac feedback around this stage. Transistor Q_8 is an emitter-follower output stage. The typical current drain of the amplifier is approximately 8 milliamperes at a total supply voltage of 10 volts.

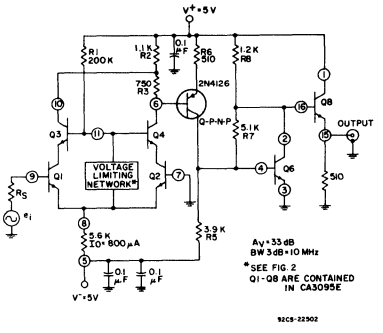


Fig. 9 – Video amplifier.

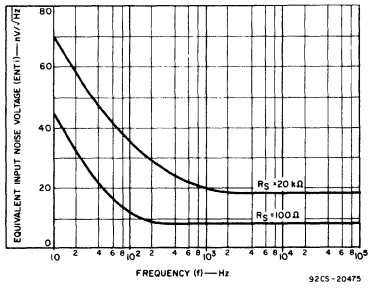


Fig. 10 – Equivalent input noise voltage vs frequency for the circuit of Fig. 9.

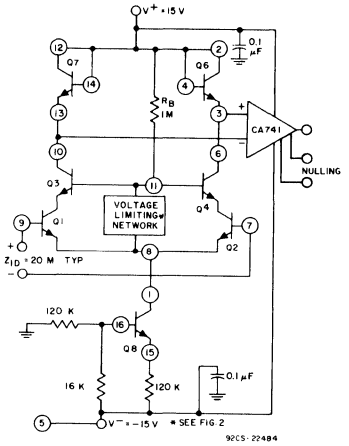


Fig. 14 – Op-amp with unity gain preamplifier.

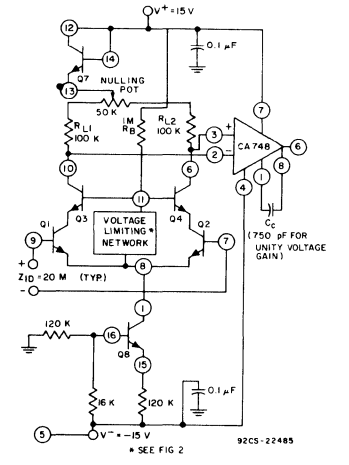


Fig. 15 – Op-amp with high-gain preamplifier.

reactance of the coupling capacitor C must be much lower than 5 megohms to achieve the high-input-impedance characteristic described above.) The low-drift, long-time-constant integrator circuit shown in Fig. 16(b) is another excellent application for the CA3095E super-beta transistor array. Because exceedingly low input bias currents permit the use of a high-value integrating resistor, R, without introducing substantial error, long-time-constant integration can be accomplished. The low input-offset-voltage drift characteristic of the super-beta transistors also contributes to low-error performance. Further reductions in error effects, particularly with temperature variation, can be achieved by using a temperature compensated bias-current source (e.g., R_1–R_3, D_1). In the circuit of Fig.15, such an arrangement could be implemented by using Q_6 in a diode connected fashion to serve as D_1. With such an arrangement, temperature-compensated bias current is applied to the inverting input terminal.

High-Input-Impedance DC-Voltmeter Circuit

The combination of a preamplifier circuit using the CA3095E in conjunction with a CA748 op-amp as described above is adaptable to dc-voltmeter circuits requiring high input impedance, as illustrated by the circuit of Fig. 17. An appropriate resistor-divider network is provided to develop a dc input signal at terminal 9 of the CA3095E with transistors Q_1 - Q_3 and Q_2 - Q_4 connected in the differential-cascode

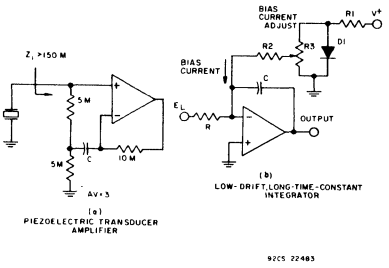


Fig. 16 – Typical super-beta op-amp applications:
(a) piezoelectric transducer amplifier
(b) low-drift, long-time-constant integrator.

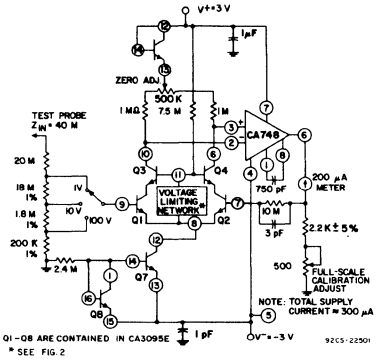


Fig. 17 – Typical high-input-impedance dc-voltmeter circuit.

arrangement. Biasing and dc feedback are applied at terminal 7 of the CA3095E through a 10-megohm resistor. The CA748 op-amp drives a 200-microampere meter calibrated in terms of the voltages to be measured. A full-scale reading occurs when the voltage applied to pin 9 is 500 millivolts dc. The entire circuit is nulled with the 500-kilohm zero-adjustment potentiometer. The total power-supply requirement is only 6 volts with a supply current of only 300 microamperes; this requirement can be met with batteries. The input impedance of this simple circuit is approximately 40 megohms on all scales.

Preamplifier for Tape-Head Signals

The exceptional low-noise characteristics of the CA3095E make it suitable for preamplifier service in professional-grade tape-playback systems. A typical circuit with equalization for NAB standards (7.5 in/s) is shown in Fig. 18. Transistors Q_1 and Q_3 are cascode-connected as the input stage, and transistor Q_6 is connected as a common-emitter post-amplifier. Transistors Q_2 and Q_4 are non-conductive because the emitter-base junction in Q_2 and the base-collector junction in Q_4 are shunted by external wiring. Equalization for the NAB tape-playback, frequency-response characteristics is provided by the R_1, C_1, C_2 network connected in the ac feedback path; DC feedback stabilization is provided by the path through resistor R_2. The amplifier has an over-all gain of about 37 db at 1 kHz, and can deliver output voltages in the order of 25 volts, peak-to-peak. The circuit configuration of Fig.18 is preferred to the differential-amplifier configuration because it limits the input-noise contribution to that of a single transistor (e.g., Q_1).

Preamplifier for Signals from Magnetic-Phonograph Cartridges

The exceptional low-noise characteristics of the CA3095E are also of great use in preamplifier service in equipment used to reproduce signals from magnetic phonograph cartridges. A typical circuit for this application with equalization for RIAA

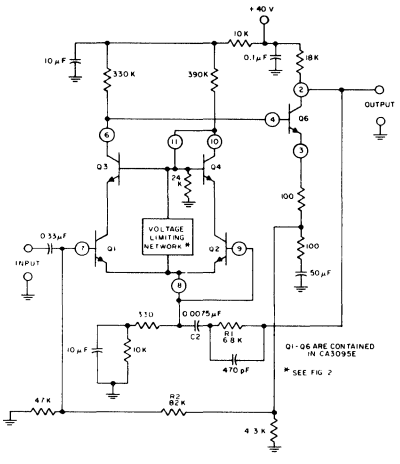


Fig. 18 – Tape play-back preamplifier equalized for NAB standards (7.5 in/s).

playback standards is shown in Fig. 19. Transistors Q_1 and Q_3 are cascode-connected as the input stage, and transistor Q_6 is connected as a common-emitter post-amplifier. Transistor Q_2 and Q_4 are non-conductive because the emitter-base junction in Q_2 and the base-collector junction in Q_4 are shunted by external wiring. Equalization for the RIAA phonograph-frequency-response characteristics is provided by the R_1, C_1 network connected in the ac feedback path. DC feedback stabilization is provided by the path through resistor R_2. The amplifier has an over-all gain of about 40 dB at 1 Hz, and can deliver output voltages in the order of 25 volts, peak-to-peak. The dynamic range of these circuits is typically about 95 dB with the gains indicated.

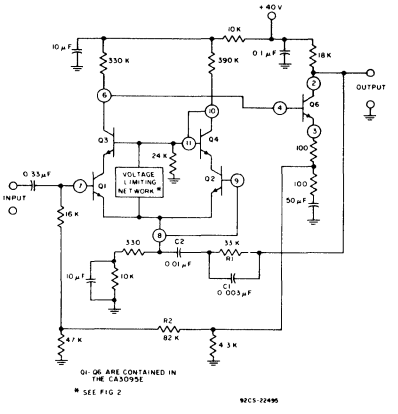


Fig. 19 – Preamplifier equalized for RIAA standards applicable to magnetic phonograph catridges.

ACKNOWLEDGMENT

The circuits of Figs. 18 and 19 were designed by L.A. Kaplan.

REFERENCES

1. "Super-Beta Transistor Array," CA3095E, RCA Data File No. 591.
2. "Measurement of Burst ("Popcorn") Noise in Linear Integrated Circuits," T. J. Robe, RCA Application Note ICAN-6732.
3. "Operational Amplifiers," RCA Data File No. 531.

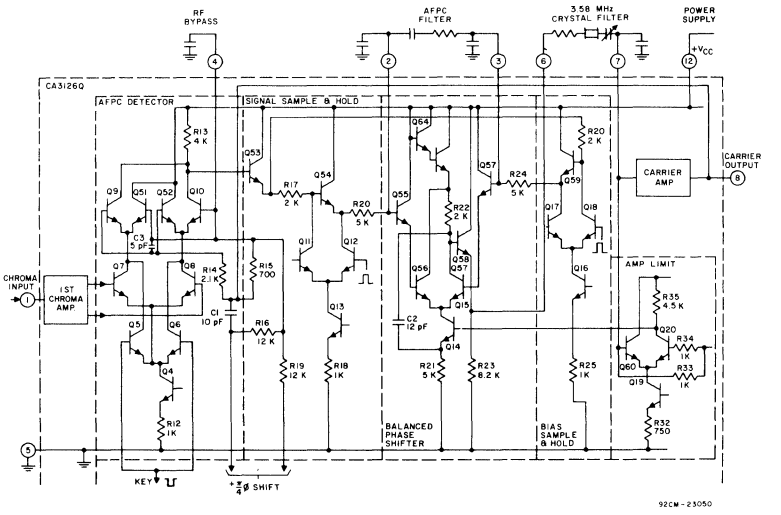


Fig. 3– Subcarrier regeneration circuit.

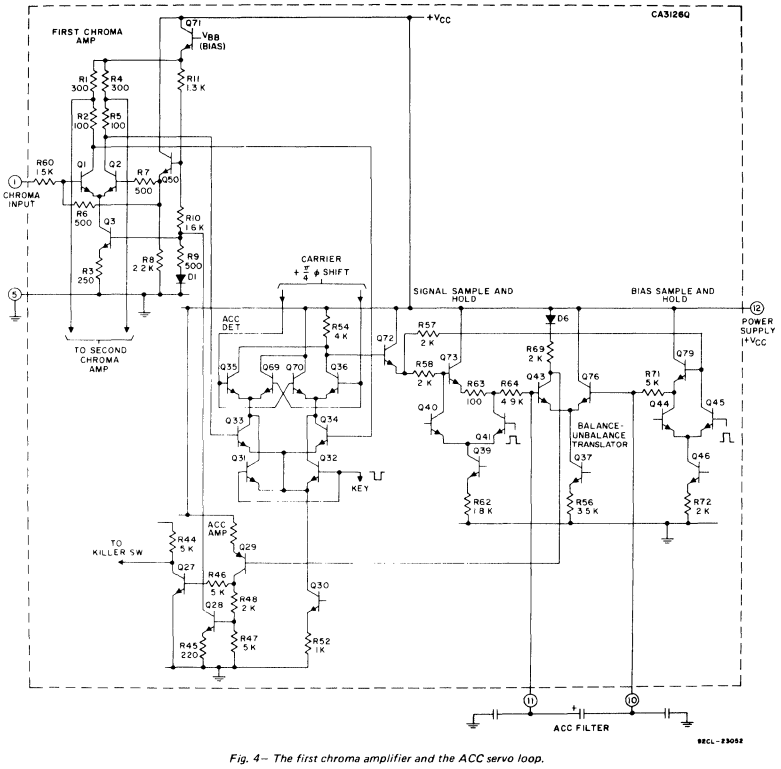


Fig. 4– The first chroma amplifier and the ACC servo loop.

detector from the switching pulses generated in the sampling circuits. The sample-and-hold action is accomplished by controlling the conduction current in transistor Q_{54} thus alternating the charge path during those intervals. During the sampling interval, transistor Q_{54} conducts and its emitter exhibits a relatively low impedance in comparison with the value of the integrated charging resistor R_{20}. The detected or sampled signal is stored in the AFPC filter capacitor which, with R_{20}, determines the time constant during this time interval. During the hold period, transistor Q_{54} is off and the filter time constant is several orders of magnitude larger than previously. The discharge of the filter capacitor is reduced to very small base bias currents only and little of the stored information is lost.

The "on" and "off" condition of the transistor Q_{54} is determined by the state of the transistor-pair Q_{11} and Q_{12}. During the "on" (sampling) interval, a signal from the horizontal rate keyer disables transistor Q_{11} and the collector current of the transistor Q_{12} maintains the transistor Q_{54} in the "on" condition. During the "off" (hold) period, transistors Q_{11} and Q_{12} change their states and the transistor Q_{54} is "off".

The bias sample-and-hold circuit, similar in structure to the above-described circuit, consists of the sampling switch Q_{59} and the transistor-pair Q_{17} and Q_{18}. This circuit, also activated by a signal from a horizontal rate keyer, samples the quiescent potential of the phase detector. The two signals, the error and the bias, processed by the sampling circuits, are stored in filter capacitors, and are applied to opposite terminals of a differential phase control. The phase control circuit synchronizes the reference carrier produced by the VCO.

Depending on the free-running frequency of the VCO, the detected signal is in the form of positive or negative going pulse trains which are then stored in a filter capacitor. The sampling switch has equal drive capabilities for both polarities of the signal; a requirement of particular importance in the presence of noise signals. Non-linear operation of the detector and sampling circuit would produce a rectified dc component causing an erroneous detuning of the VCO.

The VCO Loop

The amplification and amplitude limiting of the oscillator signal takes place in the amplifier-limiter formed by the transistor-pair Q_{60} and Q_{20}. The output from Q_{20} is fed to the dc controlled phase-shifter and returns to the amplifier through a crystal filter. The amplifier operates in a non-inverting mode, hence, the total phase shift through the phase-shifter plus crystal filter must be a multiple of 2π radians. The crystal filter is tuned to the subcarrier frequency and the filter band-width is determined by a resistor in series with the crystal. The DC controlled phase-shifter has a phase range of approximately $\pm \frac{\pi}{4}$ radians, and a phase change activated by a control signal results in a corresponding oscillator frequency change.

In the phase-shifter, the oscillator signal available at the collector of Q_{20} is applied to the base of Q_{14} from which it proceeds along two paths. An integrated capacitor C_2 couples this signal from the emitter of Q_{14} to the collector load of Q_{15} and, at this point, the signal is phase-shifted by approximately $\pi/4$ radians. In the second path, the signal arriving at the collector of Q_{15} passes through a current splitter formed by the transistor-pair Q_{56}, Q_{15}. This signal is reduced to a level determined by the control voltage at the bases of transistors Q_{56} and Q_{15}. At one extreme, transistor Q_{15} is OFF and the signal at the collector of Q_{15} arrives through the capacitor C_2 only. Conversely, with transistor Q_{15} ON, and Q_{56} OFF, the signal arriving through the transistor Q_{15} is phase-oriented so that the resultant signal has a phase of $+3/4\ \pi$ radians. The phase-control is linear throughout most of the control range.

A buffer amplifier is used to supply the CW carrier required for the demodulators, and the carrier is available at terminal 8. Internally, the buffer amplifier supplies the two synchronous detectors. Two R-C phase-shifters fed from the buffer amplifier provide the required phase orientation. A low-pass R_{14}-C_3 filter shifts the carrier to the AFPC detector by $-\pi/4$ while a high-pass filter provides a $+\pi/4$ oriented carrier for the ACC-killer detector.

AMPLITUDE CONTROL OF THE CHROMINANCE SIGNAL

Two cascaded amplifier stages serve to process the chroma signal and several signals are developed to control the gain of each stage.

First Chroma Amplifier and ACC Servo Loop

The first chroma amplifier, shown in Fig. 4, is controlled by the burst responsive ACC-killer detector only. The amplifier formed by the transistor-pair Q_1, Q_2 is driven single-ended by the applied composite chroma signal. The amplified output from this stage drives differentially the synchronous ACC-killer detector. The gain of the first amplifier is a function of the dc emitter current supplied by the constant current source Q_3. This current source is biased to provide a nominal current and, hence, a nominal gain in the first amplifier stage. The bias of the current source is reduced in response to a detected burst signal and the gain of the first stage diminishes correspondingly.

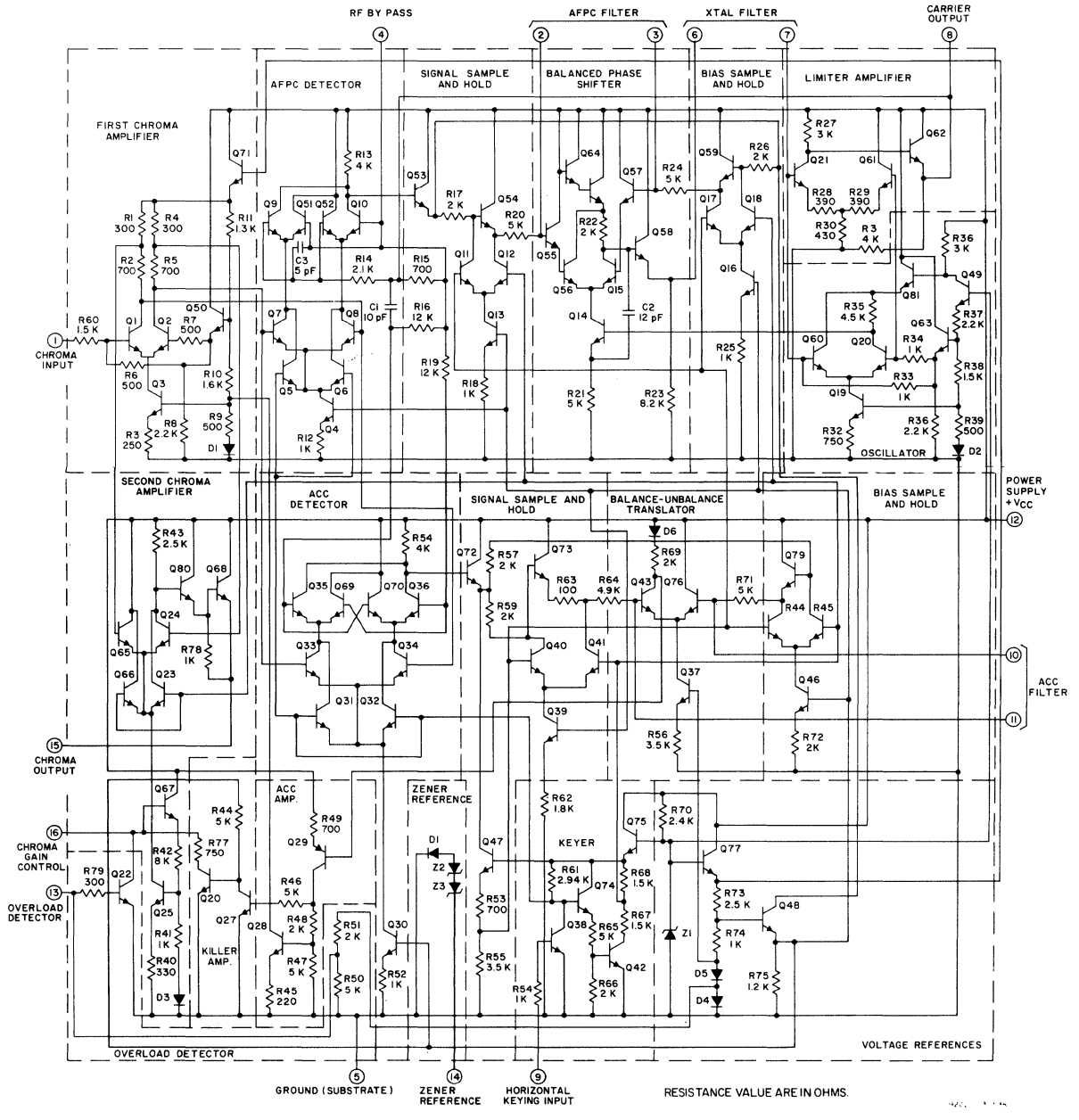


Fig. 7– Complete circuit diagram showing details of the keying circuit and internal bias circuits.

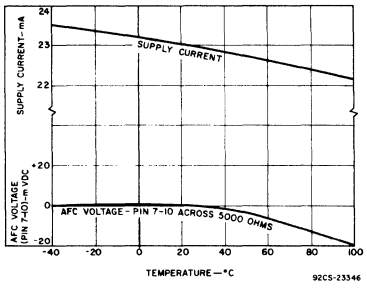
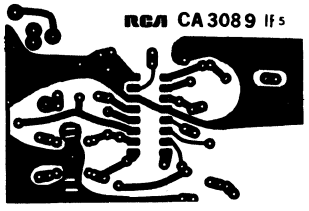


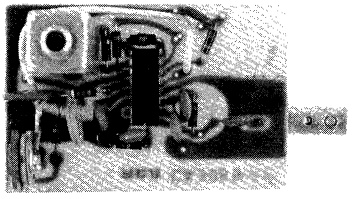
Fig. 7– Supply current and AFC voltage as a function of temperature.

exhibit inductive reactance at their terminals. The nominal input impedance of the CA3089E is approximately 9,000 ohms, and it is not recommended that an impedance match be attempted. Most commercial receivers use ceramic-filter frequency-selective elements that normally have source impedances of 500 ohms or less. When these filters are properly terminated with loading resistors, the typical source impedance is further decreased to 250 ohms or less. Higher levels of source impedance are possible with very careful circuit layout; however, the maintenance of stability could be difficult.

The CA3089E has a frequency response that is typically flat to 20 MHz; consequently, the device can provide useful gain well above that frequency. If the device is used at lower frequencies, the larger-value bypass capacitors required may not be adequate to bypass the higher frequencies. Double bypassing with lower-value capacitors can overcome such a problem. Another means of alleviating the problem is to externally reduce the frequency response by using a small capacitance across the output load of the device.



a) Bottom view of printed-circuit board.

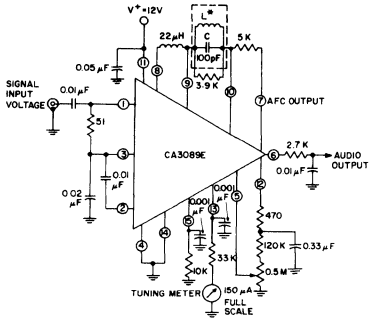


b) Component side — top view.

Fig. 8.– CA3089E and outboard components mounted on a printed circuit board.

Quadrature-Detector Circuits

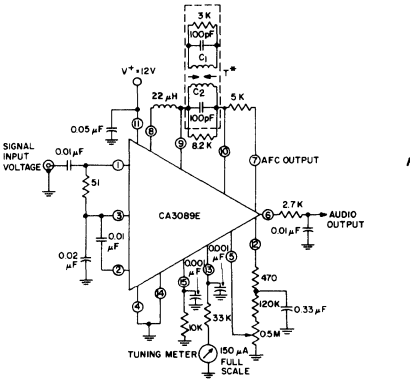
The quadrature-detector tuned circuit is connected between pins 9 and 10. The signal voltage at pin 8 is normally coupled to pin 9 through a choke. The circuit values for the detector network are determined by several factors, the primary one being distortion at a particular level of recovered audio. Distortion is determined by the phase linearity of the quadrature network and is not influenced by the device unless excessive, recovered audio overdrives the audio circuit. With a single tuned network, the phase linearity improves as the bandwidth increases; however, recovered audio decreases. A satisfactory compromise for most FM-receiver applications is reflected in the circuit of Fig. 9(a). This circuit typically provides 400 millivolts rms of recovered audio with less than 0.5-percent distortion. Because a double-tuned circuit has better phase linearity over a wider bandwidth, distortion figures of less than 0.1-percent are attainable with the network used in the circuit of Fig. 9(b). Proper alignment and coupling adjustment of the double-tuned circuit are most easily accomplished while viewing the resulting S curve. Initial adjustment of the primary tuning slug to the proper crossover is made with the secondary slug removed. The secondary tuning slug is then



ALL RESISTANCE VALUES ARE IN OHMS
*L TUNES WITH 100 pF (C) AT 10.7 MHz
Q_O(UNLOADED) ≅ 75 (G.I. AUTOMATIC MFG. DIV. EX22741 OR EQUIVALENT)

92CM-19040R1

(a)



ALL RESISTANCE VALUES ARE IN OHMS
*T: PRI. – Q_O(UNLOADED) ≅ 75 (TUNES WITH 100 pF (C1) 20 t OF 34 ø ON 7/32" DIA. FORM
SEC. – Q_O(UNLOADED) ≅ 75 (TUNES WITH 100 pF (C2) 20 t OF 34 ø ON 7/32" DIA. FORM
kQ (PERCENT OF CRITICAL COUPLING) ≅ 70 %
(ADJUSTED FOR COIL VOLTAGE V_C = 150 mV
ABOVE VALUES PERMIT PROPER OPERATION OF MUTE (SQUELCH) CIRCUIT
"E" TYPE SLUGS, SPACING 4 mm

92CM-19041R1

(b)

Fig. 9– (a) Test circuit for the CA3089E using a single-tuned detector coil, (b) test circuit for the CA3089E using a double-tuned detector coil.

adjusted until a slight "ripple" is observed moving along the S curve. If the ripple is excessive (enough to distort the S curve) the coupling is too tight. If no ripple is observed, the coupling is too loose. As the ripple moves through the crossover point, it will be observed that the S curve becomes more linear near the center frequency. Slight readjustment of both slugs may be necessary for final alignment. The best performance can then be achieved by slight adjustment while measuring distortion. The coupling may be varied by either moving the coils or by changing the value of the secondary load resistor.

Various circuit values can be used to obtain the same recovered audio, but the basic conditions of circuit bandwidth and phase linearity must be maintained. The detector circuit also sets up conditions which are required for proper operation of the mute circuit. The rf voltage on pin 9 must be held at approximately 175 millivolts rms, ±25 millivolts. The reason for this requirement is discussed subsequently in connection with the mute logic circuit. The approximate voltage at pin 9 is determined from the equivalent circuit shown in Fig. 10.

The peak-to-peak voltage on pin 9 is:

$$|V_9| \cong |V_8| \frac{R1}{\omega L_{ch}}$$

where R1 is the total parallel resistance and V8 is approximately 300 millivolts, peak-to-peak.

The Q of the tuned circuit between pins 9 and 10 may be affected by the effective Q of the choke between pins 8 and 9 and the series resistor R31 in the CA3089E. All of the above factors should be considered in selecting circuit values. Table I lists some typical combinations of component values under various conditions.

A choke is normally selected to equalize delays in the signal path and in the limiter–quadrature path. It also reduces the if harmonic content across the quadrature circuit. In some cases, such as in narrow-band applications, it may become necessary to use a capacitor as the coupling component where large values of inductance with high Q's are difficult to obtain. If a capacitor is used, the phase of the recovered audio and AFC voltage will be reversed, some asymmetry of the S curve may result, and the distortion may be adversely affected to a small degree.

As indicated above, the inductance between pins 8 and 9 tends to equalize delays in the detector signal paths. The matching of elements of the IC in the balanced detector

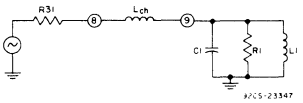


Fig. 10– Equivalent circuit used to determine approximate voltage on pin 9 of the CA3089E in Fig. 9.

circuit results in an AFC output with a very small offset when referred to the voltage at pin 10. For most applications, the inherent offset variation is well within tolerances, and does not affect circuit performance. In some narrow-band applications, however, the offset becomes more critical because of the very narrow bandwidth. In such situations, the combination of normal production variations of the device and the external circuit components results in receiver detuning when the AFC loop is closed. This detuning results in an increased distortion of the recovered audio. This distortion can be corrected with the addition of a variable capacitor from pin 8 to ground to provide phase compensation. The capacitor can be adjusted to provide zero AFC offset with minimum distortion. Generally, the offset is in one direction for a given set of conditions. The addition of a fixed capacitor will minimize variations sufficiently to satisfy many applications. A value of 5 picofarads is an effective value for the circuit of Fig. 9(a) with the recommended PC-board layout. Conversely, the offset created by using a capacitor between pins 8 and 9, as mentioned earlier, may be compensated by placing an inductance between pins 8 and 10.

Audio and AFC Circuits

The audio and AFC circuits are very similar, and both develop the same audio signal at their respective output terminals. The audio output voltage on pin 6 is developed across an internal, nominal, 5,000-ohm resistor (R49) connected to the 5.6-volt reference. In addition, the audio signal level can be attenuated by providing a direct current into pin 5 without any shift in its dc level. The audio output,

455 kHz without the use of external circuitry. The rf-AGC and mute logic circuits do not develop sufficient dc voltage

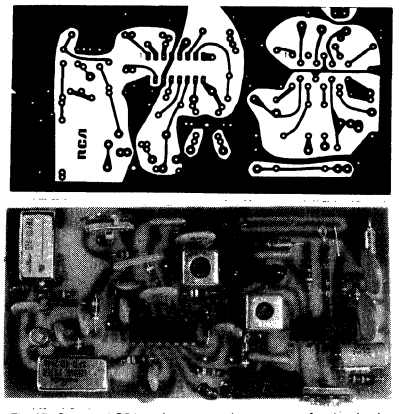


Fig. 15—Suggested PC-board pattern and parts layout for the circuit of Fig. 14.

to perform their functions, and the meter output signal loses its logarithmic characteristic and exhibits peaks and valleys as input signal is increased. Operation of the rf-AGC and mute logic circuits may be enhanced by the addition of a dc amplifier and inverter to each circuit. A simple example using a CA3096E IC transistor array is shown in Fig. 16.[3]

The CA3089E may be used effectively in narrow-band communication receivers. In double-conversion receivers, some of the functions of the CA3089E are negated at a 455-kHz intermediate frequency. However, if a 10.7-MHz intermediate frequency is used, all of the auxiliary features

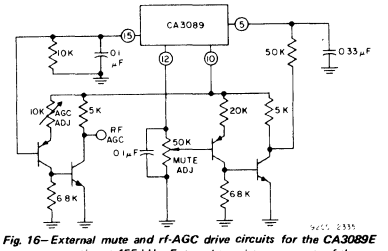


Fig. 16—External mute and rf-AGC drive circuits for the CA3089E operating at 455 kHz. External transistors are parts of the CA3096E n-p-n/p-n-p transistor array.

may be used, but another set of problems is encountered. The small deviation signals encountered in narrow-band systems require the use of high-Q circuits in the quadrature detector, as indicated in Table I. However, variations in external-component parameters with temperature changes may cause the tuned frequency of the detector to drift out of the if pass band. Normally temperature-compensated components are necessary. The CA3089E, operating in conjunction with an inexpensive operational transconductance amplifier,[4,5] provides means of locking the tuned circuit to the incoming frequency. Fig. 17 shows the block diagram of such a system. The AFC output voltage developed across the resistor between pins 7 and 10 is amplified by the op-amp and drives a varactor to maintain the tuned frequency on the incoming-signal frequency.

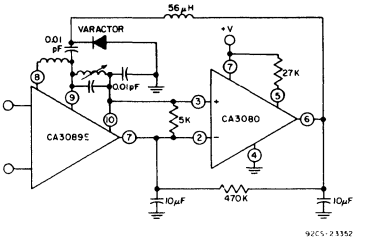


Fig. 17—Detector frequency-stabilization circuit.

The CA3089E may also be used as the core of an ultra-linear FM generator; Fig. 18 shows the circuit. The carrier is generated by the CA3089E with the introduction of feedback from the output terminal, pin 8. The carrier is modulated by the varactor connected across the tuned circuit at the input of the CA3089E. The varactor is driven by the output of the differential amplifier, A1, using a CA3028 IC.[6,7] This differential-amplifier stage is driven at one of its input terminals by the audio modulating signal. Negative feedback of the audio signal is provided by driving the other differential-amplifier input from the recovered audio output of the CA3089E at pin 6. The detector circuit uses a double-tuned transformer to produce audio with very little distortion at pin 6. This feedback technique results in a very low distortion modulation. The rf output of the CA3089E at pin 8 is essentially a square wave, and is fed to a tuned-amplifier stage to buffer the signal and restore the sine-wave-shaped rf output signal.

Acknowledgments

The author thanks Jack Craft for his aid and suggestions in many discussions and Frank Curley for his aid in circuit construction and collection of data.

Bibliography

1. "Advances in FM Receiver Design," J. Avins, IEEE Transactions on Broadcast and TV Receivers, Aug., 1971.
2. "High-Performance FM Receivers Using High-Gain Integrated-Circuit IF Amplifiers," T.J. Robe, L. Kaplan IEEE Transactions on Broadcast and TV Receivers, Sept. 1966.
3. RCA Data Bulletin, File No. 595: CA3096 NPN/PNP Transistor Array IC.
4. RCA Data Bulletin, File No. 475: CA3080 Operational Transconductance Amplifier.
5. "Applications of the CA3080 and CA3000A High-Performance Operational-Transconductance Amplifiers," H.A. Wittlinger, RCA Application Note ICAN-6668.
6. RCA Data Bulletin, File No. 382: CA3028A, Differential/Cascode Amplifiers.
7. "Application of the RCA CA3028A and CA3028B Integrated Circuit RF Amplifiers in the HF and VHF Ranges," RCA Application Note ICAN-5337.

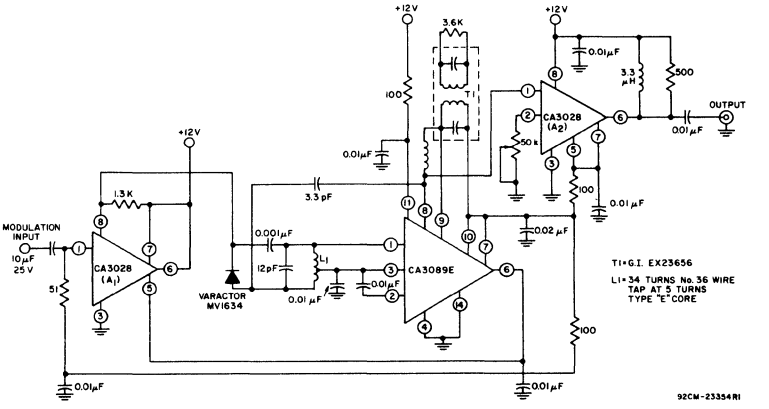


Fig. 18—FM generator circuit.

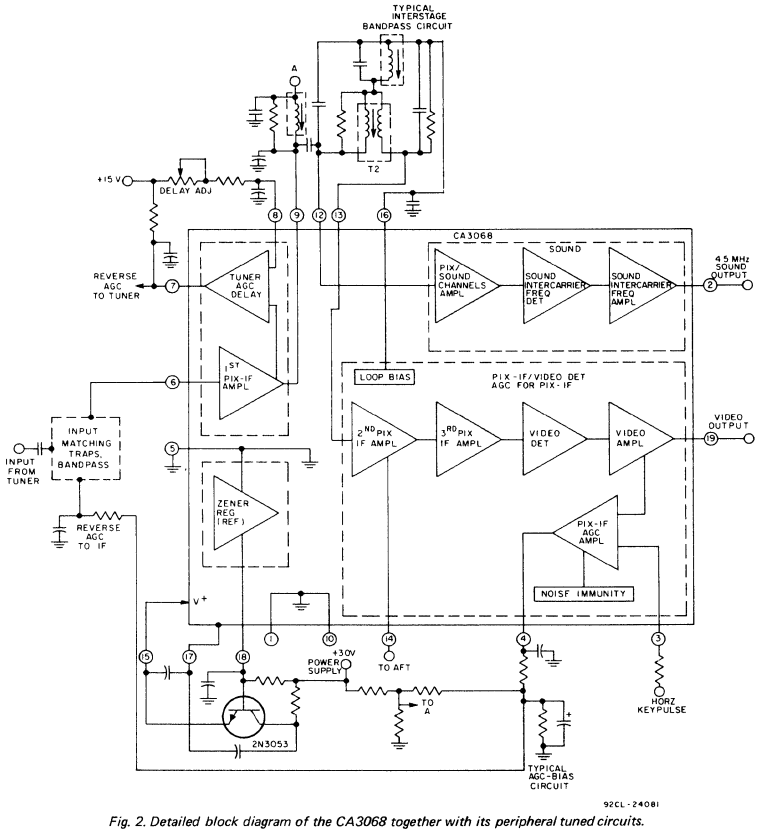


Fig. 2. Detailed block diagram of the CA3068 together with its peripheral tuned circuits.

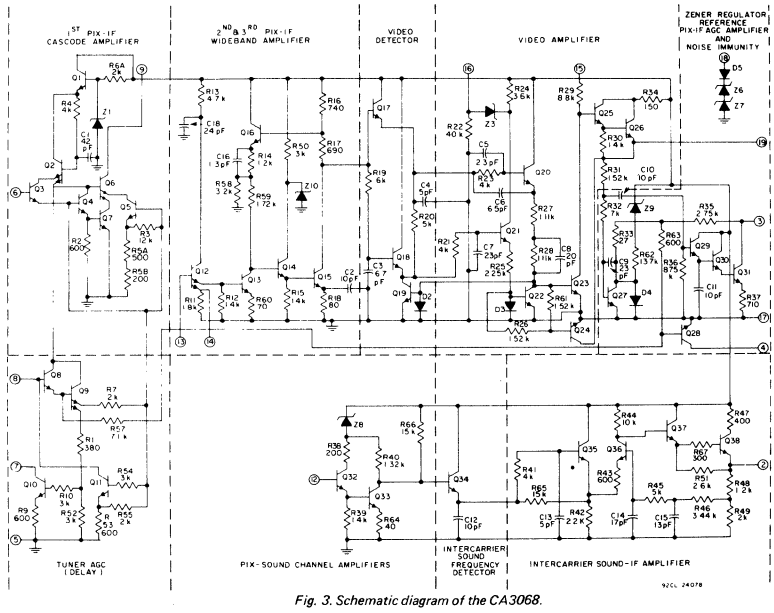


Fig. 3. Schematic diagram of the CA3068.

this composite waveform drive the keyed agc amplifier Q27, which in turn drives Q28. Without a video rf signal there is no video signal output, and Q27 conducts during the keying intervals (the horizontal pulse is connected to terminal 3). As the detected signal level increases in amplitude and the output voltage at terminal 19 approaches its typical operational level of 7 volts peak-to-peak, the peak potential at the base of Q27 begins to fall below 0.8 volt. Under these conditions, the keying current formerly channeled through Q27 is diverted through diode D4. As the signal level rises even higher, a greater portion of the Q27 collector current is diverted through D4, and the base current to Q28 is proportionately increased. A 10-microfarad capacitor is normally connected between terminal and ground and is, by this connection, put in shunt with Q28. The charge on this external capacitor is maintained through a bleeder resistor to V+. As the base current to Q28 increases, Q28 discharges the capacitor at a rate that is proportional to the base current of Q28. Integration of the total charge on the capacitor over the keying interval yields a dc level (agc voltage) that is inversely proportional to the incoming signal level; i.e., agc voltage approaches zero as the signal increases.

Any high-performance agc system must have noise-immunity characteristics in order to avoid the establishment of false agc levels. AGC developed from random noise can produce "wash-out", "blank raster" and/or a momentary "loss of sync". The CA3068 is designed with an improved noise-immunity circuit that essentially removes the keying current during periods of high noise input. The active devices responsible for providing protection against this deleterious effect of the impulse noise are the "noise detector", Q29, and the "noise clamp" Q31, which is driven by Q30. Impulse noise is channeled through the high-pass filter network consisting of C10 and R36 to the detector input Q29. Q29 and C11 comprise a conventional peak detector. The dc level across C11, which is proportional to the level of impulse noise, turn on Q30 and Q31, thereby clamping the keying supply voltage (terminal 3) to ground. In actual operation, the terminal-3 supply has a series resistance that is large enough to limit the peak current into the zener diode (Z5) to approximately 0.8 milliampere. When Q31 conducts, it shunts this current to ground.

The sound-if-channel and PIX-IF-channel signals whose "carrier" frequencies are 41.25 MHz and 45.75 MHz, respectively, are applied to terminal 12. Q32 functions as a buffer between the interstage-tuned-circuits associated with terminal 12 and the PIX/sound-channels amplifier, Q33. The intercarrier frequency (the difference frequency between the PIX and sound "carrier" frequencies) is detected by the peak detector Q34 and C12. The resultant 4.5 MHz FM sound-intercarrier signal is fed to transistor Q35. This transistor and Q36 form a differential pair that provides an amplified intercarrier sound-if signal to the base of Q37. A feedback system through the RC networks in the Darlington emitter-follower output of Q37 provides bandpass shaping in the region of 4.5 MHz while maintaining a low dc gain. The low level of dc gain is desirable because the circuit receives its bias in an open-loop manner from terminal 16. The bandpass of this amplifier system is fairly broad, and even though it is optimized for 4.5 MHz operation, there is relatively high output at other intercarrier frequencies, as shown in the curve in Fig. 4.

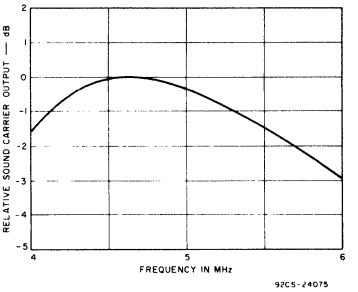


Fig. 4. Relative sound-carrier output as a function of frequency.

The internal zener reference-diode consists of the series diode arrangement shown connected between terminal 18 and the substrate in Fig. 3. A regulator-circuit configuration showing the

itor connected between terminal 4 and ground. An RC decoupling network smooths the age ripple associated with the charge and discharge of the 10-microfarad capacitor at the horizontal-oscillator frequency rate. The age system is normally keyed from the horizontal-output circuit in the TV system. This keying pulse should be applied to terminal 3. The magnitude of the pulse should be sufficient to supply a nominal peak current value of 0.8 milliampere into terminal 3. The value of the series resistor R_S associated with terminal 3 may be computed as follows: During the conduction period (with keying applied), the constant-voltage components within the integrated circuit account for:

$V_k = 8.2$ V

(It is assumed that I3 = 0.8 mA)

If the keying-pulse magnitude, V_p, is 15 V, then:

$$I3 = 0.8\ \text{mA} = \frac{15 \cdot V_k}{R_S} = \frac{(15 \cdot 8.2)\ \text{V}}{R_S}$$

$R_S = 8.5$ kilohms

The sound output is derived from terminal 2 at a level compatible with the input requirements of a TV-sound-if-subsystem IC, such as the RCA CA3065. There is also a dc component of approximately 6.7 volts present at terminal 2. Coupling networks to subsequent circuits must contain a suitable dc-blocking capacitor.

Small chokes located in the sound and video outputs (terminals 2 and 19) should be self-resonating at the intermediate frequencies to prevent if leakage into subsequent stages.

The CA3068 if subsystem has an internal zener reference-diode that permits operation of the subsystem with an external voltage-regulator pass transistor. A suggested circuit arrangement is shown as part of the over-all if schematic diagram in Fig. 5 (b). The voltage-regulator pass-transistor has a nominal output voltage of 11.2 volts. Bypassing of the V+ supply with reference to the if subsystem is important, and the suggested arrangement shown in the application circuit (Fig. 10) should be used. Specifically, terminal 15 should be bypassed to terminal 17 on the CA3068. Even though terminal 17 is at dc ground potential, it should not be tied to ground but rather should be bypassed in the manner shown to avoid mutual impedance coupling within the CA3068.

MONOCHROME TV

The delayed-age circuits used in the CA3068 were originally intended to control a MOSFET in the rf-stage of the TV tuner. This arrangement permits direct application of the delayed-age voltage from the CA3068 to the tuner. In monochrome receivers, however, it is common practice to employ a bipolar transistor in the rf-stage of the tuner, and a circuit with a "forward"-age characteristic is required to control the rf-stage. This characteristic is easily established by means of an inverter network utilizing a p-n-p transistor, as shown in the circuit of Fig. 9.

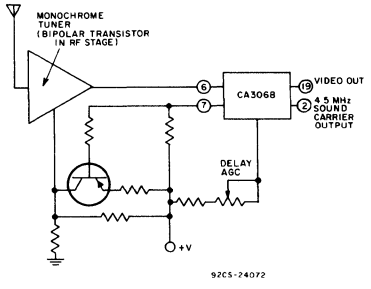


Fig. 9. Block diagram of an if system for a monochrome receiver showing peripheral age circuit.

As the input signal level increases, the forward-age delay voltage is developed at the tuner when the voltage at terminal 7 of the CA3068 decreases. The age voltage applied to the rf-stage of the tuner (Fig. 9) is derived from the collector of the p-n-p transistor. As the delay-age voltage is generated at terminal 7 of the CA3068, the base of the p-n-p inverter is driven into conduction, which causes more current to flow through the collector circuit, so that a positive (or forward) age potential is generated for the bipolar transistor in the tuner.

TV RECEIVER PIX–IF CIRCUIT APPLICATIONS

In this section, the application of the CA3068 integrated circuit in a color and a monochrome TV receiver is described. The circuits shown were constructed on single-sided copper PC boards.

As previously noted, because of the high gain encountered in PIX-IF design, positive feedback must be avoided if the amplifier is to remain free of spurious oscillation. To this end, the optimization of printed board layout and component placement is essential. The proper choice of bypassing components and signal-path layout is necessary to avoid feedback through ground loops.

IF CIRCUIT FOR COLOR TV RECEIVER

The schematic diagram of an if system for a color-TV receiver is shown in Fig. 10. A parts list and illustrations showing the PC-board component layout (top view) and the actual printed circuit (bottom view of board) are shown in Appendix A. Since most current color-TV receivers employ automatic-fine-tuning (AFT) systems, an AFT system using the CA3064 has also been included on the same board; Fig. 10 includes the AFT circuit.

The if-response is determined by the triple-tuned circuit, which consists of three traps: two preceding the IC and an interstage double-tuner circuit with one trap. In the tripled-tuned circuit, the two bridge-T traps are used to provide attenuation of the adjacent-channel picture carrier (frequency 39.75 MHz) and adjacent-channel sound carrier frequency (47.25 MHz). A

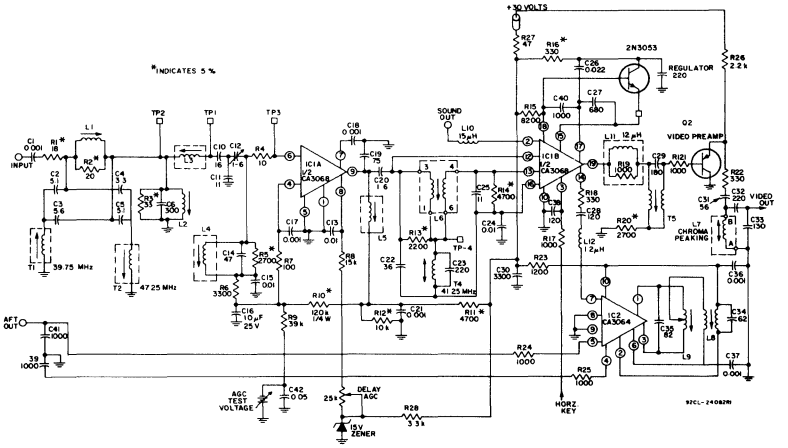


Fig. 10. Schematic diagram of a typical application of the CA3068 to a PIX-IF circuit for a color-TV system. A template of the printed circuit board used to construct this circuit, a diagram of the position of all components on the board, a block diagram of the location of major components on the board, and a circuit parts list are given in Appendix A.

common bridge impedance consisting of parallel-connected L1 and R2 is used. Adjustment of L1 for best null of the 47.25 MHz trap assures the desired 60-dB minimum attenuation.

The triple-tuned circuit provides, at center frequency, a source resistance to the IC of 800 ohms and a voltage gain of three from the input to pin 6 of the IC. The first section of the triple-tuned circuit consists of L2 and C6. Capacitor C6 is in parallel resonance with coil L2 at 44 MHz. The third section of the triple-tuned circuit consists of coil L4 and capacitor C14. Coupling and voltage-gain from L2 to L4 are provided by the second section, coil L3 and capacitors C10, C11, and C12. The inductive reactance of L3 is made 75 times larger than that of L2 to provide a high degree of tuned-circuit isolation for ease of alignment.

The circuit provides protection against interference resulting from a strong rf signal which might inadvertently be introduced between the tuner and the if stage. Parasitic resonance and couplings have been minimized to maintain a high degree of attenuation at frequencies remote from the if-resonance frequency.

The interstage double-tuned bandpass circuit, with a bifilar T-trap at 41.25 MHz, is similar to that commonly used in the third stage of color-TV receivers. The sound and picture carriers are present at the input (terminal 12) to the 4.5 MHz sound-if detector circuit. Trapping action removes the 41.25 MHz sound carrier at terminal 13 to prevent a difference-frequency beat of 0.92 MHz with the chroma subcarrier at 42.17 MHz. The picture carrier and chroma subcarrier entering terminal 13 are amplified, detected, and additionally amplified as detected video signal. If the sound carrier is not attenuated by the 41.25 MHz trap, the carrier will be detected as a large 4.5 MHz difference-signal in the video output. A 4.5 MHz trap (T5) is included to prevent interference of a residual 4.5 MHz intercarrier signal in the chroma and luminance circuits.

The chroma peaking circuit compensates for the slope of the video response, as shown in Figs. 11 (a), 11 (b) and 11 (c). The actual slope and shape of the video response between 3.08 MHz and 4.08 MHz will vary because of normal component tolerance. The chroma-peaking coil, L7, has two cores, one to adjust inductance to center the response at 3.58 MHz, and the other to adjust chroma output level and bandwidth. The latter core controls circuit Q with little effect on over-all inductance.

Photographs of the detected sweep-response characteristics are shown in Fig. 12. The sweep-response of Fig. 12 (f) shows the interstage alignment from TP3 (of Fig. 10) to terminal 9 of the CA3068. The sweep-response curves in Figs. 12 (a) through 12 (e) show 60 dB of age range from a level of 100 microvolts (Fig. 12 (e)) to 100 millivolts (Fig. 12 (a)).

The alignment procedure for the color-TV PIX-IF system using the CA3068, Fig. 10, is given in Appendix A.

IF CIRCUIT FOR MONOCHROME TV RECEIVER

The schematic diagram for a PIX-IF system for a monochrome TV system that employs the CA3068 is shown in Fig. 13. A PC-board component-layout diagram (top view), the actual printed circuit (bottom view of board), and a circuit parts list are shown in Appendix B. A sound-if system using the CA3065 has been included to show the simplicity with which it can be used in conjunction with the CA3068.

The selectivity is provided in two sections, an input single-tuned circuit with trap, and a double-tuned interstage circuit. The resistive pad, R1, R2, and R3 of Fig. 13, is used to terminate the link-cable and isolate cable effects from the high-Q input circuit. The bridge-T trap-circuit is used to give maximum attenuation to the adjacent-channel sound carrier. Precision components (R2, C1, C2) achieve a good null at 47.25 MHz

Although this Application Note describes subsystem designs in TV receivers, the CA3068 is also applicable in AM communications systems requiring performance at frequencies within the range of 10 to 70 MHz.

REFERENCES

1. RCA Data Bulletin File No. 396 concerning the CA3064 and CA3064E, "TV Automatic Fine Tuning Circuit", or the RCA DATABOOK, 1975 Series SSD-201C.
2. RCA Data Bulletin File No. 412 concerning the CA3065, "TV IF Sound System", or the RCA DATABOOK, 1975 Series SSD-201C.
3. RCA Data Bulletin File No. 467 concerning the CA3068, "Television Video IF System", or the RCA DATABOOK, 1975 Series SSD201C.

APPENDIX A – THE COLOR CIRCUIT

ALIGNMENT PROCEDURE FOR THE COLOR CIRCUIT

Preliminary Adjustments and Calibration

1. Adjust delay-agc (noise pot) fully cw.
2. Connect supplies as indicated on schematic diagram (Fig. 10), set bias to zero.
3. Set sweep generator to 10 millivolts as indicated on Boonton 91DA meter with 56-ohm termination.

Step 1 - IF Interstage Alignment

a. Ground TP1 with short clip lead.
b. Connect sweep generator with 56-ohm termination and 1000-picofarad decoupling capacitor to TP3.
c. Connect oscilloscope to video output.
d. Adjust bias for 5-volt peak-to-peak response on oscilloscope.
e. Adjust bottom core of T4 for minimum at 41.25 MHz.
f. Adjust L5 and L6 for symmetrical response with PIX and color markers equal (Fig. 12 (a)): L5 controls markers and L6 controls tilt.
g. Adjust top and bottom cores of T4 simultaneously, top core for maximum rejection of 41.25 MHz and bottom core to maintain minimum 41.25 MHz.

Step 2 - IF Overall Alignment

a. Leave ground clip lead on TP1.
b. Remove sweep input from TP3.
c. Connect TP2 through a 1000-picofarad capacitor to TP3.
d. Connect sweep generator to input.
e. Readjust variable bias to maintain 5-volts peak-to-peak response on oscilloscope.
f. Adjust T1 for minimum 39.75 MHz.
g. Adjust T2 for minimum 47.25 MHz.
h. Adjust L2 for equal height of PIX and color markers.
i. Remove ground-clip lead from TP1 and 1000-picofarad capacitor from between TP2 and TP3.
j. Maintain 5-volts peak-to-peak response on oscilloscope by re-adjusting bias.
k. Adjust L3 and L4 simultaneously for symmetrical response with PIX and color markers equal: L4 controls markers and L3 controls tilt.
l. Adjust bandpass trimmer, C12, to place PIX and color markers at 40 percent while readjusting L3 and L4 (Fig. 12 (b)).
m. Re-adjust T1 for minimum at 39.75 MHz if necessary.
n. Re-adjust T2 for minimum at 49.25 MHz. Then adjust L2 to maximize the rejection at 47.25 MHz.

AFT Alignment

a. With oscilloscope on AFT output, adjust bias for 10-volts peak-to-peak response.
b. Adjust L8 for maximum 45.75 MHz.
c. Adjust L9 for crossover at 45.75 MHz.
d. Re-adjust L8 and L9 to obtain symmetry.
e. Adjust L8 to obtain maximum width.

Color-Circuit Parts List

Capacitors		Resistors (All values in ohms)	
C1	0.001μF	R1	18
C2	5.1pF	R2	20
C3	5.6pF	R3	33
C4	3.3pF	R4	10
C5	5.1pF	R5	2.7k
C6	300pF	R6	3.3k
C10	16pF	R7	100
C11	11pF	R8	15k
C12	1-6pF	R9	39k
C13	0.01μF	R10	120k
C14	47pF	R11	4.7k
C15	0.01μF	R12	10k
C16	10μF	R13	2.2k
C17	0.001μF	R14	4.7k
C18	0.001μF	R15	8.2k
C19	7.5pF	R16	330
C20	1.6pF	R17	1k
C21	0.001μF	R18	330
C22	3.6pF	R19	1k
C23	220pF	R20	2.7k
C24	0.01μF	R21	1k
C25	11pF	R22	330
C26	0.022μF	R23	1.2k
C27	680pF	R24	1k
C28	120pF	R25	1k
C29	180pF	R26	2.2k
C30	0.022μF	R27	47
C31	56pF	R28	3.3k
C32	220pF	R29	25k
C33	130pF		
C34	62pF		
C35	82pF		
C36	0.001μF		
C40	1000pF		
C41	1000pF		
C42	1000pF		

Inductors	RCA Stock No.
L1	132159
L2	132161
L3	132839
L4	132658
L5	137126
L6	132146
T1	132839
T2	132157
T4	132150
T5	132135

APPENDIX B – THE MONOCHROME CIRCUIT

ALIGNMENT PROCEDURE FOR THE MONOCHROME-CIRCUIT

Step 1 -

1. Connect +20 volts to appropriate points on board.
2. Connect sweep generator to input
3. Connect dc bias voltage to appropriate point on board.
4. Adjust sweep generator for 10-millivolt input.
5. Adjust bias voltage for 5-volt, peak-to-peak output.

Step 2 -

1. Adjust LT for minimum response at 47.25 MHz.
2. Adjust L2 for maximum at 44.5 MHz.
3. Adjust L6, L7 for bandpass shown in Fig. 14 (b). The curve should have 3-MHz bandwidth centered at 44.5 MHz.

Monochrome-Circuit Parts List

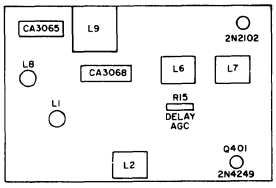
Capacitors	
C1	3.0pF
C2	3.0pF
C3	6.8pF
C4	3.9pF
C5	0.001μF
C6	12μF
C7	0.001μF
C8	0.001μF
C9	6.8pF
C10	0.01μF
C11	20pF
C12	15pF
C13	0.001μF
C14	18pF
C15	0.01μF
C16	0.001μF
C17	0.001μF
C18	5μF
C19	4700pF
C20	68pF
C21	12pF
C22	4pF
C23	82pF
C24	0.047μF
C25	0.047μF
C26	0.01μF
C27	0.047μF

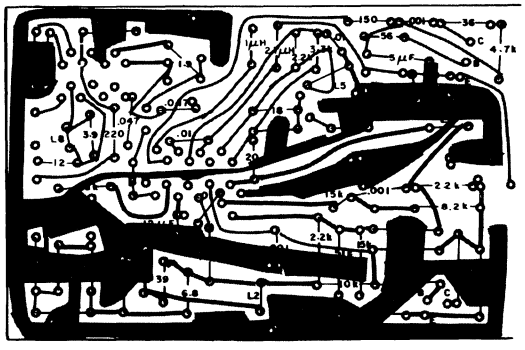
Inductors	RCA Stock No.
L1	131655
L2	133463
L3	1.0μH
L4	12.0μH
L5	134754*
L6	131465
L7	133546
L8	130120
L9	130121

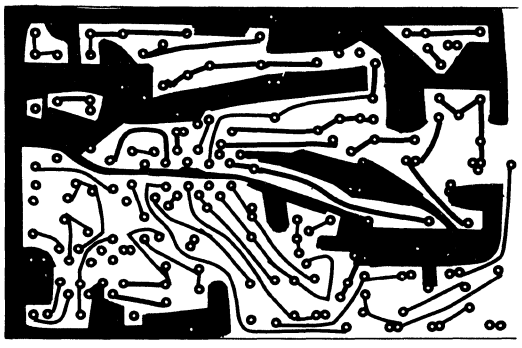
*(9 turns No. 23 wire; use 1/2 W resistor to form coil)

Resistors (All values in ohms)	
R1	18
R2	27
R3	91
R4	15k
R5	3.3k
R6	10k
R7	1.0k
R8	33k
R9	51k
R10	270
R11	2.2k
R12	120k
R13	2.2k
R14	15k
R15	25k
R16	8.2k
R17	2.2k
R18	3.3k
R19	150
R20	56
R21	36
R22	220
R23	5.6k

THE MONOCHROME CIRCUIT







figuration is used to minimize capacitive feed-through coupling via the base-collector junction of the p-n-p transistor.

Another multiplex system using the OTA's clocked by a COS/MOS flip-flop is shown in Fig. 6. The high output voltage capability of the COS/MOS flip-flop permits the circuit to be driven directly without the need for p-n-p level-shifting transistors.

A simple RC phase-compensation network is used on the output of the OTA in the circuits shown in Figs. 5 & 6. The values of the RC-network are chosen so that $\frac{1}{2\pi RC} \cong 2\text{MHz}$.

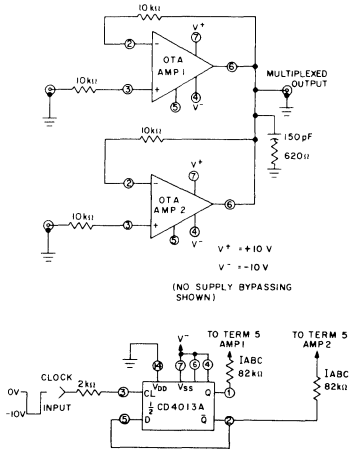


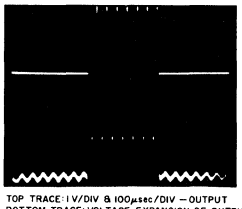
Fig. 6– Schematic diagram of a two-channel linear multiplex system using a COS/MOS flip-flop to gate two OTAs.

This RC-network is connected to the point shown because the lowest-frequency pole for the system is usually found at this point. Fig. 7 shows an oscilloscope photograph of the multiplex circuit functioning with two input signals. Fig. 8



TOP TRACE: MULTIPLEXED OUTPUT 1V/DIV & 100μsec/DIV
BOTTOM TRACE: TIME EXPANSION OF SWITCHING BETWEEN INPUTS 2V/DIV & 5μsec/DIV

Fig. 7– Voltage waveforms for circuit of Fig. 6; top trace: multiplexed output; lower trace: time expansion of switching between inputs.



TOP TRACE: 1V/DIV & 100μsec/DIV – OUTPUT
BOTTOM TRACE: VOLTAGE EXPANSION OF OUTPUT 1mV/DIV & 100μsec/DIV ISOLATION IS IN EXCESS OF 80 db

Fig. 8– Voltage waveforms for circuit of Fig. 6; top trace: output; lower trace: voltage expansion of output; isolation in excess of 80 dB.

shows an oscilloscope photograph of the output of the multiplexer with a 6-V p-p, sine wave signal (22 kHz) applied to one amplifier and the input to the other amplifier grounded. This photograph demonstrates an isolation of at least 80 dB between channels.

Sample-and-Hold Circuits

An extension of the multiplex system application is a sample-and-hold circuit (Fig. 9), using the strobing characteristics of the OTA amplifier bias-current (ABC) terminal as a means of control. Fig. 9 shows the basic system using the CA3080A as an OTA in a simple voltage-follower configuration with the phase-compensation capacitor serving the additional function of sampled-signal storage. The major consideration for the use of this method to "hold" charge is that neither the charging amplifier nor the signal readout device significantly alter the charge stored on the capacitor. The CA3080A is a particularly suitable capacitor-charging amplifier because its output resistance is more than 1000 MΩ under cut-off conditions, and the loading on the storage capacitor during the hold-mode is minimized. An effective solution to the read-out requirement involves the use of an RCA 3N138 insulated-gate field-effect transistor (MOS/FET) in the feedback loop. This transistor has a maximum gate-leakage current of 10 picoamperes; its loading on the charge "holding" capacitor is negligible. The open-loop voltage-gain of the system (Fig. 9) is approximately 100 dB if the MOS/FET is used in the source-follower mode to the CA3080A as the input amplifier. The open-loop output impedance $(\frac{1}{g_m})$ of the 3N138 is approximately 220 Ω because its transconductance is about 4,600 μmho at an operating current of 5 mA. When the CA3080A drives the 3N138 (Fig. 9), the closed loop operational-amplifier output impedance characteristic

$$Z_{out} \cong \frac{Z_O \text{ (open-loop)}}{A \text{ (open-loop voltage-gain)}}$$

$$\cong \frac{220\ \Omega}{100\text{dB}} \cong \frac{220\ \Omega}{10^5} \cong 0.0022\ \Omega$$

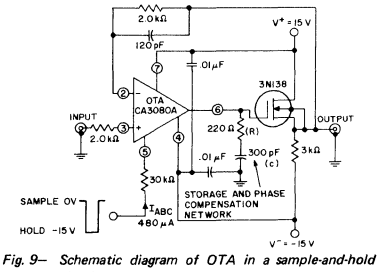
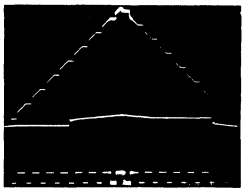


Fig. 9– Schematic diagram of OTA in a sample-and-hold circuit.

Fig. 10 shows a "sampled" triangular signal. The lower trace in the photograph is the sampling signal. When this signal goes negative, the CA3080A is cutoff and the signal is "held" on the storage capacitor, as shown by the plateaus on the triangular wave-form. The center trace is a time expansion of the top-most transition (in the upper trace) with a time scale of 2 μsec/div.



TOP TRACE: SAMPLED SIGNAL 1V/DIV & 20μsec/DIV
CENTER TRACE: TOP PORTION OF UPPER SIGNAL 1V/DIV & 2μsec/DIV
BOTTOM TRACE: SAMPLING SIGNAL 20V/DIV & 20μsec/DIV

Fig. 10– Waveforms for circuit of Fig. 9; top trace: sampled signal; center trace: top portion of upper signal; lower trace: sampling signal.

Once the signal is acquired, variation in the stored-signal level during the hold-period is of concern. This variation is primarily a function of the cutoff leakage current of the CA3080A (a maximum limit of 5 ηA), the leakage of the storage element, and other extraneous paths. These leakage currents may be either "positive" or "negative" and, consequently, the stored-signal may rise or fall during the "hold" interval. The term "tilt" is used to describe this condition. Fig. 11 shows the expected pulse "tilt" in microvolts as a function of time for various values of the compensation/storage capacitor. The horizontal axis shows three scales representing leakage currents of 50 ηA, 5 ηA, 500 pA.

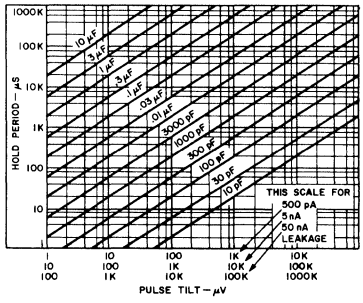
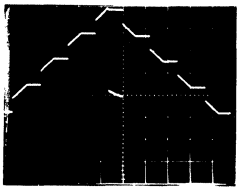


Fig. 11– Chart showing "tilt" in sample-and-hold potentials as a function of hold time with load capacitance as a parameter.

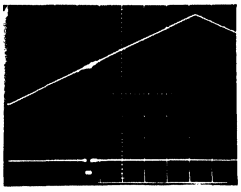
Fig. 12 shows a dual-trace photograph of a triangular signal being "sampled-and-held" for approximately 14 ms with a 300 pF storage capacitor. The center trace (expanded to 20 mV/div) shows the worst-case "tilt" for all the steps shown in the upper trace. The total equivalent leakage current in this case is only 170 pA $(I = C\frac{dv}{dt})$.



TOP TRACE: SAMPLED SIGNAL 1V/DIV & 20msec/DIV
CENTER TRACE WORSE CASE TILT 20mV/DIV & 20msec/DIV

Fig. 12– Oscilloscope photo of "triangular-voltage" being sampled by circuit of Fig. 9.

Fig. 13 is an oscilloscope photograph of a ramp voltage being sampled by the "sample-and-hold" circuit of Fig. 9. The input signal and sampled-output signal are superimposed. The lower trace shows the sampling signal. Data shown in Fig. 13 were recorded with supply voltages of ±10 V and the series input resistor at terminal 5 was 22 kΩ.



TOP TRACE: INPUT AND OUTPUT SUPERIMPOSED 1V/DIV & 2μsec/DIV
BOTTOM TRACE: SAMPLING SIGNAL 20V/DIV & 2μsec/DIV

Fig. 13– Oscilloscope photo of "ramp-voltage" being sampled by circuit of Fig. 9.

the circuit of Fig. 20 as an emitter-follower to drive the p-n-p transistor, variations due to base-emitter characteristics are considerably reduced due to the complementary nature of the n-p-n base-emitter junctions. Moreover, the temperature coefficients of the two base-emitter junctions tend to cancel one another. Fig. 21 shows a configuration using one transistor in the RCA type CA3018A n-p-n transistor-array as

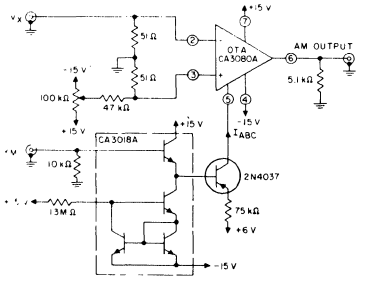


Fig. 21– Amplitude modulator using OTA controlled by p-n-p and n-p-n transistors.

an input emitter-follower, with the three remaining transistors of the transistor-array connected as a current-source for the emitter – followers. The 100-kΩ potentiometer shown in these schematics is used to null the effects of amplifier input offset voltage. This potentiometer is adjusted to set the output voltage symmetrically about zero. Figs. 22a and 22b show oscilloscope photographs of the output voltages obtained when the circuit of Fig. 19 is used as a modulator for both sinusoidal and triangular modulating signals. This method of modulation permits a range exceeding 1000:1 in the gain, and thus provides modulation of the carrier input in excess of 99%. The photo in Fig. 22c shows the excellent isolation achieved in this modulator during the "gated-off" condition.

Four-Quadrant Multipliers

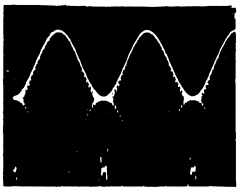
A single CA3080A is especially suited for many low-frequency, low-power four-quadrant multiplier applications. The basic multiplier circuit of Fig. 23 is particularly useful for waveform generation, doubly balanced modulation, and other signal processing applications, in portable equipment, where low-power consumption is essential and accuracy requirements are moderate. The multiplier configuration is basically an extension of the previously discussed gain-controlled configuration (Fig. 19).

To obtain a four-quadrant multiplier, the first term of the modulation equation (which represents the fixed carrier) must be reduced to zero. This term is reduced to zero by the placement of a feedback resistor (R) between the output and the inverting input terminal of the CA3080A, with the value of the feedback resistor (R) equal to $1/g_m$. The output current is $I_O = g_m(-Vx)$ because the input is applied to the inverting terminal of the OTA. The output current due to the resistor (R) is $\frac{Vx}{R}$. Hence, the two signals cancel when $R = 1/g_m$. The current for this configuration is:

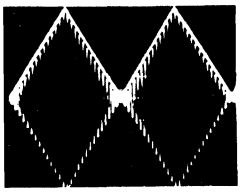
$$I_O = \frac{-19.2\ Vx\ Vm}{Rm} \text{ and } Vm = Vy$$

The output signal for these configurations is a "current" which is best terminated by a short-circuit. This condition can be satisfied by making the load resistance for the multiplier output very small. Alternatively, the output can be applied to a current-to-voltage converter shown in Fig. 24.

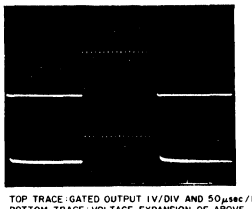
In Fig. 23, the current "cancellation" in the resistor R is a direct function of the OTA differential amplifier linearity. In the following example, the signal excursion is limited to ±10 mV to preserve this linearity. Greater signal-excursions on the input terminal will result in a significant departure from linear operation (which may be entirely satisfactory in many applications).



TOP TRACE: MODULATION FREQUENCY INPUT ≃20 VOLTS P-P & 50 μsec/DIV
CENTER TRACE AMPLITUDE MODULATE OUTPUT 500mV/DIV & 50 μsec/DIV
BOTTOM TRACE: EXPANDED OUTPUT TO SHOW DEPTH OF MODULATION 20mV/DIV & 50 μsec/DIV



TOP TRACE: MODULATION FREQUENCY INPUT 20 VOLTS & 50 μsec/DIV
BOTTOM TRACE: AMPLITUDE MODULATED OUTPUT 500mV/DIV & 50 μsec/DIV



TOP TRACE: GATED OUTPUT 1V/DIV AND 50 μsec/DIV
BOTTOM TRACE: VOLTAGE EXPANSION OF ABOVE SIGNAL – SHOWING NO RESIDUAL 1mV/DIV AND 50 μsec/DIV – AT LEAST 80 db OF ISOLATION fq = 100 kHz

Fig. 22– a) Oscilloscope photo of amplitude modulator circuit of Fig. 19 with $R_m = 40\ k\Omega$, $V^+ = 10$ v and $V^- = -10$ V. Top trace: modulation frequency input ≃ 20-V p-p; center trace: amplitude modulated output 500-mV/div.; lower trace: expanded output to show depth of modulation, 20 mV/div.; b) triangular modulation; top trace: modulation frequency input ≃ 20 V; lower trace: amplitude modulated output 500 mV/div.; c) square wave modulation, top trace: gated output 1 V/div.; lower trace: expanded scale, showing no residual (1 mV/div) and at least 80 dB of isolation at fq = 100 kHz.

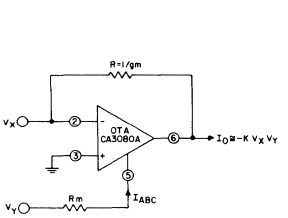


Fig. 23– Basic four quadrant analog multiplier using an OTA.

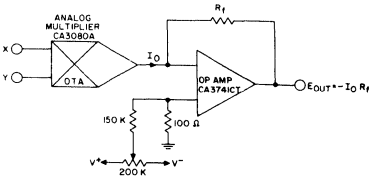


Fig. 24– OTA analog multiplier driving an op-amp that operates as a current-to-voltage converter.

Fig. 25 shows a schematic diagram of the basic multiplier with the adjustments set-up to give the multiplier an accuracy of approximately ±7 percent "full-scale". There are only three adjustments: 1) one is on the output, to

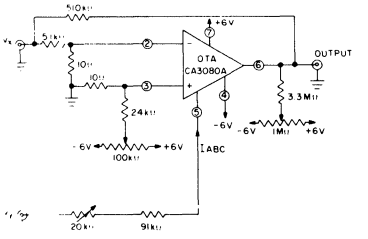


Fig. 25– Schematic diagram of analog multiplier using OTA.

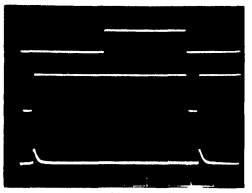
compensate for slight variations in the current-transfer ratio of the current-mirrors (which would otherwise result in a symmetrical output about some current level other than zero); 2) the adjustment of the 20-kΩ potentiometer establishes the g_m of the system equal to the value of the fixed resistor shunting the system when the Y-input is zero; 3) compensates for error due to input offset voltage.

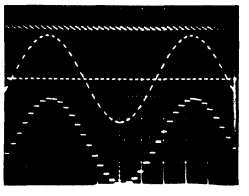
Procedure for adjustment of the circuit:

1. a) Set the 1 MΩ output-current balancing potentiometer to the center of its range
   b) Ground the X- and Y- inputs
   c) Adjust the 100 kΩ potentiometer until a zero-V reading is obtained at the output.
2. a) Ground the Y-input and apply a signal to the X-input through a low source-impedance generator. (It is essential that a low impedance source be used; this minimizes any change in the g_m balance or zero-point due to the 50-μA Y-input bias current).
   b) Adjust the 20-kΩ potentiometer in series with Y-input until a reading of zero-V is obtained at the output. This adjustment establishes the g_m of the CA3080A at the proper level to cancel the output signal. The output current is diverted through the 510-kΩ resistor.
3. a) Ground the X-input and apply a signal to the Y-input through a low source-impedance generator.
   b) Adjust the 1-MΩ resistor for an output voltage of zero-V.

There will be some interaction among the adjustments and the procedure should be repeated to optimize the circuit performance.

Fig. 26 shows the schematic of an analog multiplier circuit with a 2N4037 p-n-p transistor replacing the Y-input "current" resistor. The advantage of this system is the higher input resistance resulting from the current-gain of the p-n-p transistor. The addition of another emitter-follower preceding the p-n-p transistor (shown in Fig. 21) will further increase the current gain while markedly reducing the effect of the V_{be} temperature-dependent characteristic and the offset voltage of the two base-emitter junctions.





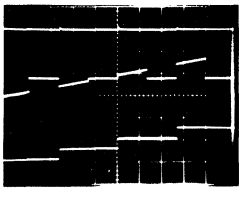


Fig. 30– (a) Waveforms showing timing of flip-flop, delay–"one-shot" and the strobing pulse to the sample-and-hold circuit (Fig. 28): top trace: flip-flop output (5 V/div); center trace: "one-shot" output (5 V/div); lower trace: pulse at collector of 2N4037 transistor (0.1 V/div); b) Waveforms showing the decoding operation from the decoder keying pulse (top traces) to the recovered "decoded" sampled output (lower traces). 1) top trace: collector of 2N4037; center trace: multiplexed output with one channel input grounded; lower trace: decoded output; 2) Expanded scale of (1).

a constant-current transistor. Phase compensation is applied at the interface of the CA3080 and the 3N138 MOS/FET shown in Fig. 9.

Another variation of this generic form of amplifier utilizes the RCA CD4007A (COS/MOS) "inverter" as an amplifier driven by the CA3080. Each of the three "inverter"/amplifiers in the CD4007A has a typical voltage gain of 30 dB. The gain of a single COS/MOS "inverter"/amplifier coupled with the 100 dB gain of the CA3080 yields a total forward-gain of about 130 dB. Use of a two-stage COS/MOS amplifier configuration will increase the total open-loop gain of the system to about 160 dB (100,000,000). Figs. 31 through 34 show examples of these configurations. Each COS/MOS "inverter"/amplifier can sink or source a current of 6 mA (typ.). In Figs. 33 and 34, two COS/MOS "inverter"/amplifiers have been connected in parallel to provide additional output current.

The open-loop slew-rate of the circuit in Fig. 31 is approximately 65 V/μsec. When compensated for the unity-gain voltage-follower mode, the slew-rate is about 1 V/μsec (shown in Fig. 32). Even when the three "inverter"/

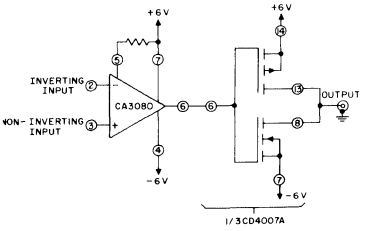


Fig. 31– Schematic diagram showing OTA driving COS/MOS Inverter/Amplifier (open-loop mode). For greater current output the two remaining amplifiers of the CD4007A may be connected in parallel with the single stage shown. Open-loop gain ≃ 130 dB.

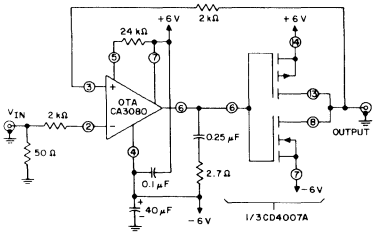


Fig. 32– Schematic diagram showing OTA driving COS/MOS Inverter/Amplifier (unity-gain closed-loop mode). For greater current output, the two remaining amplifiers of the CD4007A may be connected in parallel with the single stage shown.

amplifiers in the CD4007A are connected as shown in Fig. 33, the open-loop slew-rate remains at 65 V/μsec. A slew-rate of about 1 V/μsec is maintained with this circuit connected in the unity-gain voltage-follower mode, as shown in Fig. 34. Fig. 35 contains oscilloscope photos of input-output waveforms under small-signal and large-signal conditions for the circuits of Figs. 32 and 34. These photos illustrate the inherent stability of the OTA and COS/MOS circuits operating in concert.

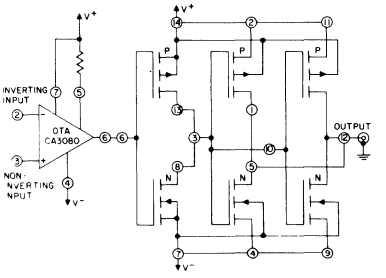


Fig. 33– Schematic diagram showing OTA driving two-stage COS/MOS Inverter/Amplifier (open-loop mode). gain ≃ 160 dB.

Precision Multistable Circuits

The micropower capabilities of the CA3080, when combined with the characteristics of the CD4007A COS/MOS "inverter"/amplifiers, are ideally suited for use in connection with precision multistable circuits. In the circuits of Figs. 31, 32, 33, and 34, for example, power-supply current drawn by the COS/MOS "inverter"/amplifier approaches zero as the output voltage swings either positive or negative, while the CA3080 current-drain remains constant.

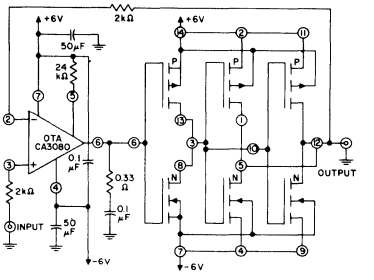


Fig. 34– Schematic diagram showing OTA driving two-stage COS/MOS Inverter/Amplifier (unity gain closed-loop mode).

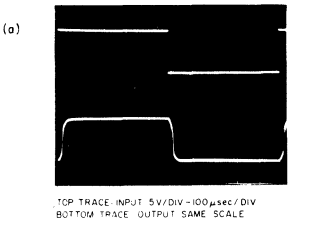


Fig. 35– a) Waveforms for circuit of Fig. 32 with large signal input; b) Waveforms for circuit of Fig. 32 with small signal input; c) Waveforms for circuit of Fig. 34 with large signal input; d) Waveforms for circuit of Fig. 34 with small signal input.

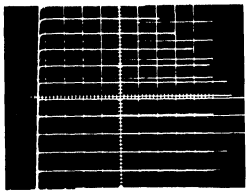


Fig. F— Photo showing results of Fig. E.

Fig. G shows the current-division within the "mirror" assuming a "unit" (1) of current in transistors (Q2 and Q3.

The resulting current-transfer ratio $I_2/I_1 = \frac{\beta^2 + 2\beta}{\beta^2 + 2\beta + 2}$; Fig. C shows this equation plotted as a function of beta. It is significant that the current transfer ratio (I_2/I_1) is improved by the β^2 term, and reduces the significance of the $2\beta + 2$ term in the denominator.

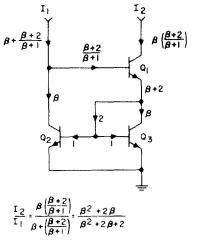


Fig. G— Current flow analysis of Fig. E.

Conclusions

The Operational Transconductance Amplifier (OTA) is a unique device with characteristics particularly suited to applications in multiplexing, amplitude modulation, analog multiplications, gain control, switching circuitry, multivibrators, comparators, and a broad spectrum of micropower circuitry. The CA3080 is ideal for use in conjunction with COS/MOS (Complementary-Symmetry MOS) IC's being operated in the linear mode.

Acknowledgements

The author is indebted to C. F. Wheatly for many helpful discussions. Valued contributions in circuit evaluation were made by A. J. Visioli Jr. and J. H. Klinger.

References

1 RCA's Linear Integrated Circuits Manual, Basic Circuits Section.
2 RCA published data for CA3060 File No. 404

provides enough gain to bring the input signal level to an amplitude suitable for fm detection, but not so high as to cause PC layout or coupling problems, Fig. 2.

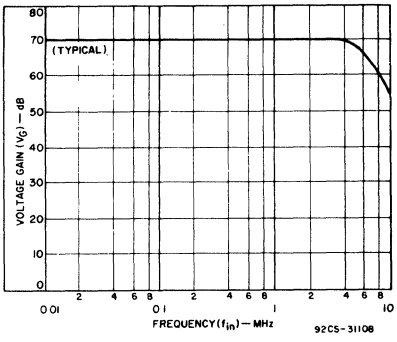


Fig. 2 - Voltage gain of if amplifier as a function of frequency.

As shown in Fig. 4, the if amplifier consists of four stages of differential amplifiers, Q15-Q16, Q19-Q20, Q23-Q24, and Q27-Q28, using resistors R13, R16, R19, and R24 as constant-current sinks; each stage is followed by emitter followers, Q17, Q21, and Q25. Because the differential amplifier functions as a limiter, am signals are eliminated and the signal into Q30 consists of constant-amplitude, frequency-modulated square waves. These square waves are shaped into approximate sine waves by Q30 and its associated RC networks to assure proper operation of the fm detector. The signal output from R31 into the base of Q41 and to terminal 10 is a constant-amplitude fm sine wave.

FM Detector

The fm sine wave at terminal 10 constitutes the input signal to the differential peak detector stage. The extracted signal contains the audio information. The detector section is formed by the differential amplifier configuration comprising transistors Q31, Q32, Q35, Q36, Q40, and Q41. Transistors Q31 and Q41 are emitter followers that operate at approximately 0.3 mA and provide high impedance at each input of the detector (terminals 10 and 11). Transistors Q32 and Q40, which operate at approximately 10 microamperes, along with the 15-picofarad capacitors C3 and C4 and the external frequency-sensitive network on terminals 10 and 11, perform peak or envelope detection. As shown in Fig. 1, this frequency-sensitive network consists of a parallel LC network in series with a 6.8-pF capacitor. The signal voltage (from Q30) is applied across the entire network connected to terminal 10. The portion of the signal from Q30 that is across the external 6.8-pF capacitor is applied to terminal 11, and the resulting difference in these signals provides the basic S curve used in the recovery of the audio signal from the fm signal.

An advantage of the differential peak detector is that it requires the alignment of only one single-tuned coil. This coil (L in Fig. 1) can be aligned by any one of the following methods (with an input terminated in 50 ohms, f_O = 4.5 MHz, f_m = 400 Hz, Δf = ± 25 kHz, and a voltage at terminal 15 (V_{15}) ≃ 100 mV rms):

1. Tune L for maximum recovered audio. To minimize thermal effects on alignment, the volume control should be adjusted so that the maximum recovered audio level at the load is limited to a low power level (approximately 0.1 watt or less).
2. Tune L for maximum recovered audio and fine tune for minimum distortion.
3. With no rf input signal, note the dc voltage at terminal 9. Then apply a 4.5-MHz cw signal and adjust the detector coil L until the dc voltage at terminal 9 is the same as the value noted.

After aligning the differential peak detector coil, align the input transformer by reducing the fm input signal level until the recovered audio level drops approximately 3 dB. Then tune the input transformer for a maximum recovered audio level while the input level of the if amplifier-limiter is below its limiting point. Fig. 3 shows the recovered audio, am rejection, and signal-to-noise ratio for the CA3134 as a function of rf input level.

Volume Control and Electronic Attenuator

Control of the audio signal detected by the differential peak detector is accomplished by differential amplifiers Q33-Q34 and Q38-Q39.

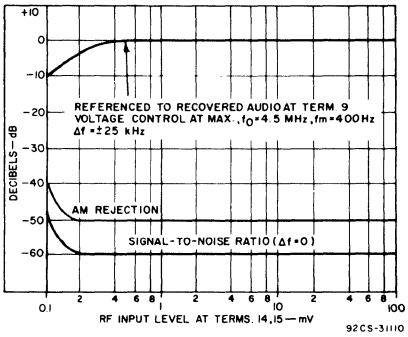


Fig. 3 - Recovered audio and signal-to-noise ratio as functions of rf input level.

The volume is controlled when the bias levels of the differential amplifiers are changed by a current flowing through an external fixed resistor between terminals 12 and 16. The amount of current flowing through this external resistor (which determines the level of recovered audio) is controlled by the position of the variable resistance (volume control) relative to ground. The voltage reference at terminal 16 is established by internal zener diode Z2, approximately 6 volts. The maximum level of recovered audio, therefore, occurs when no currents other than the base currents for Q34 and Q39 are being drawn from the zener diode through the external resistor. When the volume control is adjusted for the minimum level of recovered audio, the current drawn from terminal 16 should be limited to less than 1 milliampere.

This method of controlling the recovered audio has a very predictable volume-control taper, which can be modified to suit the designer's preference by changing the external component values. In addition, it allows for either a one- or two-wire volume control. The one-wire volume control (Fig. 4, alternate volume-control circuit) requires only one wire from the printed circuit board to the external volume control, but requires that the value of the variable resistor be large (approximately 500 kilohms) and that the resistor have an audio taper to assure an acceptable change of audio output level with a linear change (rotation) of the volume-control. The two-wire volume control allows the use of a volume control having a lower value of resistance and a linear taper.

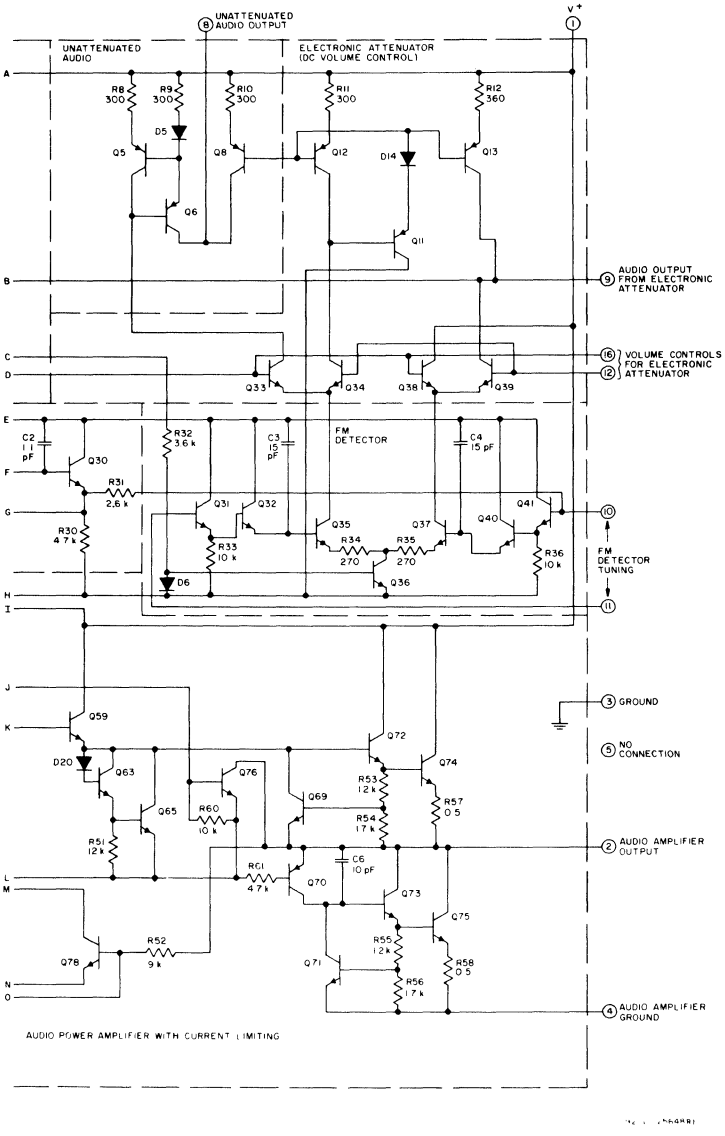


Fig. 4 – Schematic diagram of CA3134.

nents, especially costly electrolytic capacitors. The input impedance (at terminal 7) is typically 100 kilohms (R59). Fig. 5 shows the frequency response of the audio power amplifier and Fig. 6 its efficiency. Both current limiting and thermal shutdown protection are provided. Current limiting is accomplished by limiting the drive to the output transistors from the driver transistors Q72 and Q73. The limiting drive is determined by the feedback from R53, R54, and Q69 to Q72, and R55, R56, and Q71 to Q73. When the peak output current exceeds approximately 0.8 ampere, the voltage developed across the emitters of Q72 and Q73 will cause Q69 and Q71, respectively, to conduct, thereby limiting the drive to the output transistors Q74, Q75.

When the chip temperature exceeds 150 °C, the thermal-sensing portion of the CA3134 begins to shut down the power amplifier by removing the bias from the power amplifier driver stages. The temperature at which the thermal shutdown circuitry is activated is determined by the relative areas of D9, Q66, and D18 and those of Q49, D11, D12, and D13. When Q49 conducts, transistors Q79, Q68, and Q76 are in turn biased into

Acknowledgment

The author is indebted to both Jack Craft for many helpful discussions and Wayne Austin for his suggestions in the preparation of this Note. The contributions of H. Chinery in the electrical characterization of the CA3134 and Ralph Thompson in the mechanical characterization of the stud package are acknowledged.

References

1. RCA Solid State Data Sheet for CA3134 types, "TV Sound IF and Audio Output Systems," File No. 1097.

2. Method of attaching heat sinks similar to the type provided with the CA3134GM or GQM to the CA3134G. First apply a non-conductive epoxy (Uniset structural adhesive or equivalent) to the top side of the plastic package. Then apply a conductive epoxy (Dupont 5504A or equivalent) in the hole of the heat sink and around the stud projecting from the plastic package. To assure good thermal conduction, use sufficient conductive epoxy to allow the excess to be forced through the hole when the heat sink is fitted over the stud. Stress applied to the stud should be limited to less than 3 in-lbs (approximately 0.35 newton-meter), 15 lbs (approximately 65 newtons) of tension, and 100 lbs (approximately 445 newtons) of compression.

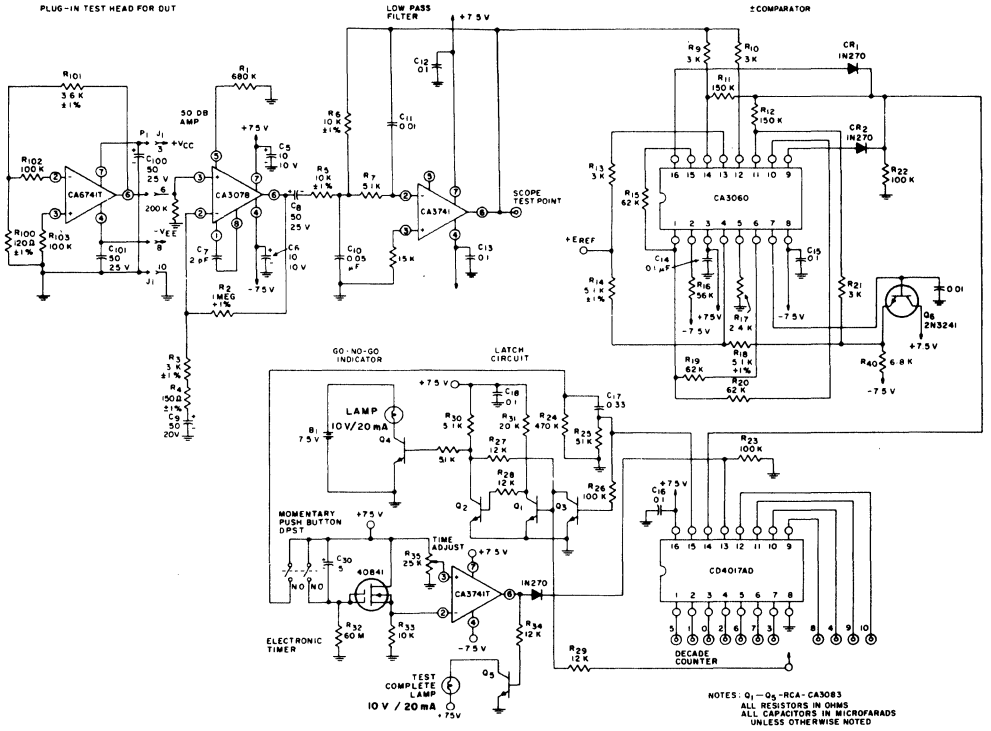


Fig. 2b— Complete schematic diagram for burst noise test-set.

currents consistent with the gain-bandwidth requirements of the particular application.

In the test for burst noise, the source resistance (Rs) seen by the input terminals of the DUT, is a key test parameter. Burst noise causes effects which are equivalent to a spurious current-source at the device input and, therefore, burst-noise current generates an equivalent input noise-voltage in proportion to the magnitude of the source resistance through which it flows. Accordingly, to increase the sensitivity of the test system, it is desirable to use the highest source resistance consistent with the input offset-current of the DUT. For example, an Op-Amp which has 0.1 μA input offset current could realistically be tested with source-resistance in the order of 100KΩ (10 mV input offset), whereas a 1 MΩ source-resistance (100 mV input offset) could cause excessive offset in the output. For 741 type Op-Amps a 100kΩ resistance is recommended.

Burst-noise generation in amplifiers is usually more pronounced at lower temperatures (particularly below 0°C). Consequently, consideration must be given to the temperature of the DUT in relation to the temperature range under which the device is expected to perform in a particular operation.

A test parameter of importance is the time duration of observation. Because the frequency of burst-noise occurrence is frequently less than once every few seconds, the minimum test period should be in the range of from 15 to 30 seconds.

Pass-Fail Criteria

A test system built to accommodate the test philosophy outlined above has the ability to reject or pass a DUT on the basis of two variables: burst-amplitude and the frequency of burst occurrence. The burst-amplitude which will trip the counter can be no lower than the background l/f noise peaks of burst-free units, otherwise normal background noise will fail the DUT.

The background noise peaks depend on the source termination Rs, the wide band l/f noise figure of the DUT, and the test system bandwidth. A good estimate of the normal background noise-peak levels can be computed from the definition of noise factor and an empirically determined noise-crest factor of approximately 6:1. The crest-factor is the ratio of the maximum peak-noise voltage to the RMS noise voltage. The noise factor is defined as the ratio of the total noise power at the amplifier output to the output-noise power due to the source resistors alone. In terms of the RMS noise voltages at the input terminals of the amplifier this is equivalent to:

$$\text{Noise Factor (F)} = \frac{E^2\text{input noise total}}{E^2\text{noise source resist}} = \frac{(E_{NTi})^2}{(E_{NRS})^2} \quad (1)$$

E_{NTi} is the total input noise-voltage, i.e., the sum of noise generated in the source termination resistance and noise generated by the DUT.

E_{NRs} is that part of E_{NTi} due to Rs alone.

$$\text{Therefore,} \quad E_{NTi} = (\sqrt{F})\,(E_{NRs}). \quad (2)$$

E_{NRs} can be computed by using the well known expression for "white-noise" generated across the terminals of a resistor (R):

$$E_{NR}(\text{RMS}) = \sqrt{4kTBR} \quad (3)$$

where k = Boltzmans Constant = 1.372×10^{-23} j/°K

T = Absolute Temperature in °K
B = Noise Bandwidth in Hz
R = Value of the resistor in ohms.

Thus, at a room temperature of 290°K

$$E_{NR}(\text{RMS}) = 1.28 \times 10^{-10}\sqrt{BR}$$

For example, a 100 kΩ resistor preceding a system with a bandwidth of 1 kHz will generate a noise-voltage of

$$(1.28 \times 10^{-10}) \quad (\sqrt{10^3 \cdot 10^5}) \quad = 1.28\ \mu V_{RMS}$$

Both inputs of an Op-Amp are usually terminated in Rs, hence it is necessary to combine the effects of both resistors to determine the effective E_{NRs} at the input of the DUT. Because the noise voltages from these two resistors are uncorrelated their voltages must be added vectorally rather than algebraically.

$$E_{NRs}\,(\text{effective}) = \sqrt{(E_{NRs1})^2 + (E_{NRs2})^2} \quad (4)$$

because $E_{NRs1} = E_{NRs2}$, when $R_{s1} = R_{s2}$

$$E_{NRs}\,(\text{effective} = (\sqrt{2})\ (E_{NRs})$$

and for 1 kHz bandwidth at 290°K

$$E_{NRs}\,(\text{effective}) = (\sqrt{2})\,(1.28\ \mu V) = 1.81\ \mu V_{RMS}.$$

If in this example, the DUT has a wideband l/f noise figure of 4 dB (2.5:1 power ratio) the total RMS background noise-voltage at the input will be

$$E_{NTi} = (\sqrt{F})\ (E_{NRs})\ \text{(from eq.(2))}$$
$$= (\sqrt{2.5})\ (1.81) = 2.9\ \mu V_{RMS}$$

operated, "On-Off" switching of nearby equipment introduces detectable transients into the system. These problems are eliminated by placing the test circuitry in a completely shielded enclosure with a hinged top for easy access to the test unit. The external noise problem is best solved by use of a shielded enclosure and by use of a battery-operated power-supply contained within the enclosure. Fig. 6 shows a photo of the circuit board layouts of the test unit.

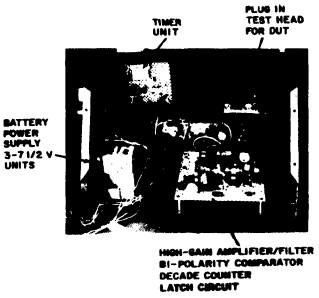


Fig. 6— Photo of circuit-board layout.

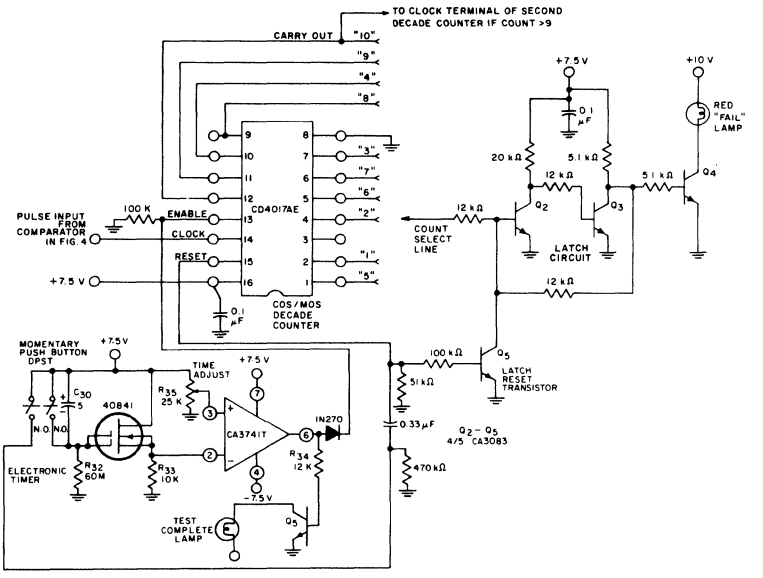


Fig. 5— Counter-latch-timer-control circuit schematic.

voltages: a 50-dB amplifier; a 10-dB, 42-MHz amplifier; a twin-T bandpass amplifier; a 20-dB, 10-MHz bandpass amplifier; and a voltage-follower.

ICAN-5269 . . . . . 7 pages
Integrated Circuits for FM Broadcast Receivers
This Note describes several approaches to FM receiver design using silicon monolithic integrated circuits. The tuner section is described first, and then the if-amplifier and detector sections. Performance characteristics are described where applicable. The FM receivers discussed are designed for use from a +9-volt supply. The key to design simplicity is the use of the RCA multifunction integrated circuits CA3005, CA3012, and CA3014. The CA3005 may be used as a cascode rf amplifier, a differential rf amplifier, a mixer-oscillator, and an if amplifier; the CA3012 and CA3014 perform if amplification, limiting, detection, and preamplification.

ICAN-5296 . . . . . 5 pages
Application of the RCA-CA3018 Integrated-Circuit Transistor Array
The CA3018 integrated circuit consists of four silicon epitaxial transistors produced by a monolithic process on a single chip mounted in a 12-lead TO-5 package. The four active devices, two isolated transistors plus two transistors with an emitter-base common connection, are especially suitable for applications in which closely matched device characteristics are required, or in which a number of active devices must be interconnected with non-integrable components such as tuned circuits, large-value resistors, variable resistors, and microfarad bypass capacitors. Such areas of application include if, rf (through 100 MHz), video, agc, audio, and dc amplifiers.

ICAN-5299 . . . . . 6 pages
Application of the RCA-CA3019 Integrated-Circuit Diode Array
The CA3019 integrated circuit diode array provides four diodes internally connected in a diode-quad arrangement plus two individual diodes. Its applications include gating, mixing, modulating, and detecting circuits. Because all the diodes are fabricated simultaneously on a single silicon chip, they have nearly identical characteristics, and their parameters track each other with temperature variations. Consequently, the CA3019 is particularly useful in circuit configurations that require either a balanced diode bridge or identical diodes.

ICAN-5337 . . . . . 10 pages
Application of the RCA-CA3028A and CA-3028B Integrated-Circuit RD Amplifiers in the HF and VHF Ranges
The CA3028A and CA3028B monolithic-silicon integrated circuits are single-stage differential amplifiers intended for service in communications systems operating at frequencies up to 100 MHz with single power supplies. This Note provides technical data and recommended circuits for use of the CA3028A and CA3028B in rf amplifiers, autodyne converters, if amplifiers, and limiters. The CA3028A and CA3028B are suitable for use in a wide range of applications in dc, audio, and pulse amplifier service; they have been used as sense amplifiers, preamplifiers for low-level transducers, and dc differential amplifiers.

ICAN-5338 . . . . . 14 pages
Application of the RCA-CA3021, CA3022, and CA3023 Integrated-Circuit, Wideband Amplifiers
The CA3021, CA3022, and CA3023 integrated circuits are multipurpose high-gain amplifiers designed for use in video and AM or FM if stages in single-power-supply systems. Specifically, they can be used in video amplifiers operating at frequencies through 30 MHz, AM and FM if amplifiers, and buffer amplifiers in which an isolation capability greater than 60 dB at 1 MHz is desired.

ICAN-5380 . . . . . 7 pages
Integrated - Circuit Frequency - Modulation if Amplifiers
The discussion in this Note shows that the simplest approach to the use of the CA3012 and CA3028 integrated circuits in FM if-amplifier strips is to replace each stage in present discrete-transistor if strips with a differential amplifier. This integrated-circuit approach requires a minimum of re-engineering because a cascade of individually tuned if stages is used. From a performance point of view, this approach results in better AM rejection than that obtained with discrete circuits because of the inherent limiting achieved with the differential-amplifier configuration.

ICAN-5766 . . . . . 8 pages
Application of the RCA-CA3020 and CA3020A Integrated-Circuit Multipurpose Wideband Power Amplifiers
The CA3020 and CA3020A integrated circuits are multipurpose, multifunction power amplifiers designed for use as power-output amplifiers and driver stages in portable and fixed communications equipment and in ac servo-control systems. The flexibility of these circuits and the high-frequency capabilities of the circuit components make these types suitable for a wide variety of applications such as broadband amplifiers, video amplifiers, and video line drivers. Voltage gains of 60 dB or more are available with a 3-dB bandwidth of 8 MHz. Applications covered include audio, wideband, and driver amplifiers.

ICAN-5831 . . . . . 5 pages
Application of the RCA-CA3044 and CA3044VI Integrated Circuits in Automatic-Fine-Tuning Systems
This Note describes the use of the CA3044 and CA3044VI integrated circuits as automatic fine-tuning (AFT) system components and discusses the advantages of integrated circuits in this application. The CA3044VI is electrically identical to the CA3044, but is supplied with formed leads for easier printed-circuit-board mounting. The construction and performance of a typical automatic-fine-tuning system for a color television system are examined.

ICAN-5841 . . . . . 4 pages
Feedback-Type Volume-Control Circuits for RCA-CA3041 and CA3042 Integrated Circuits
This Note describes feedback-type volume controls for use with RCA-CA3041 and CA3042 integrated circuits in television receivers. In television sets using these integrated circuits, the volume control is often located remote from the amplifier. The long leads required in such a configuration sometimes pick up undesirable signals that, in turn, cause the system to exhibit hum and noise at low volume levels. The proposed feedback-type volume control reduces hum and noise pick-up by reducing the gain of the system rather than the signal level, and thus eliminates the cost of shielding the leads.

ICAN-6259 . . . . . 10 pages
Integrated-Circuit Stereo Decoder Using the CA3090AQ Stereo Multiplex Demodulator
The CA3090AQ integrated-circuit provides features heretofore unavailable to the receiver designer. This device needs only a single tuning adjustment, which reduces to a minimum the manual effort during assembly; the phase-locked loop maintains performance under conditions of temperature variations, humidity, and aging. The compactness of the CA3090AQ and of the required external components, added to the other attributes, makes this stereo decoder a significant advancement in the state of the art of stereo decoder designs.

ICAN-6302 . . . . . 9 pages
Description and Application of the RCA-CA3120E Integrated-Circuit TV-Signal Processor
The CA3120E is a 16-pin, dual-in-line-monolithic-silicon integrated circuit that processes a video signal and provides the following outputs: non-inverted video output; noise-processed, inverted video output; dual-polarity, composite synchronization signals; and automatic gain-control signals (agc). The IC, which can be used in color or monochrome TV receivers, requires a single-polarity power supply (positive) and includes impulse noise inversion and delay circuits that reduce the deleterious effects of impulse noise in the receiver agc and synchronization (sync) circuits. Standard agc strobing techniques are also used. The agc and impulse-noise thresholds are automatically set and require no controls. The if maximum-gain bias and the tuner agc delay may be adjusted for optimun. TV-receiver performance; the time constant for the sync-separator input can also be optimized by the set designer.

ICAN-6724 . . . . . 8 pages
A Flexible Integrated-Circuit Color Demodulator for Color Television
This Note describes the circuit operation and application of the CA3067 in a color television receiver. The CA3067, which is supplied in a quad-in-line 16-lead plastic package, provides the following color-demodulator circuit functions: amplification, balanced chroma demodulation, dc-operated tint (phase) control, and zener-diode voltage regulation.

RCA Sales Offices Manufacturers' Representatives, and Authorized Distributors

RCA Manufacturers' Representatives

Arizona ..... **C.T. Carlberg Associates,**
4236 North Brown Ave.,
Scottsdale, AZ 85251 ..... **(602)277-2808**

California ..... **Bestronics** (San Diego Area)
7827 Convoy Court, Suite 407,
San Diego, CA 92111 ..... **(714)278-2150**

Colorado ..... **Waugaman Associates, Inc.**
4800 Van Gordon,
Wheatridge, CO 80033 ..... **(303)423-1020**

Delaware ..... **Thomas Associates, Inc.,** (See New Jersey)

Florida ..... **G.F. Bohman Associates,**
5104 No. Orange Blossom
Trail, Suite 115, Rosemont Bldg.
Orlando, FL 32804 ..... **(305)295-5760**
G.F. Bohman Associates,
3172 SW 27th Ave., Apt. 3,
Miami, FL 33133 ..... **(305)564-3081**
G.F. Bohman Associates,
4511 Bayshore Blvd. NE,
St. Petersburg, FL 33703 ..... **(813)527-0954**

Idaho ..... **Western Technical Sales, Inc.,**
(No. of Boise, see Washington)
R^2Marketing, (E. & S. of
Boise, see Utah)

Illinois ..... **Kebco,** (see Missouri)

Iowa ..... **Lorenz Sales, Inc.,** Suite 302,
Executive Plaza,
Cedar Rapids, IA 52402 ..... **(319)393-6912**

Kansas ..... **Kebco,** 7070 West 107th St., Suite 160,
Overland Park, KS 66204 ..... **(913)649-2168**

Louisiana ..... **Jackson Arnold Company,** (see Texas)

Michigan ..... **Nicon Associates,** 3835 W. Eight
Mile Rd., Detroit, MI 48221 ..... **(313)341-7688**

Minnesota ..... **Comstrand, Inc.,**
2852 Anthony Lane South,
Minneapolis, MN 55114 ..... **(612)788-9234**

Missouri ..... **Kebco,** 75 Worthington Drive,
Maryland, MO 63043 ..... **(314)576-4110/4111**

Montana ..... **R^2 Marketing,** (see Utah)

Nebraska ..... **Lorenz Sales, Inc.,** (see Iowa)

Nevada ..... **C.T. Carlberg Associates** (Clark Co.,
see Arizona)

New Jersey ..... **Thomas Associates, Inc.,**
(So. N.J.), 12 South Blackhorse Pike **(215)627-6615**
Bellmawr, NJ 08031 ..... **(609)933-2600**

New Mexico ..... **C.T. Carlberg Associates,**
PO Box 3177, Station D,
Albuquerque, NM 87110 ..... **(505)265-1579**

New York ..... **L-Mar Associates, Inc.,**
(Upstate NY), 98 Elwell Ave.
Binghamton, NY 13901 ..... **(607)723-1513**

New York ..... **L-Mar Associates, Inc.,**
(Upstate NY) PO Box 7945,
Rochester, NY 14606 ..... **(716)328-5240**
L-Mar Associates, Inc.,
216 Tilden Drive,
E. Syracuse, NY 13057 ..... **(315)437-7779**

North Dakota ..... **Lorenz Sales, Inc.,** (see Iowa)

Ohio ..... **Arthur H. Baier Company,**
67 Alpha Drive,
Cleveland, OH 44143 ..... **(216)461-6161**
Arthur H. Baier Company,
4940 Profit Way,
Dayton, OH 45414 ..... **(513)276-4128**

Oregon ..... **Western Technical Sales, Inc.,**
2271 N.E. Cornell Rd.,
Hillsboro, OR 97123 ..... **(503)640-4621**

Pennsylvania ..... **Arthur H. Baier Company,** (W. Pa., see Ohio)

Pennsylvania ..... **Thomas Associates, Inc.,** (E. Pa., see New Jersey)

South Dakota ..... **Lorenz Sales, Inc.,** (see Iowa)

Texas ..... **C.T. Carlberg Associates,** (El Paso)
Area, see New Mexico)
Jackson Arnold Company,
(Austin, Houston, San Antonio
Area), PO Box 42388,
Houston, TX 77042 ..... **(713)981-5789**

Utah ..... **R^2 Marketing,** 3688 West 2100 South,
Salt Lake City, UT 84120 ..... **(801)972-5646**

Washington ..... **Western Technical Sales, Inc.,**
PO Box 3923,
Bellevue, WA 98009 ..... **(206)641-3900**

West Virginia ..... **Arthur H. Baier Company,** (see Ohio)

Wisconsin ..... **Key Enterprises,** 850 Elm
Grove Road, Elm Grove, WI 53122 ..... **(414)784-3390**

Wyoming ..... **Waugaman Associates, Inc.,** (see Colorado)

RCA Authorized Distributors

Taiwan ..... **Hwa Sheng Electronic Co., Ltd.**, 3th Fl., #7, Ren-ai Rd., Sec. 2, Taipei, R.O.C. ..... (02)3219 311-5

Thailand ..... **Anglo-Thai Eng. Ltd.**, PO Box 18, Bangkok

Turkey ..... **Teknika TAS**, PO Box Karakoy 153, Istanbul 43 61 00
Teknim Company Ltd., Riza Sah Pehlevi Caddesi 7, Kavaklidere, Ankara 275800

Uruguay ..... **American Products S.A.**, Av. Italia 4230, Montevideo

Venezuela ..... **Telereca, C.A.**, PO Box 3975, Caracas

Yugoslavia ..... **Avtotehna**, PO Box 593, XI, Titova 36, Ljubljana 61000 ..... 317 044

UK ..... **Apex Components Ltd.**, 396 Bath Road, Slough, Berks, SL1 6JD ..... Burnham 63741
Crellon Ltd., 380/386 Bath Road, Slough, Berks, SL1 6JE ..... Burnham 4434
Distronic Ltd., 50/51 Burnt Mill, Elizabeth Way, Harlow, Essex, CM20 2HU ..... Harlow (0279)39701
ITT Electronic Services, Edinburgh Way, Harlow, Essex, CM20 2DE ..... Harlow 26811
Mogul Electronics Ltd., 273 High Street, Epping, Essex, CM 16 4DA ..... Epping 77366
Semicomps (Northern) Ltd., East Bowmont Street, Kelso, Roxboroughshire TD5 7BZ ..... Kelso 2366

U.S.

Alabama ..... **Hamilton-Avnet Electronics**, 4692 Commercial Drive N.W., Huntsville, AL 35805 ..... (205)837-7201

Arizona ..... **Hamilton-Avnet Electronics**, 2615 South 21st Street, Phoenix, AZ 85034 ..... (602)275-7851
Kierulff Electronics, Inc., 4134 East Wood Street, Phoenix, AZ 85040 ..... (602)243-4101

Arizona ..... **Liberty Electronics/Arizona**, 8155 North 24th Avenue, Phoenix, AZ 85022 ..... (602)249-2232

California ..... **Cramer/San Francisco**, 720 Palomer Avenue, Sunnyvale, CA 94086 ..... (408)739-3011
Electronic Supply Corp., 2486 Third Street, Riverside, CA 92507 ..... (714)683-7300
Elmar Electronics, Inc., 2288 Charleston Road, Mt. View, CA 94042 ..... (415)961-3611
Hamilton-Avnet Electronics, 1175 Bordeaux Drive, Sunnyvale, CA 94086 ..... (415)743-3300
Hamilton-Avnet Electronics, 8917 Complex Drive, San Diego, CA 92123 ..... (714)279-2421
Hamilton Electro Sales, 10912 W. Washington Blvd., Culver City, CA 90230 ..... (213)558-2020
Kierulff Electronics, Inc., 2585 Commerce Way, Los Angeles, CA 90040 ..... (213)685-5511
Kierulff Electronics, Inc, 3969 E. Bayshore Road, Palo Alto, CA 94303 ..... (415)968-6292
Kierulff Electronics, Inc., 8797 Balboa Avenue, San Diego, CA 92123 ..... (714)278-2112
Liberty Electronics, 124 Maryland Avenue, El Segundo, CA 90245 ..... (213)322-8100

California ..... **Liberty/San Diego**, 9525 Chesapeake Drive, San Diego CA 92123 ..... (714)565-9171
G.S. Marshall Company, 9674 Telstar Avenue, El Monte, CA 91731 ..... (213)686-0141
RPS Electronics, Inc., 1501 South Hill Street, Los Angeles, CA 90015 ..... (213)748-1271
Schweber Electronics Corp., 17811 Gillette Ave., Irvine, CA 92714 ..... (714)556-3880

Colorado ..... **Elmar Electronics/Denver**, 6777 East 50th Avenue Commerce City, CO 80022 ..... (303)287-9611
Hamilton-Avnet Electronics, 5921 North Broadway, Denver, CO 80216 ..... (303)534-1212
Kierulff Electronics, Inc., 10890 East 47th Avenue, Denver, CO 80239 ..... (303)371-6500

Connecticut ..... **Arrow Electronics, Inc.**, 295 Treadwell Street, Hamden, CT 06514 ..... (203)248-3801
Cramer/Connecticut, 12 Beaumont Rd., Wallingford, CT 06492 ..... (203)265-7741
Hamilton-Avnet Electronics, 643 Danbury Road, Georgetown, CT 06829 ..... (203)762-0361
Schweber Electronics Corp., Finance Drive, Commerce Industrial Park, Danbury, CT 06810 ..... (203)792-3500

Florida ..... **Arrow Electronics, Inc.**, 1001 NW 62nd St., Suite 402, Ft. Lauderdale, FL 33309 ..... (305)776-7790
Arrow Electronics, Inc., 115 Palm Bay Road, N.W., Suite 10, Palm Bay, FL 32905 ..... (305)725-1480
Cramer/Orlando, 345 Graham Avenue, Orlando, FL 32803 ..... (305)895-1511
Hamilton-Avnet Electronics, 6800 N.W. 20th Avenue, Ft. Lauderdale, FL 33309 ..... (305)971-2900
Hamilton-Avnet Electronics, 3197 Tech Drive No., St. Petersburg, FL 33702 ..... (813)576-3930
Schweber Electronics Corp., 2830 North 28th Terrace, Hollywood, FL 33020 ..... (305)927-0511

Georgia ..... **Arrow Electronics, Inc.**, 3406 Oak Cliff Rd., Doraville, GA 30350 ..... (404)455-4054
Cramer/Atlanta, 6456 Warren Drive, Norcross, GA 30071 ..... (404)448-9050
Hamilton-Avnet Electronics, 6700 I85 Access Road, Suite 1E Norcross, GA 30071 ..... (404)448-0800

Illinois ..... **Cramer/Chicago**, 1911 South Busse Road, Mt. Prospect, IL 60056 ..... (312)593-8230
Hamilton-Avnet Electronics, 3901 North 25th Avenue, Schiller Park, IL 60176 ..... (312)678-6310
Newark Electronics, 500 North Pulaski Road, Chicago, IL 60624 ..... (312)638-4411
Schweber Electronics Corp., 1275 Brummel Ave., Elk Grove Village, IL 60007 ..... (312)593-2740
Semiconductor Specialists, Inc., 195 Spangler Avenue, Elmhurst, IL 60126 ..... (312)279-1000

Indiana ..... **Graham Electronics Supply, Inc.**, 133 S. Pennsylvania Street, Indianapolis, IN 46204 ..... (317)634-8202

Iowa ..... **Deeco, Inc.**, 2500 16th Avenue, S.W., Cedar Rapids, IA 52801 ..... (319)365-7551

RCA Authorized Distributors

Ohio
Cramer/Cleveland,
5835 Harper Road,
Solon, OH 44139 ..... (216)248-8400
Hamilton-Avnet Electronics,
761 Beta Drive, Suite E.
Cleveland, OH 44143 ..... (216)461-1400
Hamilton-Avnet Electronics,
954 Senate Drive,
Dayton, OH 45459 ..... (513)433-0610
Hughes-Peters, Inc.,
481 East 11th Aveneu,
Columbus, OH 43211 ..... (216)464-2970
Schweber Electronics Corp.,
23880 Commerce Park Road,
Beachwood, OH 44122 ..... (216)464-2970
The Stotts Briedman Co.,
2600 East River Road,
Dayton, OH 45439 ..... (513)298-5555

Oklahoma
Radio, Inc.,
1000 S. Main Street,
Tulsa, OK 74119 ..... (918)587-9123

Pennsylvania
Herbach & Rademan, Inc.,
401 East Erie Avenue,
Philadelphia, PA 19134 ..... (215)426-1700

Pennsylvania
Semiconductor Specialists, Inc.,
1000 RIDC Plaza, Suite 207,
Pittsburgh, PA 15238 ..... (412)781-8120

Texas
Cramer/Texas,
13740 Midway Road,
Dallas, TX 75240 ..... (214)661-9300
Hamilton-Avnet Electronics,
445 Sigma Road,
Dallas, TX 75240 ..... (214)661-8661
Hamilton-Avnet Electronics,
3939 Ann Arbor Street,
Houston, TX 77063 ..... (713)780-1771
Schweber Electronics, Corp.,
14177 Proton Road,
Dallas, TX 75240 ..... (214)661-5010

Texas
Schweber Electronics Corp.,
7420 Harwin Drive,
Houston, TX 77063 ..... (713)784-3600
Sterling Electronics, Inc.,
2800 Longhorn, Suite 100,
Austin, TX 78758 ..... (512)836-1341
Sterling Electronics, Inc.,
4201 Southwest Freeway,
Houston, TX 77027 ..... (713)627-9800
Sterling Electronics, Inc.,
2875 Merrell Road,
Dallas, TX 75229 ..... (214)357-9131
Trevino Electronics, Inc.,
2826 Walnut Hill Lane,
Dallas, TX 75229 ..... (214)358-2418

Utah
Hamilton-Avnet Electronics,
1585 West 2100 South,
Salt Lake City, UT 84119 ..... (801)972-2800

Washington
Hamilton-Avnet Electronics,
13407 Northrup Way,
Bellevue, WA 98005 ..... (206)746-8750
Liberty Electronics/Northwest,
1750 132nd Ave. N.E.,
Bellevue, WA 98005 ..... (206)453-8300
Robert E. Priebe Company,
2211 5th Avenue,
Seattle, WA 98121 ..... (206)682-8242

Wisconsin
Arrow Electronics, Inc.,
434 West Rawson Avenue,
Oak Creek, WI 53154 ..... (414)764-6600
Hamilton-Avnet Electronics,
2975 South Moorland Road,
New Berlin, WI 53151 ..... (414)784-4510
Taylor Electric Company,
1000 W. Donges Bay Road,
Mequon, WI 53092 ..... (414)241-4321


RCA
Solid
State
Industrial · Industrial · Industrial · Industrial · Industrial · Industrial · Industrial
BiMOS · I2L · Gold CHIP · MOS · Bipolar · BiMOS · I2L · Gold CHIP · MOS
Consumer · Consumer · Consumer · Consumer · Consumer · Consumer · Consumer